



ALLAN DE AMORIM DOS SANTOS

**APPROACH OF NEW COATING FORMULATIONS BASED
ON CATIONIC STARCH FOR KRAFTLINER PAPER**

**LAVRAS - MG
2023**

ALLAN DE AMORIM DOS SANTOS

**APPROACH OF NEW COATING FORMULATIONS BASED ON CATIONIC
STARCH FOR KRAFTLINER PAPER**

Tese apresentada à Universidade Federal de Lavras e à Universidade de Copenhagen, como parte das exigências do Programa de Pós-Graduação em Ciência e Tecnologia da Madeira e do Programa de Pós-Graduação da Faculdade de Ciências, para obtenção do título de Doutor (dupla titulação).

Prof. Dr. Gustavo Henrique Denzin Tonoli (UFLA) - Brasil
Orientador

Prof. Dr. Anand Ramesh Sanadi (UCPH) - Dinamarca
Orientador

**LAVRAS - MG
2023**

**Ficha catalográfica elaborada pelo Sistema de Geração de Ficha Catalográfica da Biblioteca
Universitária da UFLA, com dados informados pelo(a) próprio(a) autor(a).**

Santos, Allan de Amorim dos.

Approach of new coating formulations based on cationic starch
for kraftliner paper / Allan de Amorim dos Santos. - 2023.

153 p. : il.

Orientador(a): Gustavo Henrique Denzin Tonoli.

Coorientador(a): Anand Ramesh Sanadi.

Tese (doutorado) - Universidade Federal de Lavras, 2023.

Bibliografia.

1. Eco-friendly coating. 2. Green barrier. 3. Kraft paper
packaging. I. Tonoli, Gustavo Henrique Denzin. II. Sanadi, Anand
Ramesh. III. Título.

O conteúdo desta obra é de responsabilidade do(a) autor(a) e de seu orientador(a).

ALLAN DE AMORIM DOS SANTOS

**APPROACH OF NEW COATING FORMULATIONS BASED ON CATIONIC
STARCH FOR KRAFTLINER PAPER**

**ABORDAGEM DE NOVAS FORMULAÇÕES DE REVESTIMENTO À BASE DE
AMIDO CATIONICO PARA PAPEL KRAFTLINER**

PhD thesis presented to the University of Copenhagen and to the Federal University of Lavras as part of the requirements of the Graduate Program of the Faculty of Science and the Graduate Program in Wood Science and Technology to obtain the title of Doctor (double degree).

Prof. Dr. Gustavo Henrique Denzin Tonoli (UFLA) - Brazil
Advisor

Prof. Dr. Anand Ramesh Sanadi (UCPH) - Denmark
Advisor

*This thesis has been submitted to the PhD School of The Faculty of Science, University of
Copenhagen, on December 23rd, 2022.*

**LAVRAS - MG
2023**

ALLAN DE AMORIM DOS SANTOS

**APPROACH OF NEW COATING FORMULATIONS BASED ON CATIONIC
STARCH FOR KRAFTLINER PAPER**

**ABORDAGEM DE NOVAS FORMULAÇÕES DE REVESTIMENTO À BASE DE
AMIDO CATIONICO PARA PAPEL KRAFTLINER**

Tese apresentada à Universidade Federal de Lavras e à Universidade de Copenhagen, como parte das exigências do Programa de Pós-Graduação em Ciência e Tecnologia da Madeira e do Programa de Pós-Graduação da Faculdade de Ciências, para obtenção do título de Doutor (dupla titulação).

APROVADA em 23 de fevereiro de 2023.

Dra. Juliana Cristina da Silva – Klabin S.A.

Dra. Lina Bufalino - UFRA

Dra. Lisbeth Garbrecht Thygesen - UCPH

Dra. Maria Lucia Bianchi - UFPA

Dr. Sergio Henrique Pezzin - UDESC

Prof. Dr. Gustavo Henrique Denzin Tonoli
Orientador - Brasil

**LAVRAS - MG
2023**

ALLAN DE AMORIM DOS SANTOS

**APPROACH OF NEW COATING FORMULATIONS BASED ON CATIONIC
STARCH FOR KRAFTLINER PAPER**

**ABORDAGEM DE NOVAS FORMULAÇÕES DE REVESTIMENTO À BASE DE
AMIDO CATIONICO PARA PAPEL KRAFTLINER**

PhD thesis presented to the University of Copenhagen and to the Federal University of Lavras as part of the requirements of the Graduate Program of the Faculty of Science and the Graduate Program in Wood Science and Technology to obtain the title of Doctor (double degree).

APPROVED on February 23rd, 2023.

Dr. Juliana Cristina da Silva – Klabin S.A.

Dr. Lina Bufalino - UFRA

Dr. Lisbeth Garbrecht Thygesen - UCPH

Dr. Maria Lucia Bianchi - UFLA

Dr. Sergio Henrique Pezzin - UDESC

Prof. Dr. Anand Ramesh Sanadi
Advisor - Denmark

**LAVRAS - MG
2023**

AGRADECIMENTOS

Agradeço primeiramente a Deus, em Quem deposito minha fé.

Aos meus pais Lia e Reni, minha irmã Kátia e meus sobrinhos Mariáh e Miguel. Vocês são meu porto seguro.

À Universidade Federal de Lavras e ao Programa de Pós-Graduação em Ciência e Tecnologia da Madeira pela oportunidade de estudo de qualidade. Também a todo corpo docente e técnicos do Departamento de Ciências Florestais pelo apoio e aprendizado durante o doutorado. Ainda, à Coordenação de Aperfeiçoamento de Pessoal de Nível Superior (CAPES) pelo apoio financeiro.

À Universidade de Copenhagen, docentes, técnicos e colegas do Departamento de Geociências e Gestão de Recursos Naturais e à Dinamarca. Também para meus queridos amigos Karen, Rokas e Sandra. Vocês são os melhores! Me senti muito aconchegado e acolhido.

Aos meus orientadores, Gustavo Henrique Denzin Tonoli e Anand Ramesh Sanadi, que brilhantemente me auxiliaram a crescer como pesquisador, me conduzindo com toda dedicação.

Aos colegas do Laboratório de Nanotecnologia Florestal, especialmente à Lays e ao Luiz. Nem em meus melhores sonhos eu poderia imaginar conviver com pessoas tão incríveis quanto vocês.

Também, a todos os meus amigos que estiveram ao meu lado nas fases boas e também nas fases desafiadoras. Reduto, Manhauçu, Viçosa, Lavras, Edmonton e Copenhagen só foram incríveis porque compartilhamos memórias juntos. Espero celebrar com vocês nossas próximas vitórias.

O presente trabalho foi realizado com apoio da Coordenação de Aperfeiçoamento de Pessoal de Nível Superior – Brasil (CAPES) – Código de Financiamento 001.

E finalmente, gostaria de agradecer a cada brasileiro. O investimento na educação sustentado pela população possibilitou o desenvolvimento dessa e de muitas outras pesquisas. Obrigado, Brasil!

Não há palavras suficientes que expressem minha gratidão a vocês.

MUITO OBRIGADO!

ACKNOWLEDGMENT

I first thank God, in Whom I put my faith.

To my parents Lia and Reni, my sister Kátia, my niece Mariáh, and my nephew Miguel. You are my safe haven.

To the Federal University of Lavras and the Graduate Program in Wood Science and Technology for the opportunity of high-quality study. Also, to all the professors and technicians of the Department of Forest Sciences for their support during my doctorate. In addition, to the Coordenação de Aperfeiçoamento de Pessoal de Nível Superior (CAPES) for financial support.

To the University of Copenhagen, professors, technicians, and colleagues from the Department of Geosciences and Natural Resources Management and Denmark. Also, to my dear friends Karen, Rokas, and Sandra. You guys rock! I felt very cozy and welcomed.

To my advisors Gustavo Henrique Denzin Tonoli and Anand Ramesh Sanadi, who brilliantly helped me grow as a researcher, leading me with all their dedication.

To colleagues from the Forest Nanotechnology Laboratory, especially to Lays and Luiz. Not in my best dreams could I have imagined sharing my path with people as incredible as you.

Also, to all my friends who were by my side in the sound and challenging times. Reduto, Manhuaçu, Viçosa, Lavras, Edmonton, and Copenhagen were unique because we shared memories together. I hope to celebrate with you our next victories.

This study was financed in part by the Coordenação de Aperfeiçoamento de Pessoal de Nível Superior – Brasil (CAPES) – Finance Code 001.

And finally, I would like to thank every Brazilian. Investment in education sustained by the population enabled the development of this and many other studies. Thanks, Brazil!

There are not enough words to express my gratitude to you.

THANK YOU!

RESUMO

Materiais de embalagem tradicionais baseiam-se principalmente em polietileno e polipropileno não biodegradáveis e comprometem seu descarte se deixados no ambiente. Como alternativa, o papel é amplamente utilizado como material de embalagem e uma opção de baixo custo com processo de fabricação bem estabelecido. No entanto, possui limitações de permeabilidade e hidrofobicidade. A técnica de revestimento do papel é uma excelente opção para proporcionar melhores propriedades de barreira e reduzir sua higroscopicidade. Além disso, é preferível fazer revestimentos com materiais naturais ou biodegradáveis, como amidos, para reduzir a pressão ambiental. A utilização de componentes naturais misturados ao amido em sua forma catiônica com alta viscosidade e baixo teor de sólidos para revestimento de papel kraftliner para fins de embalagem é pouco explorada na literatura. Portanto, esta tese teve como objetivo avaliar revestimentos à base de amido catiônico em papel kraftliner para criar papéis multicamadas de alta qualidade com potencial de biodegradação e reciclagem com propriedades de barreira. No primeiro artigo científico, suspensões de amido catiônico foram misturadas com cera de carnaúba nas proporções de 1:0, 3:1, 1:1, 1:3 e 0:1 (m:m). O segundo artigo estudou a adição de bentonita a 5%, 7% e 10% (m/m) às suspensões de amido catiônico. Em seguida, o terceiro artigo avaliou as suspensões de amido catiônico misturadas com poli(álcool vinílico)(PVOH) nas proporções de 1:0, 3:1, 1:1, 1:3 e 0:1 (m:m). Para cada artigo científico, misturas revestiram o papel kraftliner em duas camadas de $15,0 \pm 0,5$ g/m² e comparadas ao papel kraftliner não revestido (86 ± 1 g/m²) e papel kraftliner duplamente úmido-e-seco. As suspensões foram avaliadas quanto ao teor de sólidos, pH e viscosidade. Além disso, os papéis multicamadas foram analisados quanto às características químicas, físicas, morfológicas e mecânicas, além de barreiras à água, vapor de água, óleo e oxigênio. Todas as suspensões apresentaram pH >4,0, com boa interação sem separação de fases. Imagens de microscopia eletrônica de varredura mostraram um filme fino para cada formulação no papel, exceto para o tratamento formado por 100% de cera de carnaúba; a adição de amido catiônico à cera corrigiu essa não formação filme. Com a aplicação do revestimento, os papéis apresentaram diminuição de até 36% na resistência mecânica à tração causada pela presença de água nas suspensões, o que reduziu a interação entre as fibras do papel. O papel Kraftliner revestido com amido catiônico apresentou alta hidrofobicidade com teste Cobb de 189 ± 2 g/m², mas diminuiu 28% e 66% quando adicionado cera de carnaúba e bentonita, respectivamente. Além disso, a adição de PVOH ao amido catiônico diminuiu a permeabilidade ao vapor de água dos papéis em 57% e aumentou a barreira de óleo de 10 para 12 no kit-óleo. Em comparação com o amido catiônico puro, a barreira de óleo também aumentou quando se adicionou 7% de bentonita (m/m) ao amido catiônico. Finalmente, uma barreira de oxigênio de até 10 cc/(mm².dia) foi alcançada pela adição de até 75% (m/m) de amido catiônico ao polímero PVOH. A incorporação de cera de carnaúba, bentonita e PVOH ao amido catiônico melhorou as propriedades de barreira ao vapor de água e oxigênio, servindo como embalagem de baixa umidade para alimentos, como alimentos de panificação. Esses revestimentos atendem às demandas do mercado de embalagens primárias e secundárias com foco na excelente relação homem-ambiente.

Palavras-chave: Revestimento ecologicamente correto. Barreira verde. Embalagem de papel kraft. Embalagem multicamadas. Materiais sustentáveis.

ABSTRACT

Traditional packaging materials are based mainly on polyethylene and polypropylene, which are not biodegradable and compromise their disposal if left in the environment. As an alternative, paper is already widely used as a packaging material and a low-cost option with adequate manufacturing know-how. However, it has limitations in terms of permeability and hydrophilicity. The coating technique on the paper surface is an excellent option to provide better barrier properties and reduce its hygroscopicity. Additionally, making coatings with natural or biodegradable materials, such as starches, is preferable to reduce environmental pressure. Using natural components mixed with starch in its cationic form with high viscosity at low solid content for coating kraftliner paper for packaging purposes is underexplored in literature. Therefore, this work aimed to evaluate cationic starch-based coatings on kraftliner paper to create high-quality multilayer papers with biodegradation and recycling potential with barrier properties. In the first scientific article, cationic starch suspensions were mixed with carnauba wax in proportions of 1:0, 3:1, 1:1, 1:3, and 0:1 (m:m). The second scientific article studied the addition of bentonite in 5%, 7%, and 10% (m/m) to cationic starch suspensions. Then, the third scientific article evaluated the cationic starch suspensions mixed with poly(vinyl alcohol)(PVOH) in proportions of 1:0, 3:1, 1:1, 1:3, and 0:1 (m:m). For each scientific article, the mixtures coated the kraftliner paper in two layers of $15.0 \pm 0.5 \text{ g/m}^2$ and compared to uncoated kraftliner paper ($86 \pm 1 \text{ g/m}^2$) double wet-and-dry kraftliner paper. The suspensions were evaluated for solids content, pH, and viscosity. Also, we analyzed the multilayer papers for chemical, physical, morphological, and mechanical characteristics, in addition to barriers to water, water vapor, oil, and oxygen. All suspensions showed $\text{pH} > 4.0$ with good interaction without phase separation. The scanning electron microscopy images showed a thin film for each formulation on the paper, except for the treatment formed by 100% carnauba wax; adding cationic starch to the wax corrected this non-film formation. With coating application, papers showed a decrease of up to 36% in tensile mechanical strength caused by water in the suspensions, which reduced the interaction between paper fibers. Kraftliner paper coated with cationic starch showed high hydrophilicity with a Cobb test of $189 \pm 2 \text{ g/m}^2$ but decreased by 28% and 66% when adding carnauba wax and bentonite, respectively. Furthermore, adding PVOH to cationic starch decreased the water vapor permeability of the papers by 57% and increased the oil barrier from 10 to 12 in the kit oil. Compared to pure cationic starch, the oil barrier also increased when adding 7% bentonite (m/m) to cationic starch. Finally, an oxygen barrier of up to $10 \text{ cc}/(\text{mm}^2 \cdot \text{day})$ was achieved by adding 75% (m/m) of cationic starch to the PVOH polymer. Incorporating carnauba wax, bentonite, and PVOH into the cationic starch improved the barrier properties to water vapor and oxygen, serving as low-moisture packaging for foods, such as bakery elements. These coatings meet market demands for primary and secondary packages, focusing on an excellent human-environment relationship.

Keywords: Eco-friendly coating. Green barrier. Kraft paper packaging. Multilayer packaging. Sustainable materials.

RESUMÉ

Traditionelt anvendes materialer baserede på polyætylen og polypropylen til emballage, hvilket gør bortskaffelse og genanvendelse vanskeligt, da polyætylen ikke er biologisk nedbrydeligt. Et mindre miljøbelastende og billigere alternativ er papir, som allerede anvendes bredt. Papir har imidlertid nogle ulemper: Det er ikke tæt, og det er ydermere hydrofilt. Overfladebehandling kan forbedre barriereegenskaberne og nedsætte vandsugningsevnen. Det er at foretrække at der anvendes en belægning bestående af naturlige og biologisk nedbrydelige materialer, så som stivelse, da det nedsætter miljøbelastningen. I dette studie var formålet derfor at undersøge coating af kraft liner papir med kationiseret stivelse til fremstilling af flerlagspapir i høj kvalitet med potentiale for biologisk nedbrydelighed og gode barriereegenskaber. I det første videnskabelige studie blev suspensioner bestående af kationiseret stivelse blandet med carnaubapalmevoks i forholdene 1:0, 3:1, 1:1, 1:3 og 0:1 (m:m). I det andet videnskabelige studie blev suspensioner bestående af kationiseret stivelse tilsat bentonit i koncentrationerne 5%, 7% og 10% (m/m). I det tredje videnskabelige studie blev suspensioner bestående af kationiseret stivelse blandet med poly(vinyl alcohol)(PVOH) i forholdene 1:0, 3:1, 1:1, 1:3 og 0:1 (m:m). I hvert studie coatedes kraft liner papir med suspensionerne i to lag med en samlet vægt på 15.0 ± 0.5 g/m² og sammenlignedes med ikke-coatet kraft liner papir (86 ± 1 g/m²), der var blevet gjort vådt og tørret to gange. Suspensionernes indhold af ikke-opløselige stoffer, samt deres pH og viskositet blev bestemt. Papir overfladebehandlet med suspensionerne blev undersøgt med hensyn til kemiske, fysiske, morfologiske og mekaniske karakteristika. Herudover blev barriereegenskaber med hensyn til vand, vanddamp, olie og ilt bestemt. Alle suspensioner havde en pH-værdi på over 4.0, udviste god interaktion og skilte sig ikke ud i forskellige faser. Ved brug af elektronmikroskopi var det muligt at observere dannelsen af en tynd film på overfladen af papiret, undtagen for 100% carnaubapalmevoks; hvis der tilsattes stivelse kunne voksen imidlertid godt danne en film på papiroverfladen. Coating gav et fald i trækstyrke på op til 36% på grund af vandet i suspensionerne, som reducerede interaktionen mellem fibrene i papiret. Kraft liner papir coatet med kationiseret stivelse var meget hydrofilt; en Cobb test viste 189 ± 2 g/m², men reduceredes med henholdsvis 28% og 66% ved tilsætning af enten carnaubapalmevoks eller bentonit. Tilsætning af PVOH til suspensionen af kationiseret stivelse nedsatte vandpermeabiliteten af det coatede papir med 57% og øgede barriereegenskaberne med hensyn til olie fra 10 til 12 ifølge det anvendte olie assay. Sammenlignet med den rene suspension af kationiseret stivelse forbedredes barriereegenskaberne over for olie når der tilsattes 7% bentonit. Endelig opnåedes barriereegenskaber over for ilt på op til 10 cc/(mm².dag) ved tilsætning af 75 % stivelse til PVOH polymeren. At tilsætte carnaubapalmevoks, bentonit og PVOH til kationiseret stivelse forbedrede barriereegenskaberne over for vanddamp og ilt, hvilket åbner perspektiver overfor anvendelse af disse emballager til fødevarer med lavt vandindhold så som for eksempel bageriprodukter. Emballagerne har således et potentiale med hensyn til primær og sekundær emballage, med en miljømæssigt attraktiv profil.

Nøgleord: Miljøvenlig coating af papir. Grøn barriere. Kraftpapir emballage. Flerlags emballage. Bæredygtige materialer.

LISTA DE FIGURAS
LIST OF FIGURES

FIRST PART

| | |
|--|----|
| Figure 1 - Hierarchical classification of packages..... | 24 |
| Figure 2 - Chemical composition of starch showing (a) glucose unit structure, (b) amylose, and (c) amylopectin. | 27 |
| Figure 3 - Production of cationic starch. | 28 |
| Figure 4 - Applications of carnauba wax in the food sector..... | 29 |
| Figure 5 - Representation of the typical structure of bentonite. | 30 |
| Figure 6 - Chemical composition of poly(vinyl alcohol) in a three-dimensional representation..... | 31 |

THIRD PART

| | |
|---|----|
| Figure 1 - Graphic scheme with cationic starch granules (A); chemical representation of cationic starch, glycerol, carnauba wax, and polysorbate 80 (B); representation of suspensions and their pH, solid contents, and viscosity characteristics of cationic starch (C); cationic starch 75%/25% carnauba wax mixture (D), cationic starch 50%/50% carnauba wax mixture (E); cationic starch 25%/75% carnauba wax mixture (F); carnauba wax (G); and flowchart of the modification of suspension characteristics with the increase of cationic starch to carnauba wax in suspension (H). | 64 |
| Figure 2 - Scanning electron microscopy of the surface of coated papers and pencil hardness. | 66 |
| Figure 3 - Scanning electron microscopy of coated papers' cross-section, thickness, and density characteristics..... | 68 |
| Figure 4 - Fourier transform infrared spectroscopy of coated papers. | 69 |
| Figure 5 - Raman spectroscopy characterization of cationic starch and carnauba wax composite films. | 71 |
| Figure 6 - Water contact angle (A), wettability (B), water vapor transmission rate – WVTR (C), and water vapor permeability – WVP (D) property of coated papers and their correlation analyzed by the principal component analysis (E) and Pearson's correlation coefficient (F). . | 73 |
| Figure 7 - Surface free energy of coated papers..... | 76 |

Figure 8 - Tensile properties of coated papers in the machine direction - MD (A) and the cross direction - CD (B).....77

FOURTH PART

Figure 1 - Illustration of suspensions of cationic starch and bentonite in deionized water (A) and their interaction (B). Cationic starch granules in a scale of 200 μ (C), 100 μ (D), and 20 μ (E). Cationic starch (S) with the addition of 5 wt% (.B5), 7 wt% (.B7), and 10 wt% (.B10) of bentonite.99

Figure 2 - Surface and cross-sectional images of multilayer packaging captured using standard scanning electron microscopy. Control treatments with no coating (C1) and water coating (C2). Cationic starch (S) with the addition of 5 wt% (.B5), 7 wt% (.B7), and 10 wt% (.B10) of bentonite. 101

Figure 3 - Multilayer packing characterization by Fourier-transform infrared spectroscopy. Control treatments with no coating (C1) and water coating (C2). Cationic starch (S) with the addition of 5 wt% (.B5), 7 wt% (.B7), and 10 wt% (.B10) of bentonite..... 103

Figure 4 - Characterization of cationic starch and bentonite films using Raman spectroscopy. Cationic starch (S) with the addition of 5 wt% (.B5), 7 wt% (.B7), and 10 wt% (.B10) of bentonite. 105

Figure 5 - Tensile index x elongation curves of multilayer packaging (A) in their machine direction – MD (B) and cross direction – CD (C). Control treatments with no coating (C1) and water coating (C2). Cationic starch (S) with the addition of 5 wt% (.B5), 7 wt% (.B7), and 10 wt% (.B10) of bentonite. 106

Figure 6 - Properties of multilayer packaging for water contact angle (A), wettability (B), water vapor transmission rate (WVTR), water vapor permeability (WVP) (C), and water absorption (Cobb test) (D). The same letters in the columns do not differ according to the Scott-Knott test at 5% of significance. Control treatments with no coating (C1) and water coating (C2). Cationic starch (S) with the addition of 5 wt% (.B5), 7 wt% (.B7), and 10 wt% (.B10) of bentonite..... 109

FIFTH PART

Figure 1 - Simplified graphical abstract with the methodology used in this research..... 126

| | |
|--|-----|
| Figure 2 - Sketch of blend suspensions in deionized water with complementary proportions (m:m) of 1:0, 3:1, 1:1, 1:3, and 0:1 of cationic starch (S) and poly(vinyl alcohol)(P)..... | 131 |
| Figure 3 - Typical scanning electron microscopy images of multilayer paper surface (A, D, G, J, M) and cross-section (B, C, E, F, H, I, K, L, N, O). | 133 |
| Figure 4 - Thermogravimetry curves (A) and the first derivative (B) of multilayer paper with cationic starch and poly(vinyl alcohol) blends and control papers. | 135 |
| Figure 5 - Fourier transform infrared spectroscopy characterization of kraftliner coated paper. | 136 |
| Figure 6 - Properties of multilayer paper of water contact angle, wettability (A), water vapor transmission rate (WVTR), and water vapor permeability (WVP) (B)..... | 137 |
| Figure 7 - Properties of multilayer coated paper surface free energy with their dispersed and polar phases. | 140 |
| Figure 8 - Oxygen transmission rate of multilayer paper. | 140 |

LISTA DE TABELAS

LIST OF TABLES

THIRD PART

| | |
|--|----|
| Table 1 - Acronyms and description of the treatments used in this work. | 59 |
| Table 2 - Water absorbance and oil resistance of coated papers. | 74 |
| Table 3 - Tensile properties of multilayer paper in the machine direction (MD). | 77 |
| Table 4 - Tensile properties of multilayer paper in the cross direction (CD). | 78 |

FOURTH PART

| | |
|---|-----|
| Table 1 - Suspensions produced by cationic starch and bentonite and their pH, solids content, and viscosity characteristics. | 93 |
| Table 2 - Characterization of the thickness, density, and hardness of multilayer paper. | 100 |
| Table 3 - Mechanical properties of multilayer paper in their machine direction (MD). | 107 |
| Table 4 - Mechanical properties of multilayer paper in their cross direction (CD). | 107 |
| Table 5 - Cationic starch and bentonite multilayer paper properties of oil resistance and surface free energy. | 111 |

FIFTH PART

| | |
|---|-----|
| Table 1 - Description of treatments and characterization of pH, solids content, and viscosity of the blend suspension formed by cationic starch and poly(vinyl alcohol). | 126 |
| Table 2 - Multilayer paper thickness, density, and thermal degradation temperature characterization. | 132 |
| Table 3 - Water absorbency and oil resistance of multilayer paper. | 139 |

LISTA DE ABREVIATURAS

LIST OF ACRONYMS

| | |
|--------------------|--|
| ABNT | Associação Brasileira de Normas Técnicas |
| ANOVA | Analysis of variance |
| ASTM | American Society for Testing and Materials |
| CCD | Charge-coupled device |
| CD | Cross direction |
| Cobb | Water absorbency |
| <i>et al.</i> | <i>et alia</i> |
| FDA | Food and Drug Administration |
| FT-IR | Fourier transform infrared spectroscopy |
| ISO | International Organization for Standardization |
| MD | Machine direction |
| NBR | Norma Brasileira |
| OTR | Oxygen transmission rate |
| pH | Potential of hydrogen |
| SEM | Scanning electron microscope |
| TAPPI | Technical Association of the Pulp and Paper Industry |
| TGA | Thermogravimetric analysis |
| T _{half} | Temperature at 50% mass loss |
| T _{onset} | Temperature at the beginning of the thermal event |
| UCPH | University of Copenhagen |
| UFLA | Universidade Federal de Lavras |
| USA | United States of America |
| WVP | Water vapor permeability |
| WVTR | Water vapor transmission rate |

LISTA DE SÍMBOLOS

LIST OF SYMBOLS

| | |
|-------|---|
| B | Bentonite |
| C1 | Kraftliner paper with no coating |
| C2 | Double wet-and-dry kraftliner paper |
| P | Treatment formed by 100 wt.% poly(vinyl alcohol) |
| PVOH | Poly(vinyl alcohol) |
| S | Treatment formed by 100 wt.% cationic starch |
| S.B10 | Treatment formed by cationic starch adding 10 wt.% of bentonite |
| S.B5 | Treatment formed by cationic starch adding 5 wt.% of bentonite |
| S.B7 | Treatment formed by cationic starch adding 7 wt.% of bentonite |
| S1:1P | Blend formed by 50 wt.% cationic starch and 50 wt.% poly(vinyl alcohol) |
| S1:1W | Treatment formed by 50 wt.% cationic starch and 50 wt.% carnauba wax |
| S1:3P | Blend formed by 25 wt.% cationic starch and 75 wt.% poly(vinyl alcohol) |
| S1:3W | Treatment formed by 25 wt.% cationic starch and 75 wt.% carnauba wax |
| S3:1P | Blend formed by 75 wt.% cationic starch and 25 wt.% poly(vinyl alcohol) |
| S3:1W | Treatment formed by 75 wt.% cationic starch and 25 wt.% carnauba wax |
| W | Treatment formed by 100 wt.% carnauba wax |

SUMÁRIO
CONTENTS

| | | |
|--------------|---|-----------|
| | FIRST PART | 21 |
| | THESIS PRESENTATION | 21 |
| 1. | INTRODUCTION | 21 |
| 2. | OBJECTIVE | 22 |
| 2.1 | Main objective | 22 |
| 2.2 | Specific objectives | 23 |
| 3. | LITERATURE REVIEW | 23 |
| 3.1 | Packaging | 23 |
| 3.2 | Multilayer packaging | 24 |
| 3.3 | Kraft paper packaging | 25 |
| 3.4 | Materials as packaging coating | 26 |
| 3.4.1 | Starch | 27 |
| 3.4.2 | Carnauba wax | 28 |
| 3.4.3 | Bentonite | 30 |
| 3.4.4 | Poly(vinyl alcohol) | 31 |
| 4. | REVIEWS CONSIDERATIONS | 32 |
| | REFERENCES | 32 |
| | SECOND PART | 43 |
| 1. | RESEARCH PROJECT | 43 |
| 1.1 | Project description | 43 |
| 1.2 | Research findings | 44 |
| 1.3 | Thesis context | 47 |
| | REFERENCES | 47 |
| | THIRD PART | 54 |
| | Evaluation of paper coated with cationic starch and carnauba wax mixtures regarding barrier properties | 54 |
| | ABSTRACT | 54 |
| 1. | INTRODUCTION | 55 |
| 2. | EXPERIMENT | 57 |
| 2.1 | Material | 57 |

| | | |
|-------|---|-----------|
| 2.1.1 | Preparation of suspensions | 57 |
| 2.1.2 | Kraftliner paper coating | 58 |
| 2.2 | Methods | 59 |
| 2.2.1 | Characterization of suspensions..... | 59 |
| 2.2.2 | Physical properties of coated paper | 59 |
| 2.2.3 | Paper pencil hardness | 59 |
| 2.2.4 | Fourier transform infrared spectroscopy (FT-IR) | 60 |
| 2.2.5 | Raman spectroscopy | 60 |
| 2.2.6 | Water and oil barrier properties of coated paper | 61 |
| 2.2.7 | Oil/Grease barrier property of coated paper | 62 |
| 2.2.8 | Mechanical property of coated paper | 63 |
| 2.3 | Statistical analysis..... | 63 |
| 3. | RESULTS AND DISCUSSION | 63 |
| 3.1 | Investigation of Suspensions | 63 |
| 3.2 | Physical and morphological characteristics | 65 |
| 3.3 | Fourier transform infrared spectroscopy and Raman spectroscopy | 69 |
| 3.4 | Water and oil barrier | 72 |
| 3.5 | Mechanical characterization..... | 76 |
| 4. | CONCLUSION | 79 |
| | ACKNOWLEDGMENT | 79 |
| | REFERENCES | 80 |
| | FOURTH PART | 89 |
| | Addition of bentonite to cationic starch matrix for coating on kraftliner paper to improve grease resistance | 89 |
| | ABSTRACT | 89 |
| 1. | INTRODUCTION | 90 |
| 2. | MATERIALS AND METHODS | 92 |
| 2.1 | Material | 92 |
| 2.1.1 | Preparation of suspensions | 92 |
| 2.1.2 | Kraftliner paper coating | 93 |
| 2.2 | Methods | 94 |
| 2.2.1 | Physical properties of coated paper | 94 |
| 2.2.2 | Pencil hardness | 94 |

| | | |
|-------|--|-----|
| 2.2.3 | Attenuated total reflectance Fourier transform infrared (ATR-FTIR) spectroscopy. | 94 |
| 2.2.4 | Raman spectroscopy | 94 |
| 2.2.5 | Mechanical properties of coated paper..... | 95 |
| 2.2.6 | Water barrier properties of coated paper | 95 |
| 2.2.7 | Oil/grease barrier property of coated packaging | 97 |
| 2.3 | Statistical analysis..... | 97 |
| 3. | RESULTS AND DISCUSSION | 98 |
| 3.1 | Suspension investigation | 98 |
| 3.2 | Physical and morphological characterization | 100 |
| 3.3 | ATR-FTIR spectroscopy and Raman spectroscopy | 102 |
| 3.4 | Mechanical characterization..... | 106 |
| 3.5 | Water and oil barrier | 108 |
| 4. | CONCLUSION | 112 |
| | ACKNOWLEDGEMENT | 112 |
| | REFERENCES | 113 |
| | FIFTH PART | 122 |
| | Kraftliner paper coated with cationic starch/glycerol and poly(vinyl alcohol) blends to generate water vapor and O₂ barriers | 122 |
| | ABSTRACT | 122 |
| 1. | INTRODUCTION | 123 |
| 2. | EXPERIMENTAL | 125 |
| 2.1 | Material | 125 |
| 2.1.1 | Preparation of suspensions | 125 |
| 2.1.2 | Kraftliner paper coating | 126 |
| 2.2 | Methods | 127 |
| 2.2.1 | Physical properties of coated paper | 127 |
| 2.2.2 | Thermogravimetric analysis (TGA) | 127 |
| 2.2.3 | Fourier transform infrared spectroscopy (FT-IR) | 127 |
| 2.2.4 | Water barrier property of coated paper | 128 |
| 2.2.5 | Oil/grease barrier property of the coated paper | 129 |
| 2.2.6 | Oxygen barrier of the coated paper | 129 |
| 2.3 | Statistical analysis | 130 |
| 3. | RESULTS AND DISCUSSION | 130 |

| | | |
|-----|---|-----|
| 3.1 | Investigation of suspensions..... | 130 |
| 3.2 | Physical, morphological, and thermal characterization | 132 |
| 3.3 | Fourier transform infrared spectroscopy (FT-IR) | 135 |
| 3.4 | Paper water and oil resistance..... | 137 |
| 3.5 | Oxygen barrier..... | 140 |
| 4. | CONCLUSION | 141 |
| | ACKNOWLEDGMENT | 142 |
| | REFERENCES | 143 |
| | SIXTH PART | 152 |
| 1. | THESIS CONCLUSIONS | 152 |

FIRST PART

THESIS PRESENTATION

This thesis is divided into six parts. The first part consists of an introduction, objectives, a literature review, and final considerations of the literature review. The literature review clarifies the content addressed in the three papers presented. The final considerations of the literature review summarize the main aspects discussed throughout the chapter.

The second part presents an executive summary of the three papers that constructed this thesis, elucidating the main data found in each paper and comparing them with the literature.

The third part of the thesis (paper 1) discusses how adding carnauba wax to a cationic starch matrix influences the surface interaction of high-barrier multilayer kraftliner paper with water, water vapor, and oil/grease.

The fourth subdivision (paper 2) includes a paper that addresses the addition of different proportions of bentonite to a cationic starch matrix to produce multilayer paper with an oil/grease barrier.

The fifth part and last paper (paper 3) addresses the effect of adding cationic starch to poly(vinyl alcohol) in kraftliner paper coating to produce low-cost paper with an oxygen barrier.

Finally, the sixth part and last chapter discusses the general conclusion of this thesis, summarizing the main points observed during the thesis regarding the use of cationic starch in a kraftliner multilayer paper coating and providing suggestions for future works.

1. INTRODUCTION

Packaging materials from petroleum are conventional and widely used because they exhibit a good cost-benefit relation in terms of their strength, durability, and ease of processing. However, the lack of biodegradability of conventional polyethylene-based packaging materials leads to many environmental risks (Emoyan, Adjere, and Tesi, 2022; Mirjani, Soleimani, and Salari, 2021; Sattar, Jehan, and Siddiqui, 2021). Thus, obtaining sustainable packaging has been the objective of many research studies (Al-Gharrawi, Wang, and Bousfield, 2022; Chen *et al.*, 2022; Palai *et al.*, 2020), especially concerning paper packaging, due to its recognized production technology (Wang *et al.*, 2022a; Shankar and Rhim, 2022; Saxena *et al.*, 2020; Dilkes-Hoffman *et al.*, 2019; Muthus, 2016).

Paper can absorb water vapor from the environment or a product due to its high hygroscopicity. This absorption can cause the paper to lose its original mechanical properties and reduce the quality of the product contained in the packaging as well as its expiration date. To minimize this problem, the coating technique can be used to reduce hygroscopicity and improve the barrier properties of paper (Chen *et al.*, 2022; Shankar and Rhim, 2022; Vaezi, Asadpour, and Sharifi, 2019). Coatings are intended for water vapor and oxygen barriers, moisture resistance, and oil resistance (Chen *et al.*, 2022; Giuseppe *et al.*, 2022; Chen *et al.*, 2021; Yook *et al.*, 2020). These factors have greater or lesser relevance depending on the intended use of the paper. Natural or biodegradable products are preferable for making such a coating to lessen the pressure on the environment and petroleum-based materials. Coatings include modified starch, nanocellulose, carnauba wax, and bentonite (Behera, Mohanta, and Thirugnanam, 2022; Hong, Wang, and Rhim, 2022; Dang and Yoksan, 2021). Another approach is using potential biodegradable petroleum-based materials, such as poly(vinyl alcohol), to improve waste management approaches (Ge, Lansing, and Lewis, 2021; Patil *et al.*, 2021; Roy and Rhim, 2021).

Modified starch and cellulose-based materials show great potential, especially when countries approved a ban on disposable plastics (Wang *et al.*, 2019). In addition to being abundant and biodegradable, films based on starch and cellulose are safe for food packaging. Several studies have reported that edible films and medicinal capsules can be inexpensively developed with these films (Guzman-Puyol *et al.*, 2022; Hai *et al.*, 2021; Chaireh, Ngasatool, and Kaewtatip, 2020; Vaezi, Asadpour, and Sharifi, 2019). Therefore, this work aims to evaluate coatings based on cationic starch in kraftliner paper to produce biodegradable multilayer papers with barrier properties and high quality.

2. OBJECTIVE

2.1 Main objective

This work aims to develop a multilayer coating barrier of non-petroleum based-coatings focusing on cationic starch for water vapor, water, oxygen, and oil barriers on high-quality coated kraftliner paper.

2.2 Specific objectives

- a) Investigate the impact of carnauba wax and bentonite on the hydrophobicity and oil/grease resistance of the coatings based on carecytionic starch.
- b) Analyze the impact of adding bentonite to a cationic starch coating on oil/grease, water vapor, and water barrier to a kraftliner paper.
- c) Evaluate the interactions between poly(vinyl alcohol) and cationic starch on the oxygen barrier of multilayer kraftliner paper.

3. LITERATURE REVIEW

The literature review was divided into the following themes to present the work in a clear manner.

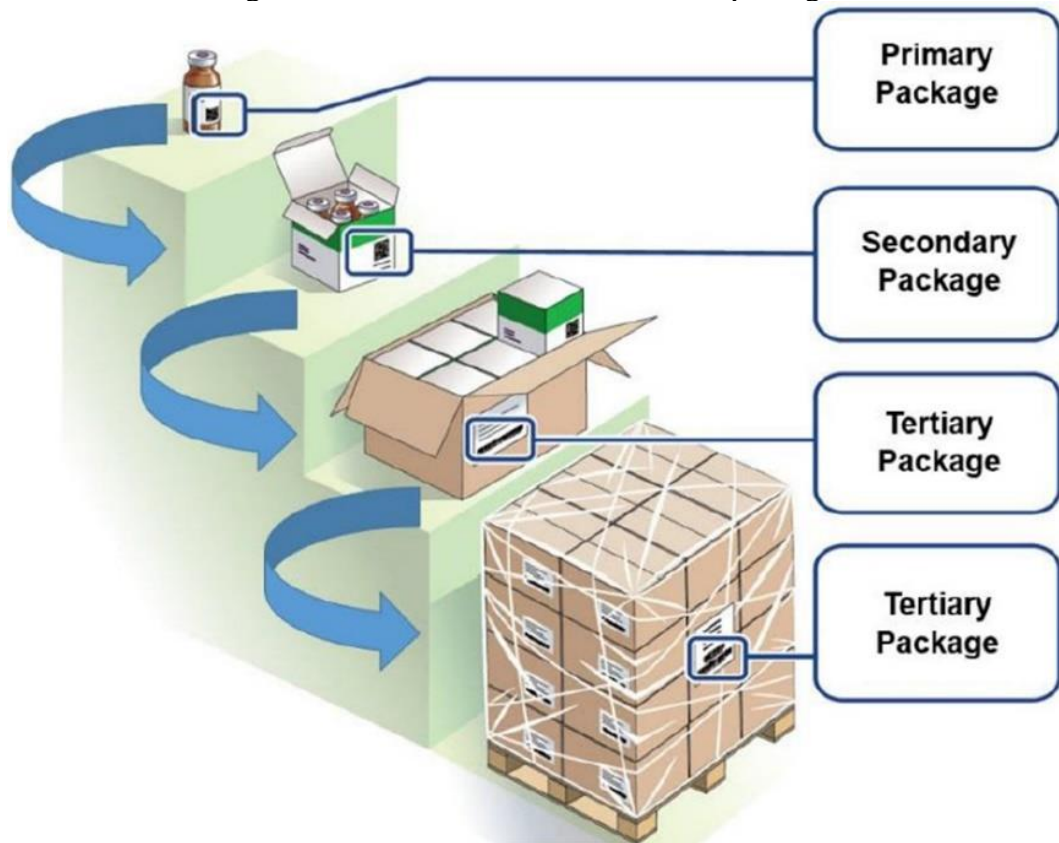
3.1 Packaging

Objects have been utilized to transport food since the prehistoric period. Primitively packaging began as leaves, shells, and other natural materials, with the primary purpose of transport and storage (Emblem and Emblem, 2012). Currently, the materials used are glass, paper, wood, metal, and plastics. The functions of packaging over time have expanded to protection, containment, communication, and convenience, extending the shelf life of products (Zhu *et al.*, 2022; Ahmad *et al.*, 2022).

Extending the shelf life of food is a primary function of packaging, which occurs by blocking the physical and chemical contact of the product with the external environment. The blockage is mainly against moisture, gases, microorganisms, vibrations, odors, and physical pressures. Even more recently, packaging functions have expanded to UV light absorption, decreased O₂ content, carbon absorption, antimicrobial activity, antioxidant activity, and even anti-fog activity (Hakke *et al.*, 2022; Wang *et al.*, 2022b; Todorova, Yavorov, and Lasheva; 2022; Ge, Lansing, and Lewis, 2021).

As it performs different functions, a packaging is hierarchically classified into primary, secondary, tertiary (Figure 1), and quaternary packaging. Primary packaging directly contacts the product or merchandise. Secondary, tertiary, and quaternary packaging are used to improve the transportation of these goods (Narancic *et al.*, 2020). Thus, packaging serves as marketing, communicates with consumers, and familiarizes customers with the product (Taylor, 2014).

Figure 1 - Hierarchical classification of packages.



Source: Adapted from Thomton *et al.* (2015).

With the deterioration of products caused by the environment and handling, the demands for packaging are increasing (Patil *et al.*, 2022; Hong, Wang, and Rhim, 2022). Furthermore, due to pressure on the environment, even more packaging must be produced with biodegradable materials, or materials with natural origins, in addition to recycling and reuse techniques.

3.2 Multilayer packaging

In the goal of increasing the shelf life of products through packaging, multilayer packaging has become an ally to utilizing biopolymers and biodegradable polymers. These packages are formed by superimposing two or more layers of the same material or different materials combined into a unified structure (Gartner, Li, and Almenar, 2015). The layers can vary from 2 to 7 layers and usually have thicknesses between 20 and 400 μm (Robert and Chartrel, 2019; Butler and Morris, 2016). This combination of different materials and several layers can offer a variety of multilayer packaging for each type of product, considering the consumer's lifestyle. Coating technology represents an efficient solution to achieve such performance (Farris, 2018), as this technique allows new properties to be incorporated into the

material (Niinivaara *et al.*, 2021). For example, water barrier polymers and UV light barrier foil were superpositioned, as in the case of Tetra Pak® multilayer packaging (Georgiopoulou *et al.*, 2021). This technique increased the quality and durability of food and materials, creating an efficient barrier to the external environment. This barrier hinders the diffusion of molecules between the external and internal environments of the packages.

The process by which molecules diffuse between two materials occurs in three steps. First, the material's surface absorbs the diffusing molecule, followed by the diffusion of the molecule through the film. Moreover, the diffusing molecule is desorbed from the surface to the other side. Steps 1 and 3 generally occur faster than when molecules move through the film, and the coating either increases or blocks this diffusion time (Nair *et al.*, 2014).

Much of the packaging focuses on petroleum-based polymers. However, using the layer-by-layer technique to produce multilayer packaging, natural and biodegradable polymers can achieve similar properties (Wang *et al.*, 2022c; Vinci *et al.*, 2019). Such polymers can be applied individually or in combination with different materials, such as kraft paper, a well-known material used as a substratum to polymer coatings (Torres *et al.*, 2020; Ghinea *et al.*, 2014).

3.3 Kraft paper packaging

The kraft process mainly consists of individualizing vegetable fibers using NaOH and Na₂S and is a process with well-established technologies. The paper produced from this pulp at different grammages exhibits high mechanical resistance, encouraging its use as packaging, and is generally used for dry foods and secondary packaging. Coating technologies are applied to kraft paper to increase its applications. Kraft paper originates from renewable materials, mainly hardwoods and softwoods, and is a recyclable material, which is advantageous. Paper fiber is recycled 3.5 times on average in Europe, but up to 15 times for corrugated paper (Kreplin, Putz, and Schabel, 2019) or even 25 cycles are technically feasible (Putz and Schabel, 2018). Recycled paper reduces waste and saves raw materials and energy (Martens and Goldmann, 2016), or even. For recycling, separate collection systems for paper and cardboard are needed since they have different chemical compositions. Chemical substances from various sources are usually present in waste paper and can eventually be transported to the recycled product (Ghinea *et al.*, 2014). Therefore, it is important that coatings have a natural and biodegradable origin so that coatings can be directed to landfills after being reused (Dilkes-Hoffman *et al.*, 2019).

Among the kraft papers currently available on the market, kraftliner paper stands out for exhibited high tensile, tearing, and compression strength, in addition to showing adequate porosity, flexibility, durability, and good printability. Thus, the paper is used as packaging to protect against impacts during transport, storage, and stacking and reduces the effects of humidity and solar radiation (Torres *et al.*, 2020). Kraftliner paper is defined as paper or cardboard composed of at least 80% fibers, usually from *Pinus* sp., and is obtained by a chemical process. Kraftliner is a paper predominantly made from primary kraft pulp with flexibility, burst resistance, and short-span compression in the cross-direction strength properties (Cepi ContainerBoard, 2017). In the production of corrugated cardboard, kraftliner paper is present in the outer and inner layers, helping to define its properties (Biermann, 1996). It is used for a high-performance packaging line and superior presentation (Paulapuro, 2000).

As a result, kraft paper stands out in the transport and packaging sector for its versatility and mechanical strength; the current research highlights the reduction in the paper's hydrophilicity and the reduction in pressure caused on the environment (Oliveira *et al.*, 2022; Wang *et al.*, 2022b; Saxena *et al.*, 2020; Li *et al.*, 2019; Matos *et al.*, 2019; Vaezi, Asadpour, and Sharifi, 2019; Shankar and Rhim, 2018).

3.4 Materials as packaging coating

Researchers are looking for new sustainable formulations in which barrier properties are achieved in one or more layers (Marangoni Júnior *et al.*, 2020; Wang *et al.*, 2020; Oudjedi *et al.*, 2019; Wrona *et al.*, 2019). The demand for materials from renewable sources that are biodegradable, repulpable, and easy to process and handle makes this search even more demanding.

The biodegradability of materials used in coating technology for water vapor and gas barriers has been the main focus due to environmental protection problems (Degli-Innocenti *et al.*, 2022; Ye *et al.*, 2022; Liao and Chen, 2021). Therefore, to replace petroleum-based materials, packaging materials should biodegrade after their useful life without causing environmental problems. Such materials are called “ecological packaging” (Rhim *et al.*, 2013; Ludueña *et al.*, 2012).

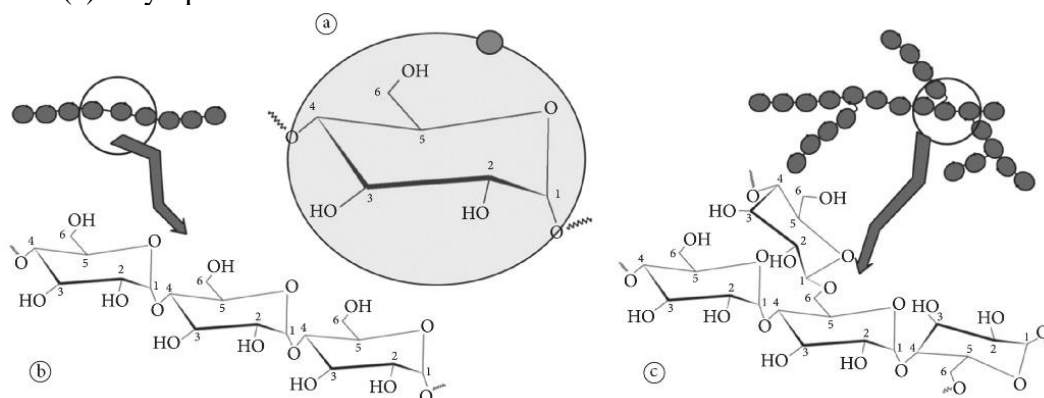
These materials can be semisynthetic polymers, such as cationic starch; vegetable wax, such as carnauba wax; natural materials with barrier properties, such as nanoclays; and potential biodegradable synthetic polymers, such as poly(vinyl alcohol). Several patents have already been registered in paper packaging using biopolymers and renewable materials with barrier

properties (Hansson, Badenlid, and Backfolk, 2019; Heiskanen *et al.*, 2019; Noda and Fukunaga, 2018; Berglund, Zhou, and Kochumalayil, 2012; Malmborg, Heijnesson-Hultén, and Sandström, 2011; Hassan and Borsinger, 2003).

3.4.1 Starch

Starch, which is among the main carbohydrates found in nature, is a reserve carbohydrate found in plants, such as corn, wheat, rice, and potatoes. Starch is formed from a mixture of two polymers. Amylose has a linear chain of 200 to 20,000 glucose units (Figure 2a), and amylopectin is highly branched. Amylose has an angulation in the α -(1-4) bond between the glucose units (Figure 2b), whereas amylopectin has short side chains containing approximately 30 units of glucose linked to an α -(1-6) bond to every 20 units of glucose (Figure 2c). Thus, amylopectin can have numerous glucose units (Ray and Bousmina, 2005).

Figure 2 - Chemical composition of starch showing (a) glucose unit structure, (b) amylose, and (c) amylopectin.



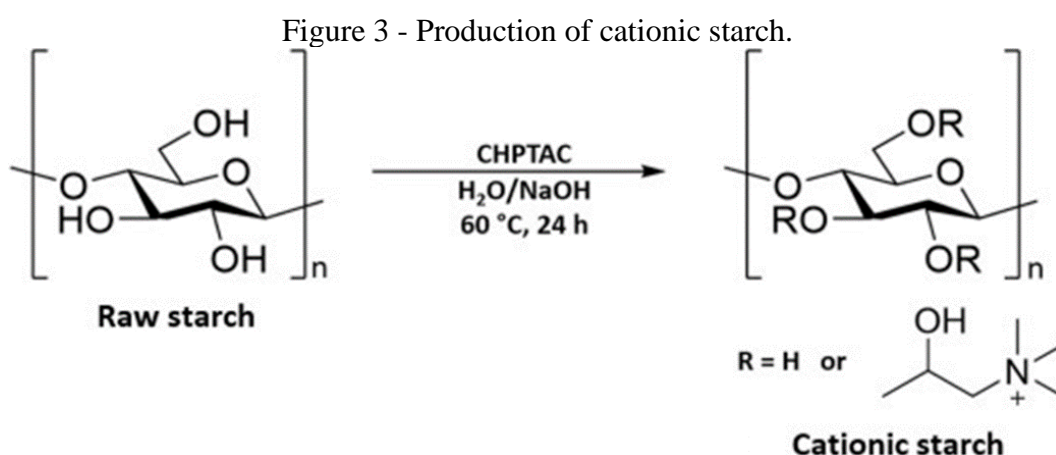
Source: Alcázar-Alay and Meireles (2015).

The film-forming property of starch derives from the bond angulation and the extent of the amylopectin chain. This process is called gelatinization. During gelatinization, the crystalline structure of the starch granules ruptures, which is an irreversible process. The gelatinization process involves granular swelling, crystalline fusion, and molecular solubilization (Wongphan *et al.*, 2022; Qiao *et al.*, 2016; Atwell *et al.*, 1988). Starch is not considered a thermoplastic; however, when added to glycerol or sorbitol, for example, it becomes more thermoplastic at high temperatures and shear.

In addition to their modification, the amylose/amylopectin ratio variation generates different sustainable films molded in an aqueous solution (Mali *et al.*, 2006; Roth and

Mehlretter, 1967). Such films have a moderate gas barrier, small moisture barrier, and low mechanical strength. Therefore, it is necessary to formulate a composite or modify the starch surface (Guo *et al.*, 2022; Hakke *et al.*, 2022; Patil *et al.*, 2021).

Cationic starch is a modified type that forms an electrostatic bond between the positive charge introduced in the starch molecule and the negative charge sites in the matrix. Cationic starch is produced (Figure 3) by treating starch with reagents such as 2-diethyl aminoethyl chloride and 2,3-(epoxypropyl)trimethylammonium chloride (Xie *et al.*, 2005). This modified starch already exhibits great applicability in the paper industry (Wang *et al.*, 2022c; You *et al.*, 2022; Eriksson *et al.*, 2005). Its films presents high hydrophilicity and low tensile strength with high permeability to water vapor (Wilhelm *et al.*, 2003). Therefore, one of the possibilities to improve its applicability is by combining biocomposites between cationic starch with other materials, improving physical, mechanical, and barrier properties (Follain *et al.*, 2022; Todorova, Yavorov and Lasheva, 2022; Wang *et al.*, 2022c).



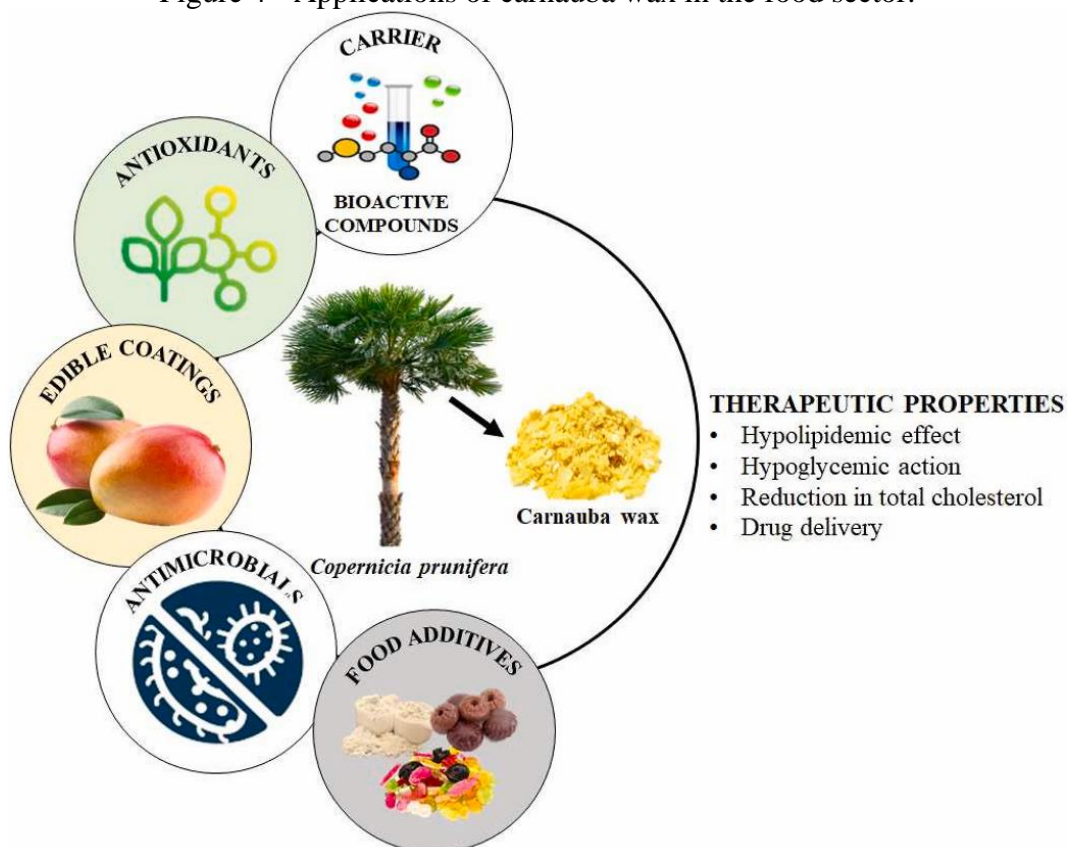
3.4.2 Carnauba wax

Carnauba wax is a complex compound extracted from the leaves of *Copernicia prunifera* (Miller) H. E. Moore (Lorenzi *et al.*, 2010). The wax in the leaves probably evolved toward the dry region to prevent excessive water loss by the plant and protect it against pathogens and predators (Carvalho and Gomes, 2008). Carnauba is composed of a mixture of esters, including aliphatic esters and diesters of cinnamic acid, aliphatic acids, free alcohols, free ω -hydroxycarboxylic acids, aromatic acids, triterpene diols, and hydrocarbons, with the esters corresponding to more than 80% of the chemical composition. With a density of 0.92 to

1.00 g/cm³, carnauba is the hardest wax with the highest melting point among the most common waxes on the market (Wang *et al.*, 2001; Laird, 1997; Vanderburg and Wilder, 1970).

Carnauba wax is used in the chemical, electronic, cosmetic, food, and pharmaceutical industries as a raw material for numerous products. It is classified as a safe compound for human health regarding application in the body and ingestion (FDA, 2018; European Food Safety Authority, 2012). Carnauba has been used as a raw material for various industrial products, such as automotive waxes, food coatings, candy additives, and paper coatings (Figure 4). As a coating, it helps to block the loss of water and maintain the shiny appearance of the fruits, adding value. Antimicrobial additives are often added to increase shelf life (Miranda *et al.*, 2022; Phothisuwan *et al.*, 2021).

Figure 4 - Applications of carnauba wax in the food sector.



Source: Devi *et al.* (2022).

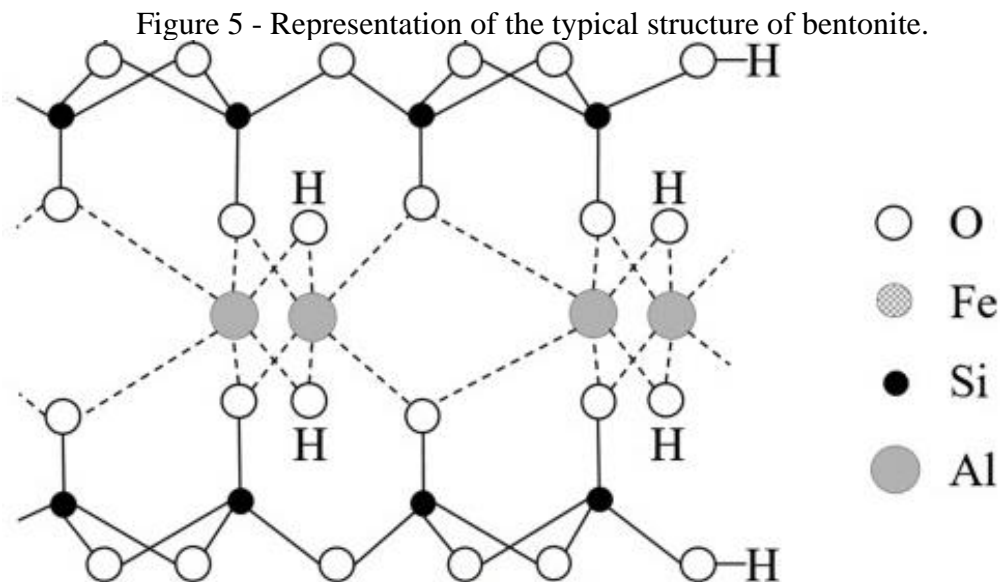
The application of carnauba wax, whether on food, paper, or other materials, aims to increase the hydrophobicity of the material (Oliveira *et al.*, 2022; Matos *et al.*, 2019). In their study, Li *et al.* (2019) developed paper packaging with carnauba wax, carrageenan, chitosan, and montmorillonite in its composition. The authors called this packaging superhydrophobic. The packaging exhibits moisture and gas barrier properties, with a contact angle of 151.4° with

water and an 83.8% reduction in the water vapor transmission rate. It is worth remembering that the surface of carnauba wax is negatively charged, and the interaction of opposite charges is more efficient in obtaining better hydrophobicity (Forsman *et al.*, 2017).

3.4.3 Bentonite

Clays are hydrated silicates of aluminum silicates. They are formed by silicon, aluminum or magnesium, oxygen, and hydroxyl groups associated with cations (Pavlidou and Papaspyrides, 2008; Gul *et al.*, 2016). Their structures are composed of layers stacked on top of each other with a variable distance between layers. The exfoliated clay particles produce nanoclays with a large surface area (Azeez *et al.*, 2013; Choudalakis and Gotsis, 2009).

Clays, such as bentonite (Figure 5), occupy pores in the composite matrix, serving as a blocking layer. The resulting structure increases and even block the gas diffusion paths (Gusev and Lusti, 2001). In addition, bentonite generates positive synergistic effects on the tensile strength and Young's modulus, which are useful for packaging. However, its overuse can result in agglomeration, interfering with the hydrogen bonds between the cellulose chains of paper and decreasing the mechanical properties of packaging (Spence *et al.*, 2011).



Source: Adapted from Wan *et al.* (2017).

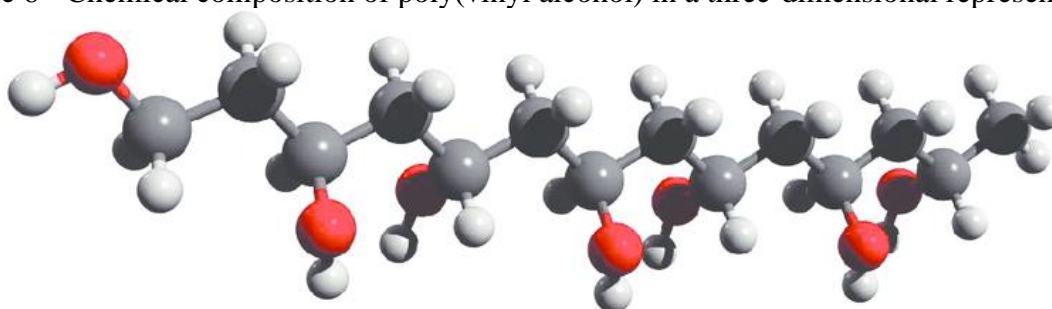
Different natural or synthetic nanoclays, such as montmorillonite (Gao, Wu, and Shi, 2022; Kumar and Udaiyakumar, 2021), kaolinite (Zhao *et al.*, 2022; Qin *et al.*, 2021), and bentonite (Behera, Mohanta, and Thirugnanam, 2022; Qureshi *et al.*, 2021), have been studied

as matrix reinforcements for coatings and films. Composites that have exfoliated nanoclays have received more attention as they exhibit better performances (Kim *et al.*, 2021; Paul and Robeson, 2008). Among different approaches, it was proposed that incorporating nanoclay into the nanocellulosic and starch matrix could improve the mechanical, thermal, and antimicrobial barrier properties (Hong, Wang, and Rhim, 2022; Garusinghe *et al.*, 2018). Such properties are achieved even with small amounts of clay (Majeed *et al.*, 2013). Its efficiency is high when the nanoclays are homogeneously dispersed in the polymeric matrix (Paul and Robeson, 2008).

3.4.4 Poly(vinyl alcohol)

The polymerization of poly(vinyl alcohol) is obtained by hydrolysis from poly(vinyl acetate) and not from vinyl alcohol since this species does not occur in a free state. With a barrier against oil/grease and good permeability to water vapor (Patil *et al.*, 2022; Suhag *et al.*, 2022; Ge, Lansing, and Lewis, 2021; Roy and Rhim, 2021), poly(vinyl alcohol) coatings exhibit a good barrier to oxygen with a low oxygen transmission rate close to 0.4 mL/m²/day (Hay and Lyon, 1967). Its chemical composition is represented in Figure 6.

Figure 6 - Chemical composition of poly(vinyl alcohol) in a three-dimensional representation.



Red structures represent oxygen, gray is carbon, and white is hydrogen.

Source: Nyflött (2014).

As a nontoxic and water-soluble polymer, poly(vinyl alcohol) acts as an emulsifier and adhesive with the capacity to form films. Its use as packaging has increased (Gaaz *et al.*, 2015). The presence of water can reduce the tensile strength of poly(vinyl alcohol), even as water vapor, but increases its elongation and tear resistance (Niinivaara *et al.*, 2021; Asrofi *et al.*, 2019). Despite being considered a synthetic polymer susceptible to biodegradation (Byrne *et al.*, 2021), poly(vinyl alcohol) is disadvantaged as only a specific number of microorganisms act upon the compound; thus its biodegradability is limited (Chiellini *et al.*, 1999) or exhibits a low rate (Mao *et al.*, 2000; Chen *et al.*, 1997).

A factor that affects the widespread use of poly(vinyl alcohol) is its higher cost compared to the daily counterparts of commodities, such as polyethylene and polypropylene. Mixing poly(vinyl alcohol) with other inexpensive renewable polymers, such as starch, could be one solution to improve its biodegradation rate and reduce the total cost (Dessie and Tadesse, 2022; Chen *et al.*, 2021; Ge, Lansing, and Lewis, 2021). Blending can improve the mechanical properties, film-forming ability, and barrier properties of starch films and reduce the cost of poly(vinyl alcohol) (Teodorescu *et al.*, 2018) and other polymers.

4. REVIEWS CONSIDERATIONS

Based on the knowledge acquired from this literature review, it was possible to build the methodology of this thesis, defining objectives and methods to achieve a product that meets the needs of academic communities and populations. How to develop biodegradable packaging based on cationic starch to meet the needs of the industry and people should be understood. Such packages must exhibit high quality and resistance with a reduced diffusion of water vapor and oxygen in films formed in kraftliner paper. These coatings are also expected to show high hydrophobicity and oil resistance.

The need to create ecologically sustainable materials grows daily, and this is the objective of several works. We hope this work can contribute to this demand.

REFERENCES

- AHMAD, S.; UTOMO, D. S.; DADHICH, P. *et al.* Packaging design, fill rate and road freight decarbonisation: A literature review and a future research agenda. **Cleaner Logistics and Supply Chain**, v. 4, p. 100066, 2022.
- ALCÁZAR-ALAY, S. C.; MEIRELES, M. A. Physicochemical properties, modifications and applications of starches from different botanical sources. **Food Science and Technology**, p. 35, n. 2, p. 215-236, 2015.
- AL-GHARRAWI, M. Z.; WANG, J.; BOUSFIELD, D. W. Improving water vapor barrier of cellulose based food packaging using double layer coatings and cellulose nanofibers. **Food Packaging and Shelf Life**, v. 33, p. 100895, 2022.
- ASROFI, M.; DWILAKSANA, D.; ABRAL, H. *et al.* Tensile, Thermal and Moisture Absorption Properties of Polyvinyl Alcohol (PVA) / Bengkuang (*Pachyrhizus erosus*) Starch Blend Films. **Material Science Research India**, v. 16, p. 70-75, 2019.

ATWELL, W. A.; HOOD, L. F.; LINEBACK, D. R. *et al.* The terminology and methodology associated with basic starch phenomena, **Cereal Foods World**, v. 33, p. 306-311, 1988.

AZEEZ, A. A.; RHEE, K. Y.; PARK, S. J. *et al.* Epoxy clay nanocomposites – processing, properties, and applications: a review. **Composites Part B: Engineering**, v. 45, p. 308–320, 2013.

BEHERA, L.; MOHANTA, M.; THIRUGNANAM, A. Intensification of yam-starch based biodegradable bioplastic film with bentonite for food packaging application. **Environmental Technology and Innovation**, v. 25, p. 102180, 2022.

BERGLUND, L.; ZHOU, Q.; KOCHUMALAYIL, J. J. **Oxygen barrier for packaging applications**. Depositante: KTH Holding AB. EP2705099A1. Depósito: 04 mai. 2012. Concessão: 01 jul. 2015.

BIERMANN, C. J. **Handbook of Pulping and Papermaking**. 2nd Edition, 1996.

BUTLER, T. I.; MORRIS, B. A. PE-based multilayer film structures. p. 281-310. In J. R. Wagner, Jr. (Ed.), **Multilayer flexible packaging**, 2016.

BYRNE, D.; BOEIJE, G.; CROFT, I. *et al.* Biodegradability of Polyvinyl Alcohol Based Film Used for Liquid Detergent Capsules: Biologische Abbaubarkeit der für Flüssigwaschmittelkapseln verwendeten Folie auf Polyvinylalkoholbasis. **Tenside Surfactants Detergents**, v. 58, n. 2, p. 88-96, 2021.

CARVALHO, F. P. A.; GOMES, J. M. A. Eco-efficiency in the production of Carnaúba wax in the municipality of Campo Maior, Piauí, 2004. **Revista de Economia e Sociologia Rural**, v. 46, n. 2, p. 421-453, 2008.

CEPI CONTAINERBOARD. European list of corrugated base papers. 5th edition, 22 p., 2017.

CHAIREH, S.; NGASATOOL, P.; KAEWTATIP, K. Novel composite foam made from starch and water hyacinth with beeswax coating for food packaging applications. **International Journal of Biological Macromolecules**, v. 165, Part A, p. 1382-1391, 2020.

CHEN, L.; IMAN, S. H.; STEIN, T. M. *et al.* Starchpolyvinyl alcohol cast film-performance and biodegradation. **Polymer Preprints**, v. 37, p. 461–462, 1997.

CHEN, L.; QIANG, T.; CHEN, X. *et al.* Fabrication and evaluation of biodegradable multi-cross-linked mulch film based on waste gelatin. **Chemical Engineering Journal**, v. 419, p. 129639, 2021.

CHEN, Y.; LI, Y.; QIN, S. *et al.* Antimicrobial, UV blocking, water-resistant and degradable coatings and packaging films based on wheat gluten and lignocellulose for food preservation. **Composites Part B: Engineering**, v. 238, p. 109868, 2022.

CHIELLINI, E.; CORTI, A.; SOLARO, R. Biodegradation of poly (vinyl alcohol) based blown films under different environmental conditions. **Polymer Degradation and Stability**, v. 64, p. 305–312, 1999.

CHOUDALAKIS, G.; GOTSIS, A. D. Permeability of polymer/clay nanocomposites: a review. **European Polymer Journal**, v. 45, p. 967–984, 2009.

DANG, K. M.; YOKSAN, R. Thermoplastic starch blown films with improved mechanical and barrier properties. **International Journal of Biological Macromolecules**, v. 188, p. 290-299, 2021.

DEGLI-INNOCENTI, F.; BARBALE, M.; CHINAGLIA, S. *et al.* Analysis of the microplastic emission potential of a starch-based biodegradable plastic material. **Polymer Degradation and Stability**, v. 199, p. 109934, 2022.

DESSIE, Y.; TADESSE, S. Optimization of polyvinyl alcohol binder on PANI coated pencil graphite electrode in doubled chamber microbial fuel cell for glucose biosensor. **Sensing and Bio-Sensing Research**, v. 36, p. 100484, 2022.

DEVI, L. M.; KALITA, S.; MUKHERJEE, A. *et al.* Carnauba wax-based composite films and coatings: recent advancement in prolonging postharvest shelf-life of fruits and vegetables. **Trends in Food Science and Technology**, v. 129, p. 296–305, 2022.

DILKES-HOFFMAN, L. S.; PRATT, S.; LANT, P. A. *et al.* 19 - The Role of Biodegradable Plastic in Solving Plastic Solid Waste Accumulation. In: AL-SALEM, S. M. *Plastics to Energy*. **William Andrew Publishing**, p. 469-505, 2019.

EMBLEM, A.; EMBLEM, H. **Packaging Technology: Fundamentals, Materials and Processes**. Cambridge: Woodhead Publishing Ltd., 2012.

EMOYAN, O. O.; ADJERESE, W.; TESI, G. O. Concentrations, Origin, and Associated Exposure Risk of Polycyclic Aromatic Hydrocarbons in Soil Depths from Selected Petroleum Tank Farms in Western Delta, Nigeria. **Polycyclic Aromatic Compounds**, 2022.

ERIKSSON, M.; PETTERSSON, G.; WÅGBERG, L. Application of polymeric multilayers of starch onto wood fibres to enhance strength properties of paper. **Nordic Pulp and Paper Research Journal**, v. 20, p. 270–276, 2005.

EUROPEAN FOOD SAFETY AUTHORITY. Scientific Opinion on the re-evaluation of carnauba wax (E 903) as a food additive. **EFSA Journal**, v. 10, 2012.

FARRIS, S. Engineering properties of packaging films. In: M. W. Siddiqui, M. S. Rahman, and A. A. Wani (Eds.). *Innovative packaging of fruits and vegetables: Strategies for safety and quality maintenance* (p. 211–226). Waretown, New Jersey: **Apple Academic Press**, 2018.

FDA. **Food and Drug Administration**. Chapter 9 - federal food, drug, and cosmetic act, Subchapter II - Definitions, Sec. 321 – Definitions; generally, Code of Federal Regulations, Title 21, Sec. 321, 2018.

FOLLAIN, N.; REN, J.; POLLET, E. *et al.* Study of the water sorption and barrier performances of potato starch nano-biocomposites based on halloysite nanotubes. **Carbohydrate Polymers**, v. 277, p. 118805, 2022.

FORSMAN, N.; LOZHECHNIKOVA, A.; KHAKALO, A. *et al.* Layer-by-layer assembled hydrophobic coatings for cellulose nanofibril films and textiles, made of polylysine and natural wax particles. **Carbohydrate Polymers**, v. 173, p. 392-402, 2017.

GAAZ, T. S.; SULONG, A. B.; AKHTAR, M. N. *et al.* Properties and Applications of Polyvinyl Alcohol, Halloysite Nanotubes and Their Nanocomposites. **Molecules**, v. 20, n. 12, p. 22833-22847, 2015.

GAO, Q.; WU, X.; SHI, F. Novel superhydrophobic NIR reflective coatings based on Montmorillonite/SiO₂ composites for Energy-saving building. **Construction and Building Materials**, v. 326, p. 126998, 2022.

GARTNER, H.; LI, Y.; ALMENAR, E. Improved wettability and adhesion of polylactic acid/chitosan coating for bio-based multilayer film development. **Applied Surface Science**, v. 332, p. 488-493, 2015.

GARUSINGHE, U. M.; VARANASI, S.; RAGHUWANSHI, V. S. *et al.* Nanocellulose-montmorillonite composites of low water vapour permeability. **Colloids and Surfaces A: Physicochemical and Engineering Aspects**, 540:233–241, 2018.

GE, C.; LANSING, B.; LEWIS, C. L. Thermoplastic starch and poly(vinyl alcohol) blends centered barrier film for food packaging applications. **Food Packaging and Shelf Life**, v. 27, p. 100610, 2021.

GEORGIOPOULOU, I.; PAPPA, G. D.; VOUYIOUKA, S. N. *et al.* Recycling of post-consumer multilayer Tetra Pak® packaging with the Selective Dissolution-Precipitation process. **Resources, Conservation and Recycling**, v. 165, p. 105268, 2021.

GHINEA, C.; PETRARU, M.; SIMION, I. M. *et al.* Life Cycle assessment of waste management and recycled paper systems. **Environmental Engineering and Management Journal**, v. 13, n. 8 p. 2073-2085, 2014.

GIUSEPPE, F.; COFFIGNIEZ, F.; AOUF, C. *et al.* Activated gallic acid as radical and oxygen scavenger in biodegradable packaging film. **Food Packaging and Shelf Life**, v. 31, p. 100811, 2022.

GUL, S.; KAUSAR, A.; MUHAMMAD, B. *et al.* Research progress on properties and applications of Polymer/Clay nanocomposite. **Polymer-Plastics Technology and Engineering**, v. 55, p. 684-703, 2016.

GULARTE, M. S.; QUADRADO, R. F. N.; PEDRA, N. S. *et al.* Preparation, characterization and antitumor activity of a cationic starch-derivative membrane embedded with a β -cyclodextrin/curcumin inclusion complex. **International Journal of Biological Macromolecules**, v. 148, p. 140-152, 2020.

GUO, X.; YAO, S.; WANG, Q. *et al.* The impact of packaging recyclable ability on environment: Case and scenario analysis of polypropylene express boxes and corrugated cartons. **Science of The Total Environment**, v. 822, p. 153650, 2022.

GUO, Z.; GOU, Q.; YANG, L. *et al.* Dielectric barrier discharge plasma: A green method to change structure of potato starch and improve physicochemical properties of potato starch films. **Food Chemistry**, v. 370, p. 130992, 2022.

GUSEV, A. A.; LUSTI, H. R. Rational design of nanocomposites for barrier applications. **Advanced Materials**, v. 13, p. 1641–1643, 2001.

GUZMAN-PUYOL, S.; HIERREZUELO, J.; BENÍTEZ, J. J. *et al.* Transparent, UV-blocking, and high barrier cellulose-based bioplastics with naringin as active food packaging materials. **International Journal of Biological Macromolecules**, v. 209, Part B, p. 1985-1994, 2022.

HAI, L. V.; MUTHOKA, R. M.; PANICKER, P. S. *et al.* All-biobased transparent-wood: A new approach and its environmental-friendly packaging application. **Carbohydrate Polymers**, v. 264, p. 118012, 2021.

HAKKE, V. S.; LANDGE, V. K.; SONAWANE, S. H. *et al.* The physical, mechanical, thermal and barrier properties of starch nanoparticle (SNP)/polyurethane (PU) nanocomposite films synthesised by an ultrasound-assisted process. **Ultrasonics Sonochemistry**, v. 88, p. 106069, 2022.

HANSSON, S.; BADENLID, R.; BACKFOLK, K. **Paperboard and laminate comprising a bio-barrier**. Depositante: Sstora Enso Oyj. O2021/005451. Depósito: 9 jul. 2019. Concessão: 14 jan. 2021.

HASSAN, A.; BORSINGER, G. **Aqueous wax emulsions and their coating applications**. Depositante: HRD Corp. WO2004083310A1. Depósito: 17 mar. 2003. Concessão: 11 nov. 2004.

HAY, J. M.; LYON, D. Vinyl Alcohol: a Stable Gas Phase Species? **Nature**, v. 216, p. 790-791, 1967.

HEISKANEN, I.; BACKFOLK, K.; KANKKUNEN, J. *et al.* **Method of producing paper, cardboard or coated film and paper, cardboard or coated film**. Depositante: Stora Enso Oyj. BR112020020682. Depósito: 12 abr. 2019. Concessão: 10 jan. 2021.

HONG, S.; WANG, L.; RHIM, J. Preparation and characterization of nanoclays-incorporated polyethylene/thermoplastic starch composite films with antimicrobial activity. **Food Packaging and Shelf Life**, v. 31, p. 100784, 2022.

KIM, J.; HLAING, S. P.; LEE, J. *et al.* Exfoliated bentonite/alginate nanocomposite hydrogel enhances intestinal delivery of probiotics by resistance to gastric pH and on-demand disintegration. **Carbohydrate Polymers**, v. 272, p. 118462, 2021.

KREPLIN, F.; PUTZ, H.; SCHABEL, S. Multiple recycling of paperboard: Paperboard characteristics and maximum number of recycling cycles-Part I: Multiple recycling of corrugated base paper. **TAPPI Journal**, v. 18, n. 11, p. 631-638, 2019.

KUMAR, D. K. M.; UDAIYAKUMAR, K. C. Investigation on mechanical properties of sugarcane bagasse ash reinforced with incorporation of HDPE - montmorillonite composite materials. **Materials Today: Proceedings**, v. 45, Part 7, p. 6123-6127, 2021.

LAIRD, T. **Ullmann's Encyclopedia of Industrial Chemistry**. 5th Edition VCH, v. 1, n. 5, p. 391-392. Weinheim: Organic Process Research and Development, 1997.

LI, H.; HE, Y.; YANG, J. *et al.* Fabrication of food-safe superhydrophobic cellulose paper with improved moisture and air barrier properties. **Carbohydrate Polymers**, v. 211, p. 22-30, 2019.

LIAO, J.; CHEN, Q. Biodegradable plastics in the air and soil environment: Low degradation rate and high microplastics formation. **Journal of Hazardous Materials**, v. 418, p. 126329, 2021.

LORENZI, H.; NOBLICK, L.; KAHN, F. *et al.* Arecaceae (Palmeiras). Flora Brasileira. **Instituto Plantarum**: Nova Odessa, p. 368. 2010.

LUDEÑA, L.; VÁZQUEZ, A.; ALVAREZ, V. Effect of lignocellulosic filler type and content on the behavior of polycaprolactone based eco-composites for packaging applications. **Carbohydrate Polymers**, v. 87, p. 411–421, 2012.

MALI, S.; GROSSMANN, M. V. E.; GARCIA, M. A. *et al.* Effects of controlled storage on thermal, mechanical and barrier properties of plasticized films from different starch sources. **Journal of Food Engineering**, 75, p. 453–460, 2006.

MALMBORG, K.; HEIJNESSON-HULTÉN, A. M.; SANDSTRÖM, J. **Cellulosic barrier composition comprising anionic polymer**. Depositante: Akzo Nobel Chemicals International BV. WO2011147823A1. Depósito: 27 mai. 2010. Concessão: 01 dez. 2011.

MAO, L. J.; IMAM, S.; GORDON, S. *et al.* Extruded cornstarch–glycerol–polyvinyl alcohol blends: Mechanical properties, morphology and biodegradability. **Journal of Polymers and the Environment**, v. 8, n. 4, p. 205–211, 2000.

MARANGONI JÚNIOR, L.; OLIVEIRA, L. M.; BÓCOLI, P. F. J. *et al.* Morphological, thermal and mechanical properties of polyamide and ethylene vinylalcohol multilayer flexible packaging after high-pressure processing. **Journal of Food Engineering**, v. 276, 109913, 2020.

MARTENS, H.; GOLDMANN, D. Recyclingtechnik. Fachbuch für Lehre und Praxis, second ed. **Springer Fachmedien Wiesbaden**, Germany, 2016.

MATOS, L. C.; ROMPA, V. D.; DAMÁSIO, R. A. P. *et al.* Incorporation of nanomaterials and emulsion of waxes in the development of multilayer papers. **Scientia Forestalis**, v. 47, n. 122, p. 177-191, 2019.

MIRANDA, M.; RIBEIRO, M. M. M.; SPRICIGO, P. C. *et al.* Carnauba wax nanoemulsion applied as an edible coating on fresh tomato for postharvest quality evaluation. **Heliyon**, v. 8, n. 7, p. 109803, 2022.

MIRJANI, M.; SOLEIMANI, M.; SALARI, V. Toxicity assessment of total petroleum hydrocarbons in aquatic environments using the bioluminescent bacterium *Aliivibrio fischeri*. **Ecotoxicology and Environmental Safety**, v. 207, p. 111554, 2021.

NAIR, S.S.; ZHU, J.Y.; DENG, Y. *et al.* High performance green barriers based on nanocellulose. **Sustainable Chemical Processes**, v. 2, n. 23, 2014.

NARANCIC, T.; CERRONE, F.; BEAGAN, N. *et al.* Recent advances in bioplastics: Application and biodegradation. **Polymers**, v. 12, n. 4, p. 1-38, 2020.

NIINIVAARA, E.; DESMAISONS, J.; DUFRESNE, A. *et al.* Film thickness limits of a buckling-based method to determine mechanical properties of polymer coatings. **Journal of Colloid and Interface Science**, v. 582, Part A, p. 227-235, 2021.

NODA, T.; FUKUNAGA, M. **Barrier material**. Depositante: Nippon Paper Industries Co. Ltda, WO2019/069963. Depósito: 3 out. 2018. Concessão: 29 jul. 2020.

NYFLÖTT, Å. **Structural Studies and Modelling of Oxygen Transport in Barrier Materials for Food Packaging**. 2014. Dissertação de Mestrado - Karlstad University Studies - Karlstad, p.64, 2014.

OLIVEIRA, M.L.C., MIRMEHDI, S., SCATOLINO, M.V. *et al.* Effect of overlapping cellulose nanofibrils and nanoclay layers on mechanical and barrier properties of spray-coated papers. **Cellulose**, v. 29, p. 1097–1113, 2022.

OUDJEDI, K.; MANSO, S.; NERIN, C. *et al.* New active antioxidant multilayer food packaging films containing Algerian Sage and Bay leaves extracts and their application for oxidative stability of fried potatoes. **Food Control**, v. 98, p. 216-226, 2019.

PALAI, B.; MOHANTY, S.; NAYAK, S. Synergistic effect of polylactic acid(PLA) and Poly(butylene succinate-co-adipate) (PBSA) based sustainable, reactive, super toughened eco-composite blown films for flexible packaging applications. **Polymer Testing**, v. 83, 106130, 2020.

PATIL, S.; BHARIMALLA, A. K.; MAHAPATRA, A. *et al.* Effect of polymer blending on mechanical and barrier properties of starch-polyvinyl alcohol based biodegradable composite films. **Food Bioscience**, v. 44, Part A, p. 101352, 2021.

PATIL, S.; BHARIMALLA, A. K.; NADANATHANGAM, V. *et al.* Nanocellulose reinforced corn starch-based biocomposite films: Composite optimization, characterization and storage studies. **Food Packaging and Shelf Life**, v. 33, p. 100860, 2022.

PAUL, D. R.; ROBESON, L. M. Polymer nanotechnology: nanocomposites. **Polymer**, v. 49, p. 3187–3204, 2008.

PAULAPURO, H. Papermaking science and technology: Paper and Board Grades, **TAPPI press**, v. 18. First Edition, 2000.

PAVLIDOU, S.; PAPANAYIDES, C. D. A review on polymer-layered silicate nanocomposites. **Progress in Polymer Science**, v. 33, p. 1119–1198, 2008.

- PHOTHISUWAN, S.; KOOMHIN, P.; MATAN, N. *et al.* Quality maintenance of salacca fruit with a carnauba wax coating containing orange oil and detection of sensory perception improvement with electroencephalography to appraise brain responses. **LWT**, v. 147, p. 111628, 2021.
- PUTZ, H.; SCHABEL, S. The Myth of Limited Fibre Life Cycles On the potential of paper fibre. **Wochenblatt für Papierfabrikation**, v. 6, p. 350-357, 2018.
- QIAO, D.; YU, L.; ZOU, W. *et al.* Insights into the hierarchical structure and digestion rate of alkali modulated starches with different amylose contents. **Carbohydrate Polymers**, v. 144, p. 271-281, 2016.
- QIN, L.; ZHANG, Y.; ZHANG, Y. *et al.* Efficient preparation of coal-series kaolinite intercalation compounds via a catalytic method and their reinforcement for styrene butadiene rubber composite. **Applied Clay Science**, v. 213, p. 106237, 2021.
- QURESHI, D.; BEHERA, K. P. MOHANTY, D. *et al.* Synthesis of novel poly (vinyl alcohol)/tamarind gum/bentonite-based composite films for drug delivery applications. **Colloids and Surfaces A: Physicochemical and Engineering Aspects**, v. 613, p. 126043, 2021.
- RAY, S. S.; BOUSMINA, M. Biodegradable polymers and their layered silicate nanocomposites: In greening the 21st century materials world. **Progress in Materials Science**, v. 50, p. 962–1079, 2005.
- RHIM, J. W.; PARK, H. M.; HA, C. S. Bio-nanocomposites for food packaging applications. **Progress in Polymer Science**, v. 38, p. 1629–1652, 2013.
- ROBERT, C.; CHARTREL, J. F. U.S. Patent No. 10,201,952. Washington, DC: U.S. **Patent and Trademark Office**, 2019.
- ROTH, W. B.; MEHLTRETTER, C. L. Some properties of hydroxypropylated amylo maize starch films. **Food Technology**, v. 21, p. 72–74, 1967.
- ROY, S.; RHIM, J. Antioxidant and antimicrobial poly(vinyl alcohol)-based films incorporated with grapefruit seed extract and curcumin. **Journal of Environmental Chemical Engineering**, v. 9, n. 1, p. 104694, 2021.
- SATTAR, S.; JEHAN, S.; SIDDIQUI, S. Potentially toxic metals in the petroleum waste contaminated soils lead to human and ecological risks in Potwar and Kohat Plateau, Pakistan: Application of multistatistical approaches. **Environmental Technology and Innovation**, v. 22, p. 101395, 2021.
- SAXENA, P.; BISSACCO, G.; MEINER, K. *Æ. et al.* Mold design and fabrication for production of thermoformed paper-based packaging products. **Journal of Manufacturing Processes**, v. 58, p. 311-321, 2020.
- SHANKAR, S.; RHIM, J. Effects of poly(butylene adipate-co-terephthalate) coating on the water resistant, mechanical, and antibacterial properties of Kraft paper. **Progress in Organic Coatings**, v. 123, p. 153-159, 2018.

SPENCE, K. L.; VENDITTI, R. A.; ROJAS, O. J. *et al.* Water vapor barrier properties of coated and filled microfibrillated cellulose composite films. **BioResources**, v. 6, p. 4370–4388, 2011.

SUHAG, A.; BISWAS, K.; SINGH, S. *et al.* Crosslinking effect on polyvinyl alcohol resin for barrier properties of barrier biaxial orientation films. **Progress in Organic Coatings**, v. 163, p. 106662, 2022.

TAYLOR, S. L. **Innovations in food packaging**. 2nd Edition. Plano: PepsiCo Corporate RandD/PepsiCo Advanced Research, 2014.

TEODORESCU, M.; BERCEA, M.; MORARIU, S. Biomaterials of poly(vinyl alcohol) and natural polymers. **Polymer Reviews**, v. 58, p. 247–287, 2018.

THOMTON, D.; DEGROOTE, B.; KRISTENSEN, D. *et al.* VPPAG Bar Code Implementation Technical Guideline. **Technical guideline for the identification and marking of vaccines purchased through WHO, UNICEF, Gavi, The Vaccine Alliance**, 11 April 2015. Disponível em: https://www.dcvmn.org/IMG/pdf/vppag_bar_code_implementation_guideline_-_release_v1_0_-_20150411_-_for_release.pdf. Acesso em: 29 jun, 2022.

TODOROVA, D.; YAVOROV, N.; LASHEVA, V. Improvement of barrier properties for packaging applications. **Sustainable Chemistry and Pharmacy**, v. 27, p. 100685, 2022.

TORRES, F.I.; DA SILVA, J.C.; VIEIRA, O. *et al.* Eukalinertm: the first 100% hardwood kraftliner in the world. In: 53RD ABTCP INTERNATIONAL PULP AND PAPER CONGRESS AND EXHIBITION AND 9TH. 2020. São Paulo, **Anais [...]** São Paulo: ABCTP, 2020.

VAEZI, K.; ASADPOUR, G.; SHARIFI, S. H. Effect of coating with novel bio nanocomposites of cationic starch/cellulose nanocrystals on the fundamental properties of the packaging paper. **Polymer Testing**, v. 80, p. 106080, 2019.

VANDENBURG, L. E.; WILDER, E. A. The structural constituents of carnauba wax. **Journal of the American Oil Chemists Society**, v. 47, n. 12, p. 514-518, 1970.

VINCI, G.; D'ASCENZO, F.; ESPOSITO, A. *et al.* Glass beverages packaging: innovation by sustainable production in trends in beverage packaging. **Academic Press**, v. 16, p. 105–133, 2019.

WAN, D.; WANG, G.; LI, W. *et al.* Investigation into the morphology and structure of magnetic bentonite nanocomposites with their catalytic activity. **Applied Surface Science**, v. 413, p. 398 – 407, 2017.

WANG, L.; ANDO, S.; ISHIDA, Y. *et al.* Quantitative and discriminative analysis of carnauba waxes by reactive pyrolysis-GC in the presence of organic alkali using a vertical microfurnace pyrolyzer. **Journal of Analytical and Applied Pyrolysis**, v. 58-59, p. 525-537, 2001.

- WANG, W.; THEMELIS, N. J.; SUN, K. *et al.* Current influence of China's ban on plastic waste imports. **Waste Disposal and Sustainable Energy**, v. 1, p. 67-78, 2019.
- WANG, L.; CHEN, C.; WANG, J. *et al.* Cellulose nanofibrils versus cellulose nanocrystals: Comparison of performance in flexible multilayer films for packaging applications. **Food Packaging and Shelf Life**, p. 100464, 2020.
- WANG, F.; WANG, L.; ZHANG, X. *et al.* Enhancement of oil resistance of cellulose packaging paper for food application by coating with materials derived from natural polymers. **Journal of Food Engineering**, v. 332, p. 111039, 2022a.
- WANG, F.; WANG, L.; ZHANG, X. *et al.* Study on the barrier properties and antibacterial properties of cellulose-based multilayer coated paperboard used for fast food packaging. **Food Bioscience**, v. 46, p. 101398, 2022b.
- WANG, X.; HOU, X.; ZOU, P. *et al.* Cationic starch modified bentonite-alginate nanocomposites for highly controlled diffusion release of pesticides. **International Journal of Biological Macromolecules**, v. 213, p. 123-133, 2022c.
- WILHELM, H. M.; SIERAKOWSKI, M. R.; SOUZA, G. P. *et al.* Starch films reinforced with mineral clay. **Carbohydrate Polymers**, v. 52, p. 101-110, 2003.
- WONGPHAN, P.; PANRONG, T.; HARNKARNSUJARIT, N. Effect of different modified starches on physical, morphological, thermomechanical, barrier and biodegradation properties of cassava starch and polybutylene adipate terephthalate blend film. **Food Packaging and Shelf Life**, v. 32, p. 100844, 2022.
- WRONA, M.; BLASCO, S.; BECERIL, R. *et al.* Antioxidant and antimicrobial markers by UPLC®-ESI-Q-TOF-MSE of a new multilayer active packaging based on *Arctostaphylos uva-ursi*. **Talanta**, v. 1961, p. 498-509, 2019.
- XIE, S. X.; LIU, Q.; CUI, S. W. *et al.* Food Carbohydrates: Chemistry, Physical Properties, and Applications. **Taylor and Francis**, pp. 357-406, 2005.
- YE, C.; YU, F.; HUANG, Y. *et al.* Hydrochar as an environment-friendly additive to improve the performance of biodegradable plastics. **Science of The Total Environment**, v. 832, p. 155124, 2022.
- YOOK, S.; PARK, H.; PARK, H. *et al.* Barrier coatings with various types of cellulose nanofibrils and their barrier properties. **Cellulose**, v. 27, p. 4509-4523, 2020.
- YOU, Y.; YANG, L.; SUN, X. *et al.* Synthesized cationic starch grafted tannin as a novel flocculant for efficient microalgae harvesting. **Journal of Cleaner Production**, v. 344, p. 131042, 2022.
- ZHAO, Y.; CAO, Z.; ZUH, A. A. *et al.* Synthesis of bismuth oxyiodide/kaolinite composite with enhanced photocatalytic activity. **Journal of Physics and Chemistry of Solids**, v. 161, p. 110424, 2022.

ZHU, Z.; LIU, W.; YE, S. *et al.* Packaging design for the circular economy: A systematic review. **Sustainable Production and Consumption**, v. 32, p. 817-832, 2022.

SECOND PART

1. RESEARCH PROJECT

1.1 Project description

Petroleum-based packaging materials have traditionally been used due to their cost-effectiveness in terms of strength, durability, and workability, representing 19.5% of packaging waste by volume in the European Union in 2020 (Eurostat, 2022). However, the lack of biodegradability of such traditional materials leads to many environmental risks (Jakubowska *et al.*, 2023; Rojas-Lema *et al.*, 2023; Emoyan, Adjerese, and Tesi, 2022; Hong, Wang, and Rhim, 2022; Kan and Miller, 2022; Patil *et al.*, 2022; Mirjani, Soleimani, and Salari, 2021; Sattar, Jehan, and Siddiqui, 2021; Bassi *et al.*, 2020; Reichert *et al.*, 2020; Dilkes-Hoffman *et al.*, 2019). Achieving sustainable packaging through the coating technique is therefore the goal of many research studies, especially those related to paper packaging (Farris, 2018; Dilkes-Hoffman *et al.*, 2019; Muthus, 2016; Farris, 2018).

Paper is found in different forms on the market, with specific characteristics. Kraftliner stands out with high-performance printable kraft paper with flexibility, durability, extensibility, and with tensile resistance. It is highly hygroscopic and can absorb water vapor from the environment and from the product (Torres *et al.*, 2020; Paulapuro, 2000; Biermann, 1996). To minimize this problem, layer-by-layer coating techniques can be used to reduce moisture absorption and improve the paper's barrier properties (Chen *et al.*, 2022; Giuseppe *et al.*, 2022; Shankar and Rhim, 2022; Chen *et al.*, 2021; Yook *et al.*, 2020; Vaezi, Asadpour, and Sharifi, 2019). Natural and potential biodegradable materials are preferred for making such coatings in order to reduce the pressure on the environment (Behera, Mohanta, and Thirugnanam, 2022; Hong, Wang, and Rhim, 2022; Oliveira *et al.*, 2022; Wang *et al.*, 2022; Dang and Yoksan, 2021; Vinci *et al.*, 2019).

Starches, for instance, are not only abundant and biodegradable, but they are also safe for food packaging. In addition, starches are already used as a paper component in the pulp and paper industry (Podshivalov *et al.*, 2017). They have recognized oil barriers with good film formation, also serving as a physical block on the surface's paper. However, its hygroscopic characteristics reduce its application, requiring the incorporation of other biopolymers and materials such as blends or composites (Follain *et al.*, 2022; Todorova, Yavorov and Lasheva, 2022; Wang *et al.*, 2022).

More efficient barrier properties can be achieved by combining starch with carnauba wax, bentonite, and poly(vinyl alcohol) polymer for an amphiphilic component (Behera, Mohanta, and Thirugnanam, 2022; Hong, Wang, and Rhim, 2022; Oliveira *et al.*, 2022; Dang and Yoksan, 2021). Some works already make such combinations with the purpose of barrier, however, without the application in kraft paper (Ge, Lansing, and Lewis, 2021; Patil *et al.*, 2021; Roy and Rhim, 2021). There are still some works with this coating composition for paper, however, the starch in its cationic form at high viscosity and low solid content combined with such materials is not explored. This thesis, therefore, aimed to evaluate cationic starch-based coatings on kraftliner papers to produce biodegradable multilayer papers with barrier properties at high quality in order to extend shelf life by serving as a physical and chemical blocking between the product and the environment. In addition, the data obtained by this thesis can serve as a basis for other theoretical works regarding sustainable packaging based on cationic starch.

1.2 Research findings

This thesis presents three articles. The first associating cationic starch-glycerol (4,000 cP) and carnauba wax-polysorbate 80 as formulations in proportions 1:0, 3:1, 1:1, 1:3, 0:1 (m:m) applied in two layers of the same grammage ($\sim 7.5 \pm 0.5$ g/m² in total) on kraftliner paper. The first layer corrects the porosity of the paper surface, while the second layer forms the film that serves as a block, possibly having barrier properties. In the second article, the addition of 5%, 7%, and 10% (m/m) of bentonite to the cationic starch-glycerol matrix was explored, also applying it in two layers of the same grammage. Finally, the third article studies coatings composed of cationic starch-glycerol and poly(vinyl alcohol) as formulations in proportions 1:0, 3:1, 1:1, 1:3, 0:1 (m:m) also applied in two layers of the same grammage (15.0 ± 0.5 g/m² in total) on kraftliner paper.

In all three papers, the suspensions were applied with an auto-bar coating machine, evenly spread and avoiding film discontinuity. Between the layers and at the end of the coating process, the multilayer papers were dried at 103 ± 2 °C for 5 min to completely remove the water from the suspension. Coated papers were further compared to uncoated kraftliner paper and twice wet and dry kraftliner paper to assess the impact of water on packaging production. The packages were characterized in terms of chemical, physical, morphological, and mechanical properties, as well as a barrier to water, water vapor, oil/grease, and oxygen. For all suspension formulations, the biodegradation potential and food safety of the materials were considered.

The first paper (third part) reports the application of carnauba wax in a cationic starch-glycerol matrix as coating on kraftliner paper. Carnauba wax has already been used to coat fruits, vegetables, and objects, like cars, to increase their hydrophobicity (Cheng *et al.*, 2023; Devi *et al.*, 2022; Miranda *et al.*, 2022; Trinh, Smith, and Mekonnen, 2022; Todorova, Yavorov, and Lasheva, 2022; Vaezi, Asadpour, and Sharifi, 2019; Despond *et al.*, 2005; Larotonda *et al.*, 2005). However, studies on using wax as paper coating are limited. Still, the applications found in the literature as coating do not associate carnauba wax with cationic starch-glycerol applied on high quality kraftliner paper (Cheng *et al.*, 2023; Devi *et al.*, 2022; Liu *et al.*, 2022; Oliveira Filho *et al.*, 2022; Diyana *et al.*, 2021; Oliveira Filho *et al.*, 2020; Chiumarelli and Hubinger, 2014; 2012; Rodrigues *et al.*, 2014; Muscat *et al.*, 2013).

Through the first paper, we concluded that more than 25 wt.% of cationic starch-glycerol in the starch/wax composites suspension increased the melting temperature of the wax promoting a layer over the paper rather than completely penetrating them, as found for isolated wax coating application. When compared to 100% cationic starch coating, carnauba wax incorporated into the starch at a proportion of 3:1 increased the water contact angle by 22%, improving the coating hydrophobicity. On the other hand, wax incorporation in the suspension decreased the dispersion and polar phases of surface free energy of the coated paper by 28%, impairing ink penetration into the packaging, thus preventing the paper printability. In addition, when compared with carnauba wax coating, increasing starch at a proportion of 75 wt.% in the coating composition decreased the composite wettability by 82% and increased its oil resistance from kit oil n. 6 to n. 9. The starch/wax interaction produced 70% less water absorption through the Cobb test than the individual starch polymer. However, they were not inferior to those found on the control kraftliner paper.

The second paper (fourth part) addresses the addition of bentonite clay into a cationic starch-glycerol matrix as a kraftliner paper coating. Bentonite does not form a film itself. It is applied to the matrix as a reinforcing additive to improve other properties when in its exfoliated form. Bentonite is already used in papers as a reinforcement but its use in a high viscosity cationic starch-glycerol coating formulations differs from other works (Behera, Mohanta, and Thirugnanam, 2022; Oliveira *et al.*, 2022; Ahmed *et al.*, 2021; Sarkar *et al.*, 2021; Shanmathy, Mohanta, and Thirugnanam, 2021; Zamrud, Ng, and Salleh, 2021; Lendvai, Sajó, and Karger-Kocsis, 2019; Monteiro *et al.*, 2018; Rihayat *et al.*, 2018).

Throughout the second paper, we concluded that adding 5 and 7% (m/m) of bentonite to a cationic starch-glycerol suspension increased the water contact angle by 18%, implying increasing their hydrophobicity. Furthermore, the papers coated with cationic starch-glycerol +

bentonite showed a decrease in the tensile index when compared to the control uncoated kraftliner paper. The water present in the suspensions is the main cause of such a decrease in the tensile index, both in the machine direction and in the cross direction. The hydroxyl's water replaced the intermolecular interactions between the hydroxyls of the fibers, causing movements between the cells, and facilitating the paper rupture at a lower load.

Adding 10 wt.% bentonite to the starch matrix in the coating suspensions generated a 66% decrease in water absorption by the Cobb test of coated papers when compared to 100% cationic starch coating, proving synergism between bentonite and starch. Furthermore, following the same comparison, the addition of 7 wt.% bentonite increased the oil barrier as the kit oil was increased from n. 10 to n. 12, the maximum oil barrier level.

The third and last paper (fifth part) explores the blending of cationic starch-glycerol with poly(vinyl alcohol) formulations for kraftliner paper coating. Both polymers have the ability to form thin films with barrier properties. Each polymer with a different function. While starch has better thermal stability with a temperature of degradation close to 310 °C, poly(vinyl alcohol) initiates its thermal degradation at 230 °C. In contrast, poly(vinyl alcohol) produces an oxygen barrier, differently from starch.

In the third paper, a greater use of starch and poly(vinyl alcohol) as a coating for kraft paper is noticeable when compared to the previous papers. The literature already portrays the use of both polymers as blends for oxygen barrier and decrease of water vapor permeance (Garavand *et al.*, 2022; Kochkina, Butikova, and Lukin, 2022; Khazael *et al.*, 2021; Kumar *et al.*, 2021; Lee *et al.*, 2021; Liu *et al.*, 2021; Patil *et al.*, 2021; Qin *et al.*, 2021; Wu *et al.*, 2021; Yao *et al.*, 2021; Gómez-Alpada *et al.*, 2020; Mittal, Garg, and Bajpai, 2020; Christophliemk *et al.*, 2017). However, the use of starch in its cationic form with high viscosity at low solids content for coating formulations is not well explored. The incorporation of poly(vinyl alcohol) starch as a coating on kraftliner paper decreased the contact angle with water by 12% and increased wettability by 33% when compared to paper coated purely with poly(vinyl alcohol), indicating more hydrophilicity. However, adding up to 75 wt.% of cationic starch-glycerol to poly(vinyl alcohol) suspensions effectively maintains the oxygen barrier of coated paper lower than 10 cc/(mm².day), conditions that state a good barrier package. In addition, many authors use mild conditions in the characterization of water vapor permeance and also in water absorption by the Cobb test.

When compared to literature, water vapor permeability differs in methodology. While most authors use mild conditions to measure water vapor transmission rate (25 °C and 50% of relative humidity) (Clegg *et al.*, 2019; Mueller *et al.*, 2011; Ning *et al.*, 2009; Park *et al.*, 2002),

the three papers in this thesis report a more drastic condition, using 38 °C and 90% relative humidity, simulating conditions that may occur during the transport and maintenance of food and products. Still, low water vapor transmission rate values around 580 g/m².day were observed for suspension-coated kraftliner papers containing 25 wt.% and 75 wt.% cationic starch and poly(vinyl alcohol), respectively. In this work, we also explored more severe conditions for the water absorption test, which can explain high Cobb values. Many authors use 60 s for water absorption to occur, different from the 120 s reported in the three papers (Vaysi and Vaghari; 2021).

Each kind of packaging requires different barrier conditions. Some focus on low values of Cobb, oxygen permeability, water vapor transmission, and wettability as low as 0, and some needs higher achievements such as water contact angle higher than 150°. These conditions direct the use of the package (Wang *et al.*, 2018). The high hydrophilicity observed for all packaging tested in this thesis impaired their use in humid environments and with polar liquids, thus being more suitable for dried products.

1.3 Thesis context

The manufacturing process for kraftliner paper coatings to create packaging with a physical barrier to gases and liquids are demanding. In addition, the need to produce biodegradable packaging and at same time from a renewable source, accessible and affordable, makes the research even more challenging.

Thus, this thesis presents relevant technical data to assist in understanding the interaction between paper, cationic starch polymer and materials with potential biodegradation characteristics (carnauba wax and PVOH) in the construction of industrial applicable coating formulations that meet market demands for primary and secondary packages, focusing on a good human-environment relationship.

REFERENCES

AHMED, H. E.; BETIHA, M. A.; EL-DARDIR, M. *et al.* High-Performance Rheology Modifiers And Fluid Loss Of Starch-Bentonite System Based Mud Fluids: Experimental And Optimization Study. **Egyptian Journal of Chemistry**, v. 64, n. 4, p. 1653-1664, 2021.

BASSI, S. A.; BOLDRIN, A.; FARACA, G. *et al.* Extended producer responsibility: How to unlock the environmental and economic potential of plastic packaging waste? **Resources, Conservation and Recycling**, v. 162, p. 105030, 2020.

- BEHERA, L.; MOHANTA, M.; THIRUGNANAM, A. Intensification of yam-starch based biodegradable bioplastic film with bentonite for food packaging application. **Environmental Technology and Innovation**, v. 25, p. 102180, 2022.
- BIERMANN, C. J. **Handbook of Pulping and Papermaking**. 2nd Edition, 1996.
- CHEN, L.; QIANG, T.; CHEN, X. *et al.* Fabrication and evaluation of biodegradable multi-cross-linked mulch film based on waste gelatin. **Chemical Engineering Journal**, v. 419, p. 129639, 2021.
- CHEN, Y.; LI, Y.; QIN, S. *et al.* Antimicrobial, UV blocking, water-resistant and degradable coatings and packaging films based on wheat gluten and lignocellulose for food preservation. **Composites Part B: Engineering**, v. 238, p. 109868, 2022.
- CHENG, Y.; ZHAI, X.; WU, U. *et al.* Effects of natural wax types on the physicochemical properties of starch/gelatin edible films fabricated by extrusion blowing. **Food Chemistry**, v. 401, p. 134081, 2023.
- CHIUMARELLI, M.; HUBINGER, M. D. Evaluation of edible films and coatings formulated with cassava starch, glycerol, carnauba wax and stearic acid. **Food Hydrocolloids**, v. 38, p. 20-27, 2014.
- CHIUMARELLI, M.; HUBINGER, M. D. Stability, solubility, mechanical and barrier properties of cassava starch – Carnauba wax edible coatings to preserve fresh-cut apples. **Food Hydrocolloids**, v. 28, n. 1, p. 59-67, 2012.
- CHRISTOPHLIEMK, H.; ULLSTEN, H.; JOHANSSON, C. *et al.* Starch-poly(vinyl alcohol) barrier coatings for flexible packaging paper and their effects of phase interactions. **Progress in Organic Coatings**, v. 111, p. 13-22, 2017.
- CLEGG, F.; BREEN, C.; MURANYI, P. *et al.* Antimicrobial, starch based barrier coatings prepared using mixed silver/sodium exchanged bentonite. **Applied Clay Science**, v. 179, p. 105144, 2019.
- DANG, K. M.; YOKSAN, R. Thermoplastic starch blew films with improved mechanical and barrier properties. **International Journal of Biological Macromolecules**, v. 188, p. 290-299, 2021.
- DESPOND, S.; ESPUCHE, E.; CARTIER, N. *et al.* Barrier properties of paper-chitosan and paper-chitosan-carnauba wax films. **Journal of Applied Polymer Science**, v. 98, p. 704–710, 2005.
- DEVI, L. S.; KALITA, S.; MUKHERJEE, A. *et al.* Carnauba wax-based composite films and coatings: recent advancement in prolonging postharvest shelf-life of fruits and vegetables. **Trends in Food Science and Technology**, v. 129, p. 296–305, 2022.
- DILKES-HOFFMAN, L. S.; PRATT, S.; LANT, P. A. *et al.* 19 - The Role of Biodegradable Plastic in Solving Plastic Solid Waste Accumulation. In: AL-SALEM, S. M. **Plastics to Energy**. William Andrew Publishing, p. 469-505, 2019.

DIYANA, Z. N.; JUMAIDIN, R.; SELAMAT, M. Z. *et al.* Thermoplastic starch/beeswax blend: Characterization on thermal mechanical and moisture absorption properties. **International Journal of Biological Macromolecules**, v. 190, p. 224–232, 2021.

EMOYAN, O. O.; ADJERESE, W.; TESI, G. O. Concentrations, Origin, and Associated Exposure Risk of Polycyclic Aromatic Hydrocarbons in Soil Depths from Selected Petroleum Tank Farms in Western Delta, Nigeria. **Polycyclic Aromatic Compounds**, 2022.

EUROSTAT. Packaging waste statistics, **Eurostat – Statistics Explained**, 10 de outubro de 2022. Disponível em: https://ec.europa.eu/eurostat/statistics-explained/index.php?title=Packaging_waste_statistics. Acesso em: 18 nov. 2022.

FARRIS, S. Engineering properties of packaging films. In: M. W. Siddiqui, M. S. Rahman, and A. A. Wani (Eds.). *Innovative packaging of fruits and vegetables: Strategies for safety and quality maintenance* (p. 211–226). Waretown, New Jersey: **Apple Academic Press**, 2018.

FOLLAIN, N.; REN, J.; POLLET, E. *et al.* Study of the water sorption and barrier performances of potato starch nano-biocomposites based on halloysite nanotubes. **Carbohydrate Polymers**, v. 277, p. 118805, 2022.

GARAVAND, Y.; TAHERI-GARAVAND, A.; GARAVAND, F. *et al.* Starch-Polyvinyl Alcohol-Based Films Reinforced with Chitosan Nanoparticles: Physical, Mechanical, Structural, Thermal and Antimicrobial Properties. **Applied Sciences**, v. 12, n. 3, p. 1111, 2022.

GE, C.; LANSING, B.; LEWIS, C. L. Thermoplastic starch and poly(vinyl alcohol) blends centered barrier film for food packaging applications. **Food Packaging and Shelf Life**, v. 27, p. 100610, 2021.

GIUSEPPE, F.; COFFIGNIEZ, F.; AOUF, C. *et al.* Activated gallic acid as radical and oxygen scavenger in biodegradable packaging film. **Food Packaging and Shelf Life**, v. 31, p. 100811, 2022.

GÓMEZ-ALDAPA, C. A.; VELASQUEZ, G.; GUTIERREZ, M. C. *et al.* Effect of polyvinyl alcohol on the physicochemical properties of biodegradable starch films. **Materials Chemistry and Physics**, v. 239, p. 122027, 2020.

HONG, S.; WANG, L.; RHIM, J. Preparation and characterization of nanoclays-incorporated polyethylene/thermoplastic starch composite films with antimicrobial activity. **Food Packaging and Shelf Life**, v. 31, p. 100784, 2022.

JAKUBOWSKA, E.; GIERSZEWSKA, M.; SZYDŁOWSKA-CZERNIAK, a. *et al.* Development and characterization of active packaging films based on chitosan, plasticizer, and quercetin for repassed oil storage. **Food Chemistry**, v. 399, p. 133934, 2023.

KAN, M.; MILLER, S. A. Environmental impacts of plastic packaging of food products, **Resources, Conservation and Recycling**, v. 180, p. 106156, 2022.

KHAZAEI, A.; NATEGHI, L.; ZAND, N. *et al.* Evaluation of Physical, Mechanical and Antibacterial Properties of Pinto Bean Starch-Polyvinyl Alcohol Biodegradable Films Reinforced with Cinnamon Essential Oil. **Polymers**, v. 13, n. 16, p. 2778, 2021.

KOCHKINA, N.E.; BUTIKOVA, O.A.; LUKIN, N.D. Ecofriendly films based on low-substituted starch acetate enhanced by polyvinyl alcohol additions. **Iranian Polymer Journal**, v. 31, p. 1361–1371, 2022.

KUMAR, P.; TANWAR, R.; GUPTA, V. *et al.* Pineapple peel extract incorporated poly(vinyl alcohol)-corn starch film for active food packaging: Preparation, characterization and antioxidant activity. **International Journal of Biological Macromolecules**, v. 187, p. 223-231, 2021.

LAROTONDA, F. D. S.; MATSUI, K. N.; SOBRAL, P. J. A. *et al.* Hygroscopicity and water vapor permeability of Kraft paper impregnated with starch acetate. **Journal of Food Engineering**, v. 71, n. 4, p. 394-402, 2005.

LEE, S.; ZHANG, M.; WANG, G. *et al.* Characterization of polyvinyl alcohol/starch composite films incorporated with p-coumaric acid modified chitosan and chitosan nanoparticles: A comparative study. **Carbohydrate Polymers**, v. 262, p. 117930, 2021.

LENDVAI, L.; SAJÓ, I.; KARGER-KOCSIS, J. Effect of Storage Time on the Structure and Mechanical Properties of Starch/Bentonite Nanocomposites. **Starch – Stärke**, v. 71, p. 1800123, 2019.

LIU, D.; DANG, S.; ZHANG, L. *et al.* Corn starch/polyvinyl alcohol based films incorporated with curcumin-loaded Pickering emulsion for application in intelligent packaging. **International Journal of Biological Macromolecules**, v. 188, p. 974-982, 2021.

LIU, S.; LIU, L.; LI, B. *et al.* Size effect of carnauba wax nanoparticles on water vapor and oxygen barrier properties of starch-based film. **Carbohydrate Polymers**, v. 296, p. 119935, 2022 Miranda *et al.*, 2022;

MIRJANI, M.; SOLEIMANI, M.; SALARI, V. Toxicity assessment of total petroleum hydrocarbons in aquatic environments using the bioluminescent bacterium *Aliivibrio fischeri*. **Ecotoxicology and Environmental Safety**, v. 207, p. 111554, 2021.

MITTAL, A.; GARG, S.; BAJPAI, S. Fabrication and characteristics of poly (vinyl alcohol)-starch-cellulosic material based biodegradable composite film for packaging application. **Materials Today: Proceedings**, v. 21, n. 3, p. 1577-1582, 2020.

MONTEIRO, M. K. S.; OLIVEIRA, V. R. L.; SANTOS, F. K. G. *et al.* Incorporation of bentonite clay in cassava starch films for the reduction of water vapor permeability. **Food Research International**, v. 105, p. 637–644, 2018.

MUELLER, C. M. O.; LAURINDO, J. B.; YAMASHITA, F. Effect of nanoclay incorporation method on mechanical and water vapor barrier properties of starch-based films. **Industrial Crops and Products**, v. 33, p. 605–610, 2011.

- MUSCAT, D.; ADHIKARI, R.; MCKNIGHT, S. *et al.* The physicochemical characteristics and hydrophobicity of high amylose starch–glycerol films in the presence of three natural waxes. **Journal of Food Engineering**, v. 119, p. 205–219, 2013.
- MUTHU, S.S. Environmental Footprints of Packaging. **Springer Singapore**, v. 1, n. 1, 192 p. 2016.
- NING, W.; XINGXIANG, Z.; NA, H. *et al.* Effect of citric acid and processing on the performance of thermoplastic starch/montmorillonite nanocomposites. **Carbohydrate Polymers**, v. 76, p. 68–73, 2009.
- OLIVEIRA, M. L. C.; MIRMEHDI, S.; SCATOLINO, M. V. *et al.* Effect of overlapping cellulose nanofibrils and nanoclay layers on mechanical and barrier properties of spray-coated papers. **Cellulose**, v. 29, p. 1097–1113, 2022.
- OLIVEIRA FILHO, J. G.; ALBIERO, B. R.; CALISTO, I. H. *et al.* Bio-nanocomposite edible coatings based on arrowroot starch/cellulose nanocrystals/carnauba wax nanoemulsion containing essential oils to preserve quality and improve shelf life of strawberry. **International Journal of Biological Macromolecules**, v. 219, p. 812–823, 2022.
- OLIVEIRA FILHO, J. G.; BEZERRA, C. C. O. N.; ALBIERO, B. R. *et al.* New approach in the development of edible films: The use of carnauba wax micro- or nanoemulsions in arrowroot starch-based films. **Food Packaging and Shelf Life**, v. 26, p. 100589, 2020.
- PARK, H.; LI, X.; JIN, C. *et al.* Preparation and properties of biodegradable thermoplastic starch/clay hybrids. **Macromolecular Materials and Engineering**, v. 287, p. 553–558, 2002.
- PATIL, S.; BHARIMALLA, A. K.; MAHAPATRA, A. *et al.* Effect of polymer blending on mechanical and barrier properties of starch-polyvinyl alcohol based biodegradable composite films. **Food Bioscience**, v. 44, n. 1, p. 101352, 2021.
- PATIL, S.; BHARIMALLA, A. K.; NADANATHANGAM, V. *et al.* Nanocellulose reinforced corn starch-based biocomposite films: Composite optimization, characterization and storage studies. **Food Packaging and Shelf Life**, v. 33, p. 100860, 2022.
- PAULAPURO, H. Papermaking science and technology: Paper and Board Grades, **TAPPI press**, v. 18. First Edition, 2000.
- PODSHIVALOV, A.; ZAKHAROVA, M.; GLAZACHEVA, E. *et al.* Gelatin/potato starch edible biocomposite films: Correlation between morphology and physical properties. **Carbohydrate Polymers**, v. 157, p. 1162–1172, 2017.
- QIN, Y.; YUN, D.; XU, F. *et al.* Smart packaging films based on starch/polyvinyl alcohol and Lycium ruthenicum anthocyanins-loaded nano-complexes: Functionality, stability and application. **Food Hydrocolloids**, v. 119, p. 106850, 2021.
- REICHERT, C. L.; BUGNICOURT, E.; COLTELLI, M. B. *et al.* Bio-Based Packaging: Materials, Modifications, Industrial Applications and Sustainability. **Polymers**, v. 12, n. 7, p. 1558, 2020.

RIHAYAT, T.; SURYANI, S.; SATRIANANDA, S. *et al.* Poly lactic acid (PLA)/chitosan/bentonite nanocomposites based on cassava starch for materials in biomedical applications. **The 3rd International Seminar on Chemistry AIP Conference Proceedings**, v. 2049, p. 020021-1–020021-6, 2018.

RODRIGUES, L. D. A.; HURTADO, C. R.; MACEDO, E. F. *et al.* Colloidal properties and cytotoxicity of enzymatically hydrolyzed cationic starch-graft-poly(butyl acrylate-co-methyl methacrylate) latex by surfactant-free emulsion polymerization for paper coating application. **Progress in Organic Coatings**, v. 145, p. 105693, 2020.

ROJAS-LEMA, S.; NILSSON, K.; LAGTON, M. *et al.* The effect of pine cone lignin on mechanical, thermal and barrier properties of faba bean protein films for packaging applications. **Journal of Food Engineering**, v. 339, p. 111282, 2023.

ROY, S.; RHIM, J. Antioxidant and antimicrobial poly(vinyl alcohol)-based films incorporated with grapefruit seed extract and curcumin. **Journal of Environmental Chemical Engineering**, v. 9, n. 1, p. 104694, 2021.

SARKAR, A.; BISWAS, D. R.; DATTA, S. C. *et al.* Preparation of novel biodegradable starch/poly(vinyl alcohol)/bentonite grafted polymeric films for fertilizer encapsulation. **Carbohydrate Polymers**, v. 259, p. 117679, 2021.

SATTAR, S.; JEHAN, S.; SIDDIQUI, S. Potentially toxic metals in the petroleum waste contaminated soils lead to human and ecological risks in Potwar and Kohat Plateau, Pakistan: Application of multistatistical approaches. **Environmental Technology and Innovation**, v. 22, p. 101395, 2021.

SHANKAR, S.; RHIM, J. Effects of poly(butylene adipate-co-terephthalate) coating on the water resistant, mechanical, and antibacterial properties of Kraft paper. **Progress in Organic Coatings**, v. 123, p. 153-159, 2018.

SHANMATHY, M.; MOHANTA, M.; THIRUGNANAM, A. Development of biodegradable bioplastic films from Taro starch reinforced with bentonite. **Carbohydrate Polymer Technologies and Applications**, v. 2, p. 100173, 2021.

TODOROVA, D.; YAVOROV, N.; LASHEVA, V. Improvement of barrier properties for packaging applications. **Sustainable Chemistry and Pharmacy**, v. 27, p. 100685, 2022.

TORRES, F.I.; DA SILVA, J.C.; VIEIRA, O. *et al.* Eukalinertm: the first 100% hardwood kraftliner in the world. In: 53RD ABTCP INTERNATIONAL PULP AND PAPER CONGRESS AND EXHIBITION AND 9TH. 2020. São Paulo, **Anais [...]** São Paulo: ABCTP, 2020.

TRINH, B. M.; SMITH, M.; MEKONNEN, T. H. A nanomaterial-stabilized starch-beeswax Pickering emulsion coating to extend produce shelf-life. **Chemical Engineering Journal**, v. 431, p. 133905, 2022.

VAEZI, K.; ASADPOUR, G.; SHARIFI, S. H. Effect of coating with novel bio nanocomposites of cationic starch/cellulose nanocrystals on the fundamental properties of the packaging paper. **Polymer Testing**, v. 80, p. 106080, 2019.

VAYSI, R.; VAGHARI, K. The effect of using cationic starch, long fiber and nano-clay on physical and mechanical properties of recycled pulp. **Iranian Journal of Wood and Paper Science Research**, v. 36, n. 4, 2021.

VINCI, G.; D'ASCENZO, F.; ESPOSITO, A. *et al.* Glass beverages packaging: innovation by sustainable production in trends in beverage packaging. **Academic Press**, v. 16, p. 105–133, 2019.

WANG, J.; GARDNER, D. J.; STARK, N. M. *et al.* Moisture and Oxygen Barrier Properties of Cellulose Nanomaterial-Based Films. **ACS Sustainable Chemistry and Engineering**, v. 6, p. 49–70, 2018.

WANG, X.; HOU, X.; ZOU, P. *et al.* Cationic starch modified bentonite-alginate nanocomposites for highly controlled diffusion release of pesticides. **International Journal of Biological Macromolecules**, v. 213, p. 123-133, 2022.

WU, F.; ZHOU, Z.; LI, N. *et al.* Development of poly(vinyl alcohol)/starch/ethyl lauroyl arginate blend films with enhanced antimicrobial and physical properties for active packaging. **International Journal of Biological Macromolecules**, v. 192, p. 389-397, 2021.

YAO, X.; QIN, Y.; ZHANG, M. *et al.* Development of active and smart packaging films based on starch, polyvinyl alcohol and betacyanins from different plant sources. **International Journal of Biological Macromolecules**, v. 183, p. 358-368, 2021.

YOOK, S.; PARK, H.; PARK, H. *et al.* Barrier coatings with various types of cellulose nanofibrils and their barrier properties. **Cellulose**, v. 27, p. 4509-4523, 2020.

ZAMRUD, Z.; NG, W. M.; SALLEH, H. M. Effect of bentonite nanoclay filler on the properties of bioplastic based on sago starch. **IOP Conf. Series: Earth and Environmental Science**, v. 765, p. 012009, 2021.

THIRD PART

Evaluation of paper coated with cationic starch and carnauba wax mixtures regarding barrier properties

Allan de Amorim dos Santos^{ab*}, Lays Camila Matos^a, Maressa Carvalho Mendonça^{ac}, Marcelo Coelho dos Santos Muguet^c, Andrea Ponzecchi^b, Anand Ramesh Sanadi^b, Gustavo Henrique Denzin Tonoli^a.

^a Department of Forest Science, University of Lavras, University Campus, P.O. Box 3037, 37200-000, Lavras, MG, Brazil.

^b Department of Geosciences and Natural Resource Management, University of Copenhagen, Rolighedsvej 23 – 1958, Frederiksberg, Denmark.

^c Klabin, Technology Center, Industrial R&D+I, Fazenda Monte Alegre, St. Harmonia, 84275-000, Telêmaco Borba, PR, Brazil.

*Corresponding author: *allan.santos1@estudante.ufla.br*

The manuscript can be modified according to the suggestions of the journal's reviewers.

ABSTRACT

Studies of single-use packaging have aimed to replace materials obtained from non-renewable sources with biodegradable materials from renewable sources in response to environmental concerns. Their barrier properties maximize shelf life and product safety. To provide such green packaging, this work aimed to describe the chemical, physical, morphological, and barrier properties of bilayer coatings made from mixtures of cationic starch (S) and carnauba wax (W) on kraftliner paper (86 ± 1 g/m²). Two coating layers (15.0 ± 0.5 g/m²) of both materials in different proportions were compared to uncoated paper and double wet-and-dry paper. The addition of cationic starch to carnauba wax raised the melting point of the wax, preventing it from completely entering the paper's pores but instead producing a layer on top of them. The hydroxyl groups present in coated paper S contributed to its hydrophilicity, showing a high Cobb value, absorbing 153 g/m² more water than control samples. Further, the mixtures showed higher hydrophobicity than the cationic starch-treated samples, with a high-water contact angle ($100\pm 4^\circ$), similarly found for the W treatment. In addition, mixtures showed 0.35 %/s less wettability than the W treatment. In terms of mechanical strength, the lower tensile strength and Young's modulus of the coated sheets brought on by hornification appear to have been predominantly caused by water in the suspensions. The addition of carnauba wax to the cationic starch decreased the resistance of coated papers to oil. However, there was an

improvement in the water barrier by decreased water absorption and wettability and an increase in water contact angle.

Keywords: Green packaging. Kraft paper. Kraftliner packaging. Palm tree wax. Sustainable coating.

1. INTRODUCTION

With growing concerns about the human–environment relationship, studies of single-use packaging have sought to replace fossil-derived material with biodegradable materials from renewable sources (Jakubowska *et al.*, 2023; Rojas-Lema *et al.*, 2023; Reichert *et al.*, 2020). Assuring long shelf life and product safety is a central matter in packaging, and gradually tuning the barrier properties of packages is a viable way to develop a functional product (Kruk *et al.*, 2023; Nilsen-Nygaard *et al.*, 2021). Paper packaging is the main renewable alternative to fossil packaging, and kraftliner paper stands out for its high tensile strength, durability, and high performance (Torres *et al.*, 2020; Petersen *et al.*, 1999). However, kraftliner paper is porous and hygroscopic and water uptake can negatively affect its mechanical properties as well as increase the permeation of gases and water. Thus, applying natural coatings such as cationic starch and waxes can improve its barrier properties without introducing toxic chemicals to the paper (Dilkes-Hoffman *et al.*, 2019; Muthus, 2016).

Starch generally contains 20 to 25% amylose and 75 to 80% amylopectin by mass. Amylose is amorphous and has a long linear structure linked by $\alpha(1\rightarrow4)$ bonds, while amylopectin is highly branched and linked by $\alpha(1\rightarrow4)$ and $\alpha(1\rightarrow6)$ bonds (Tomasik and Schilling, 2004). With good film-forming properties, starch is a highly available, biodegradable, oil-resistant, edible and low-cost polysaccharide, attracting the attention of the packaging industry (Podshivalov *et al.*, 2017). However, starch films have poor mechanical properties, and the addition of a glycerol plasticizer can improve their mechanical fragility. Due to the high content of hydroxyl groups, starch is hydrophilic and readily interacts with water molecules either in the vapor or liquid states (Basiak *et al.*, 2018). Thus, oil and natural waxes have to be added to the starch suspension to improve its hydrophobicity.

Carnauba wax, extracted from the leaf exudate of the Brazilian palm *Copernicia prunifera* (Mill.) H. E. Moore, is a non-toxic natural product. It comprises unsaturated wax specimens with a mixture of hydrocarbons, fatty acids, hydroxylated fatty acids, long-chain alcohols, diols, esters, and cinnamic acid derivatives, of which myricyl cerotate is the main constituent (Edwards and Falk, 1997). It is approved as a food additive (FDA, 2012) and has a

highly hydrophobic nature. It is mainly found in Brazil's northern region and has a mid-yellow color (Edwards and Falk, 1997). Carnauba wax has been successfully used as a coating for fruits and vegetables to increase their shelf life (Cheng *et al.*, 2023; Devi *et al.*, 2022; Miranda *et al.*, 2022; Trinh, Smith, and Mekonnen, 2022). Because the wax forms a fragile film, emulsifiers such as polysorbate can be used to stabilize the film (Matos *et al.*, 2019; Dickinson, 1993). Further, temperature increase during the coating process, paper processing, or transport, can cause the carnauba wax to reach the melting point of 82 °C (Tinto, Elufioye, and Roach, 2017). Therefore, using carnauba wax alone in paper coatings is unfeasible, but incorporating it with other biopolymers can increase its melting point.

Studying the production of starch/gelatin films with different types of wax for coating fruits and vegetables, Cheng *et al.* (2023) compared beeswax, candelilla, and carnauba wax for their physical and barrier properties. The authors concluded that carnauba wax incorporated into starch produced films with stronger molecular interactions, causing better crystallinity and increased hydrophobicity. Devi *et al.* (2022) used waxes in mixture films as plant coatings to extend the shelf life of fruits and vegetables. The authors recorded a reduced water loss and respiration rate of the foods coated with carnauba wax. In addition, incorporating starch into carnauba wax, improved the barrier properties of the film, as well as its mechanical and thermal stability. By coating kraft paper with cationic starch and cellulose nanocrystals, Vaezi, Asadpour, and Sharifi (2019) intensified the mechanical and barrier properties of packaging. The addition of nanocrystals to the cationic starch matrix decreased water absorption by 50% and increased tensile strength by 20%.

Chiumarelli and Hubinger (2014) studied four formulations of glycerol, cassava starch, stearic acid, and carnauba wax for the production of edible films. The authors found that films with higher carnauba wax content did not present a significant barrier to water vapor and oxygen, also showing discontinuity of film formation. In addition, glycerol increased the film solubility in water. The best formulation found by the authors was composed of 3% (m/m) cassava starch with 1.5% (m/m) glycerol and 0.2% (m/m) carnauba wax with 0.8% (m/m) stearic acid, promoting a continuous film with increased mechanical properties, a barrier to moisture and oxygen. Rodrigues *et al.* (2014) proposed a film formed by distinct proportions of cashew tree gum, cassava starch, and carnauba wax. They found that adding carnauba wax to the film formulation promoted a decrease in water vapor permeability and water solubility, but negatively decreased the film stiffness and strength. Forsman *et al.* (2020) analyzed the application of coatings formed by natural wax particles and polymers covering cellulosic fabrics as a repellent to water. The authors compared different coating curing temperatures and their

effect on the properties of the coating and found that the wetting property was directly correlated to the textile surface roughness with an optimal temperature of curing of 70 °C. Korhonen *et al.* (2020) applied depositions layer-by-layer of carnauba wax and cationic starch with different methodologies of coating application and curing. The authors found that the water contact angle was affected by dipping the substrates into cationic starch suspension, followed by the carnauba wax dispersion. The best curing was found for partially melting the carnauba wax. Yet, the dipping methodology showed films with heterogeneous surface, impacting negatively on tensile properties.

Generally, the application of cationic starch and carnauba wax to improve the barrier properties of a film has been applied individually or with other biopolymers (Todorova, Yavorov, and Lasheva, 2022; Vaezi, Asadpour, and Sharifi, 2019; Despond *et al.*, 2005; Larotonda *et al.*, 2005) as a direct coating of fruits but never as a paper coating (Cheng *et al.*, 2023; Devi *et al.*, 2022; Liu *et al.*, 2022; Oliveira Filho *et al.*, 2022; Diyana *et al.*, 2021; Forsman *et al.*, 2020; Korhonen *et al.*, 2020; Oliveira Filho *et al.*, 2020; Chiumarelli and Hubinger, 2014; 2012; Rodrigues *et al.*, 2014; Muscat *et al.*, 2013). In this work, we characterize bilayer coatings formed by cationic starch and carnauba wax in the proportions of 1:0, 3:1, 1:1, 1:3, and 0:1 (m:m), on kraftliner paper by means of several analytical methods toward greener packaging solutions.

2. EXPERIMENT

2.1 Material

Klabin S/A (Paraná, Brazil) provided kraftliner paper (kappa number 100, 86 ± 1 g/m²) and cationic starch (95 wt.%, amylose content 42%, degree of substitution 0.243). Êxodo Científica (São Paulo, Brazil) provided glycerol ($\geq 99\%$), Fenix Ceras e Produtos Ltda. (São Paulo, Brazil) provided carnauba wax, and Sigma Aldrich (Missouri, USA) provided polysorbate 80 emulsifier (Tween 80, HLB = 15).

2.1.1 Preparation of suspensions

Cationic starch 4.0 wt.% was prepared following the cold–heat suggestions of Gao *et al.* (2020). Complete cationic starch solubilization occurred at 23 °C (400 rpm) for 30 min,

followed by heating at 60 °C (500 rpm) until complete gelatinization and the addition of 20 wt.% glycerol.

The carnauba wax emulsion, prepared at a concentration of 10% wax (w/v), followed the methodology described by Matos *et al.* (2019). Ten grams of wax was melted in a water bath (90 °C) together with ten grams of emulsifier (polysorbate 80) and stirred for 10 min at 800 rpm. Subsequently, while still in a water bath, mechanical agitation (Ultra Turrax, Tecnal TE-102, Brazil) commenced at 14,000 rpm with the slow addition of 80 mL of deionized water. After 10 min of mechanical agitation, the emulsion was removed from the water bath and kept under continuous agitation at 4,000 rpm until completely cooled.

Utilizing the suspensions, mixtures with complementary proportions (m:m) of 1:0, 3:1, 1:1, 1:3, and 0:1 of cationic starch-glycerol (S) and carnauba wax-surfactant (W) were prepared. Each mixture was stirred at 400 rpm by mechanical agitation for 10 min.

2.1.2 Kraftliner paper coating

The suspension was applied in two layers on a 297×210 mm kraftliner paper through a coating machine with a 4 m/min speed following ASTM D646-13 (ASTM, 2013). First, the suspension was uniformly spread with a cylinder (bar n. 220), reaching 7.5 ± 0.5 g/m². Then, the coated paper was submitted to heating at 103 ± 2 °C for 5 min. The second layer followed the same procedure (bar n. 100), reaching 15.0 ± 0.5 g/m², followed by the same drying. The solid content and viscosity predetermined the amount for each layer. The first layer fulfills the roughness and porosity of the paper, while the second layer evens out the surface, forming a continuous film. Suspension application followed the fiber direction in the kraftliner paper's machine direction (MD). For comparison, kraftliner paper without a coating was used (C1), as well as kraftliner with a double wet-and-dry treatment with only deionized water (C2) to evaluate the effect of water on the coating, totaling seven treatments (Table 1).

Table 1 - Acronyms and description of the treatments used in this work.

| Acronym | Description of treatments |
|---------|--|
| C1 | Uncoated kraftliner paper |
| C2 | Double wet-and-dry kraftliner paper with deionized water |
| S | Kraftliner paper coated with cationic starch/glycerol |
| S3:1W | Kraftliner paper coated with a mixture of 75% m/m cationic starch/glycerol and 25% m/m carnauba wax/polysorbate 80 |
| S1:1W | Kraftliner paper coated with a mixture of 50% m/m cationic starch/glycerol and 50% m/m carnauba wax/polysorbate 80 |
| S1:3W | Kraftliner paper coated with a mixture of 25% m/m cationic starch/glycerol and 75% m/m carnauba wax/polysorbate 80 |
| W | Kraftliner paper coated with carnauba wax/polysorbate 80 |

Source: From the author (2023).

2.2 Methods

2.2.1 Characterization of suspensions

Suspensions were characterized by their characteristics of solid content (NBR 8877 - ABNT, 2020), pH measurement (W38 Bel Engineering, Brazil), and viscosity (NBR 9277 - ABNT, 2020), following current standards.

2.2.2 Physical properties of coated paper

The thickness and density of the multilayer packaging were measured using a Regmed micrometer (ESP/SA-10, Brazil) following the ISO 534:2011 (ISO, 2011) standard, where density is the grammage (g/cm^2) ratio to its given thickness (cm). The packaging surface and cross-section were evaluated by field emission scanning electron microscopy (SEM) in a Tescan Clara (UHR, Libusina, Czech Republic) under working conditions of 10 kV and 8 mm distance. Samples were cut with liquid nitrogen and coated with gold using a Balzer spray coating technique (SCD 050) and then placed on aluminum stubs with carbon tape on aluminum foil.

2.2.3 Paper pencil hardness

The pencil hardness was evaluated with a Wolf Wilborn durometer (TKB Erichsen Comercial e Técnica Ltda., São Paulo, Brazil) following the ASTM D3363-22 pencil test

(ASTM, 2022). A softer pencil (10B, 9B, 8B, 7B, 6B, 5B, 4B, 3B, 2B, B, HB) is attached to the instrument at a 45° angle to the paper, dragging the device. After removal, if there were no signs of damage to the coating, the test was repeated with a pencil at a higher hardness grade (F, H, 2H, 3H, 4H, 5H, 6H, 7H, 8H, 9H, 10H). The pencil that does not damage the coating expresses the maximum pencil hardness.

2.2.4 Fourier transform infrared spectroscopy (FT-IR)

Attenuated total reflectance Fourier transform infrared spectroscopy (FT-IR) was performed to identify the chemical structure of the coating and possible interactions between its components. Spectra were determined with a Nicolet 6700 FT-IR equipped with a Pike Technologies Gladi ATR diamond spectrometer (Thermo Scientific, Waltham, MA, USA) with an average of 60 scans recorded at 4 cm⁻¹ resolution in a range of 4000 to 500 cm⁻¹ at room temperature (23 °C).

2.2.5 Raman spectroscopy

Raman spectra were acquired in triplicate with a confocal Raman microscope (alpha 300, WITec GmbH, Ulm, Germany) equipped with a 10x air objective (NA = 0.25, Carl Zeiss GmbH Jena, Germany). A linear polarized laser with a wavelength of 532 nm (Crysta Laser, Reno, NV, USA) and a power of 10 mW was focused on a diffraction-limited spot size of $0.61 \times \lambda/NA$. Each Raman spectrum was the average of 10 accumulations acquired with 0.1 s exposure time. Raman light was detected with a backlit, air-cooled charge-coupled device (CCD) detector (DV401_BV, Andor, Belfast, UK) with a spectral resolution of 6 cm⁻¹. A baseline was created for each analyzed spectrum using Origin Pro 8.5 software (OriginLab, USA) to remove residual fluorescence, followed by smoothing. As the kraftliner paper showed intense autofluorescence, preventing the characterization by Raman spectroscopy, the analysis was performed on mixture films only. First, the films were formed by casting in 5 cm diameter Petri dishes. Then, 10 mL of the suspension (1.0 wt.%) was dried in a circulating oven (Solab SL-100, Brazil) for 48 h at 45 °C.

2.2.6 Water and oil barrier properties of coated paper

The contact angle of the water with the surface of the coated papers was evaluated using a Krüss Drop Shape Analyzer Goniometer (DSA25, Hamburg, Germany) in triplicate at room temperature (23 °C). A deionized water drop was deposited on the sample surface through a syringe 20 mm away. A camera captured the drop image, and Advance software determined the average contact angle between the water drop and the paper surface. The analysis was performed at ten average angles at the time of contact when the drop stabilized.

Determining the wettability of multilayer papers followed the procedures proposed by ASTM D724-99 (ASTM, 2003) in triplicate. This method measures the angle at 5 s after contact with the coated paper surface and after 55 s (total of 60 s). Increased dispersion generates smaller angles and, consequently, higher wettability. Wettability (°/s) is calculated using Equation 1.

$$\text{Wettability} = \frac{(C-c)}{55} \quad (1)$$

‘C’ represents the contact angle with water in 5 s (°), ‘c’ represents the contact angle with the water after 60 s (°), and ‘55’ represents the time (s) for the paper to absorb the water.

The water absorption test (Cobb test) followed TAPPI T441 om-13 (TAPPI, 2013). First, 15×15 cm samples were prepared, and 100 mL of deionized water was poured into a ring instrument for 120 s. Then, a 10 kg roller pressed the “wet samples” between two absorbent papers to remove trapped moisture. The sample was weighed before and after the procedure. The Cobb index shows the relationship between the mass of water absorbed by the multilayer paper and the wetted area (g/m²).

The measurements of water vapor transmission rate (WVTR) and water vapor permeability (WVP) followed the adaptation of the ASTM E96/E96M-16 (2016) standard method, as used by Guimarães Jr. *et al.* (2015). Samples with 16 mm diameter were coupled to permeation cells filled with silica. These cells were conditioned at 38 °C and 90% relative humidity (RH) for eight days and weighed each day. The 90% RH environment created in a desiccator containing a saturated saline solution was produced based on ASTM E104-02 (2012). WVTR (g/m².day) and WVP (g.mm/day.m².kPa) were calculated following Equations 2 and 3, respectively:

$$\text{WVTR} = \frac{(M/t)}{A} \quad (2)$$

$$\text{WVP} = \text{WVTR} \cdot \frac{\text{Th}}{S} \cdot (R^1 - R^2) \quad (3)$$

'M' is the mass (g), 't' is the time (d), 'M/t' is the angular coefficient from the linear regression of day (d) and mass gain (g), and 'A' is the test area (m²). 'Th' is the paper thickness (μm), 'S' is the saturation vapor pressure at the test temperature (kPa), 'R¹' is the relative humidity in the desiccator (90%), and 'R²' is the relative humidity of the test environment (0%). All samples were tested in triplicate.

2.2.7 Oil/Grease barrier property of coated paper

Oil resistance was evaluated according to T 559 cm-12 (TAPPI, 2012). Multilayer paper samples were tested with oil kit solutions ranging from 1 to 12, which contained specific proportions of three reagents: castor oil, toluene, and n-heptane. Kit test 1 contained only castor oil, while kit test 12 contained toluene and n-heptane, with the lowest surface energy. A drop of the kit test was applied to the paper surface at a height of 13 mm. After 15 s, excess oil was removed. The kit test that remained on the paper surface and not absorbed by the paper was reported as the kit test for the sample. A paper with kit test 12 indicated a more oil/grease-resistant coating.

The same kit test procedure was performed on a crease produced on the sample following the same methodology. The crease was made by repeatedly folding the paper, simulating a possible discontinuity of the thin coating when folding the multilayer paper.

The sessile drop OWRK method described by Lago *et al.* (2021) was used for surface free energy analysis. The values of polar and dispersive surface energies, expressed in mN/m, were taken after the contact angles formed in the samples by five different solvents measured by Advance software at room temperature (23 °C). The solvents used were deionized water, glycerol, diiodomethane, ethylene glycol, and 1-bromonaphthalene. Polarity was calculated as the ratio between the polar component estimates and the paper's total surface energy.

2.2.8 Mechanical property of coated paper

The tensile strength test, performed in a Shimadzu testing machine (AGS-X, Japan), followed the ASTM D828-22 (ASTM, 2022) standard with a distance between the claws of 122 mm, a speed of 25.4 mm/min, and a 10 kN load cell. Ten 25.4×254.0 mm samples per treatment were analyzed. Tensile strength is the maximum force applied to the specimen before failure, while the tensile index is the tensile strength divided by the sample's grammage; tensile energy absorption is the amount of work performed when a specimen is strained to rupture under tension under certain conditions. Tensile stiffness is the tangent of the linear region of a tensile strength–strain curve in the elastic region and represents the elastic characteristic of multilayer paper (Santos and Yoshida, 2011). Finally, elongation is the specimen's response when stress is applied, increasing its size. Kraftliner paper is an anisotropic material with different properties in the machine direction (MD) and in the cross direction (CD) of the paper sheets, being necessary to characterize the two directions in the papers coated in each treatment. Data were analyzed using Trapezium software, version 1.5.4.

2.3 Statistical analysis

The results were submitted to a one-way analysis of variance (ANOVA) and the Scott–Knott test, with 5% significance, to evaluate the properties of multilayer paper and uncoated kraftliner paper. Data were processed by Sisvar 5.6 software (Ferreira, 2014). The metan package in the R software (Olivoto and Lúcio, 2020) evaluated the correlation between the water barrier properties through principal component analysis (PCA) and by applying Pearson's correlation ($p < 0.01$), analyzed by correlogram in the software R (R Core Team 2020).

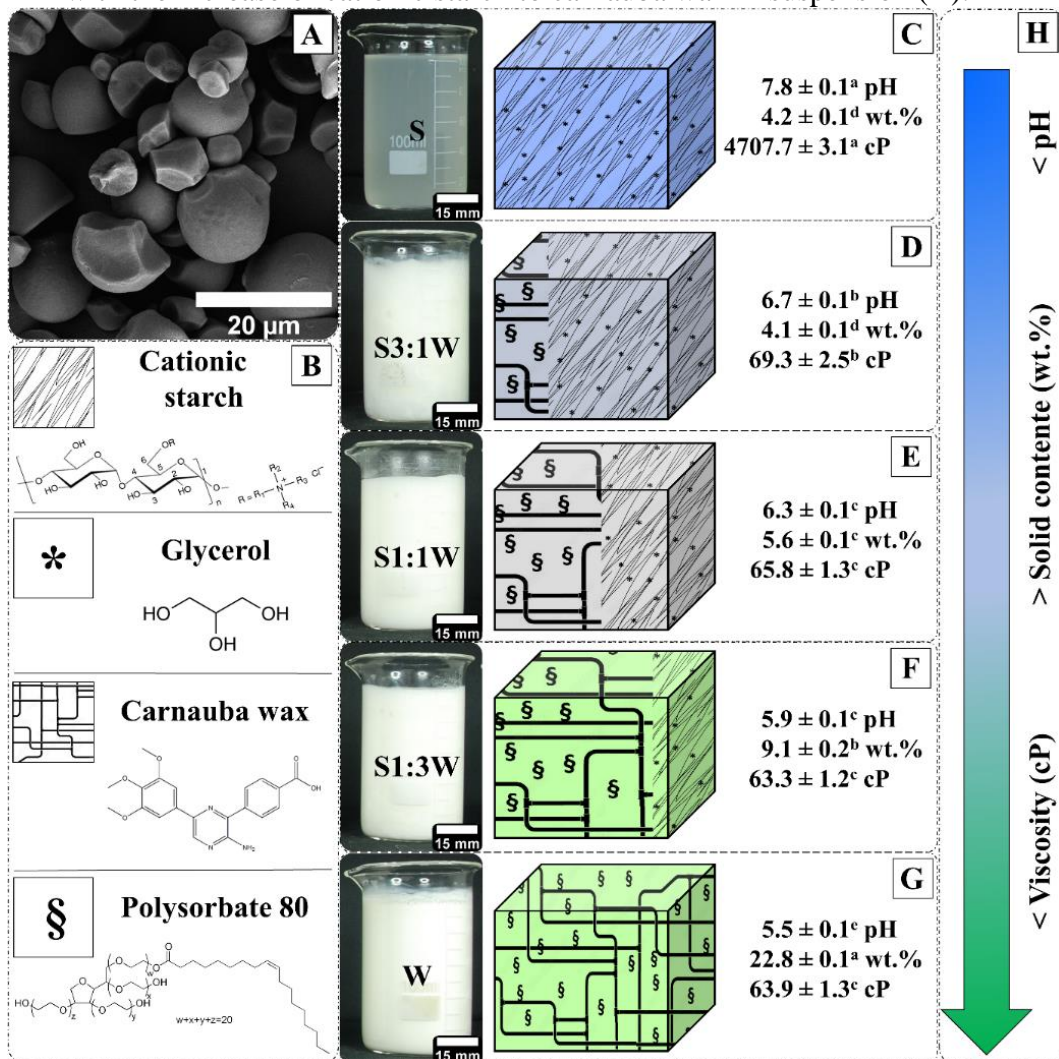
3. RESULTS AND DISCUSSION

3.1 Investigation of Suspensions

Cationic starch and carnauba wax tend to have poor or no compatibility in their natural forms. For example, Cheng *et al.* (2023) observed low compatibility between natural carnauba wax and modified cassava starch, affecting the film's surface and decreasing its barrier properties. In addition, the natural lubrication of the wax facilitates the movement of the starch polymer chain, resulting in phase separation (Firoozmand, Murray, and Dickinson, 2009).

However, the suspensions of cationic starch/carnauba wax mixtures in this work did not show phase separation (Figure 1).

Figure 1 - Graphic scheme with cationic starch granules (A); chemical representation of cationic starch, glycerol, carnauba wax, and polysorbate 80 (B); representation of suspensions and their pH, solid contents, and viscosity characteristics of cationic starch (C); cationic starch 75%/25% carnauba wax mixture (D), cationic starch 50%/50% carnauba wax mixture (E); cationic starch 25%/75% carnauba wax mixture (F); carnauba wax (G); and flowchart of the modification of suspension characteristics with the increase of cationic starch to carnauba wax in suspension (H).



Treatments with complementary proportions (m:m) of 1:0, 3:1, 1:1, 1:3, and 0:1 of cationic starch (S) and carnauba wax (W). Image of scanning electron micrography of cationic starch granules.

Source: From the author (2023).

The insertion of glycerol plasticizer and polysorbate 80 emulsifier into the mixture resulted in a single-phase suspension. Starch and glycerol bind to water via hydrogen bonds due to their hydrophilic nature (Ciannamea *et al.*, 2018), and the emulsifier assists in the binding between the cationic starch and the wax. Thus, the dispersion becomes homogeneous and

contributes to more significant contact between the carnauba wax and the cationic starch, avoiding phase separation.

When carnauba wax was added to the cationic starch suspension in different proportions (3:1, 1:1, and 1:3), the cationic starch/wax mixture showed an instant increase in viscosity but after five minutes of stirring, the mixtures became homogeneous, and the viscosity decreased to values between 69.3 and 63.3 cP (Figure 1). This increase was due to differences in components' polarity and nonimmediate interactions while the sudden decrease in viscosity may be due to the retrogradation of the starch and the bonds forming between the polymer and the wax (Ebnesajjad, 2012).

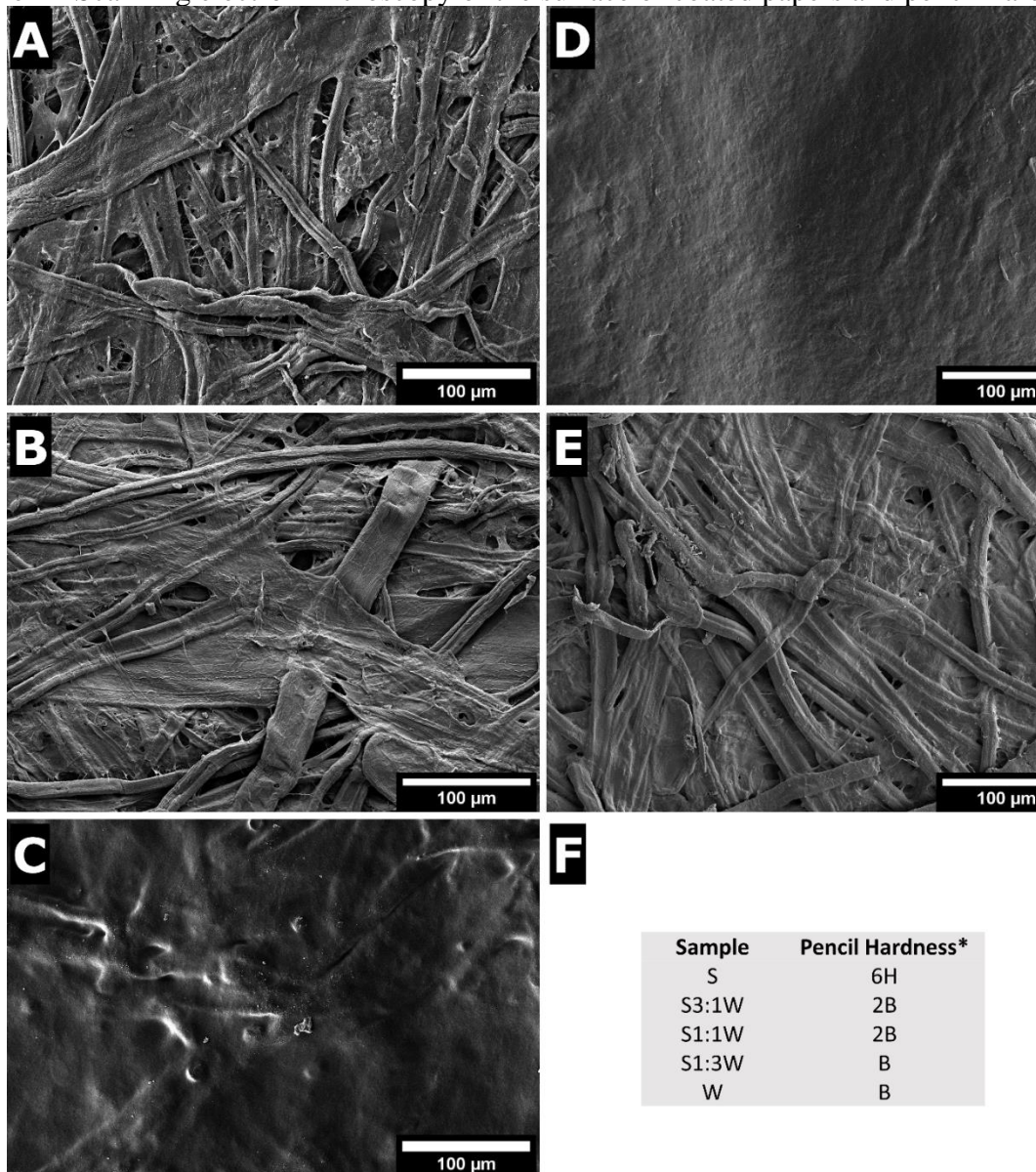
The mixture of cationic starch and wax generates an amphiphilic mixture, where the aliphatic chains of the wax are associated with the hydrophobic phase of polysorbate 80, and the hydroxyls of the polysorbate interact with the hydroxyls of cationic starch through ionic bonds or hydrogen bonds (Trinh, Smith, and Mekonnen, 2022). The addition of the emulsifier facilitates mixing but also increases the hydroxyl groups of the system, becoming more hydrophilic.

The pH of the mixtures varied between 6.7 in the S3:1W and 5.9 in the S1:3W samples. A pH value greater than 4.0 is needed to limit starch hydrolysis and stabilize the film permeability (Olsson *et al.*, 2013), which was observed for all mixture samples and pure cationic starch.

3.2 Physical and morphological characteristics

Samples coated with cationic starch and glycerol (S) showed the highest hardness with 6H, which agrees with what other authors found (Noè *et al.*, 2021; Ma, Kovash Jr., and Webster, 2017). Instead, W and S1:3W samples had the lowest hardness (B) while S3:1W and S1:1W had a moderate 2B hardness (Figure 2F). The pencil hardness depends on the flexibility of the coating chains, and gives an indication of the adhesion of the film to the paper (Gadhawe, Mahanwar, and Gadekar, 2019).

Figure 2 - Scanning electron microscopy of the surface of coated papers and pencil hardness.



* Following ASTM D 3363-22 standard (ASTM, 2022). Control treatments with no coating - C1 (A) and double wet-and-dry - C2 (B). Treatments with complementary proportions (m:m) of 1:0 (C), 1:1 (D), and 0:1 (E) of cationic starch - S and carnauba wax - W. Pencil Hardness (F).

Source: From the author (2023).

It is known that kraft papers are formed by flat fibers with significant porosity (Petersen *et al.*, 1999), as shown in Figure 2A, where water, oil, and gas molecules are transported. SEM images showed that the double coating with water and drying (C2) caused a significant flattening of the fibers and an increase in the porosity of the paper (Figure 2B), which facilitates the transport of the molecules through the material. This fibrous and interwoven characteristic of the paper gives it mechanical strength, which is excellent for use in packaging.

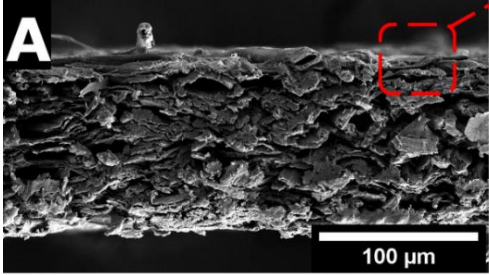
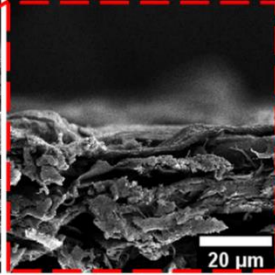
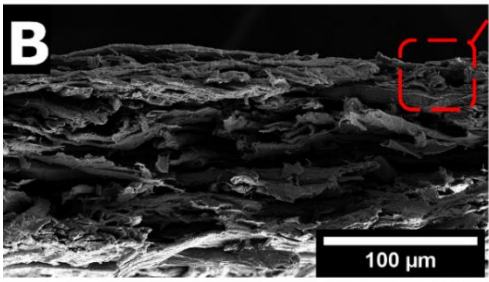
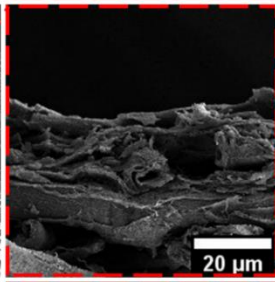
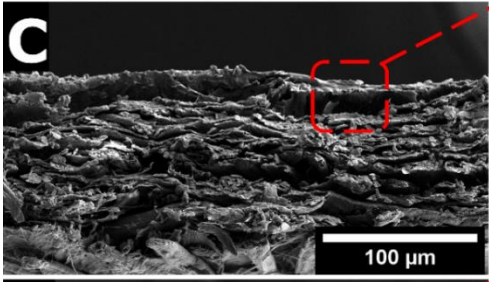
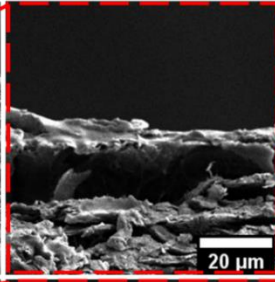
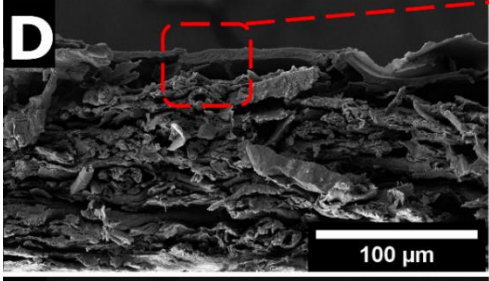
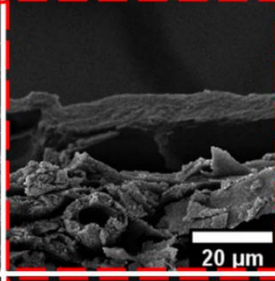
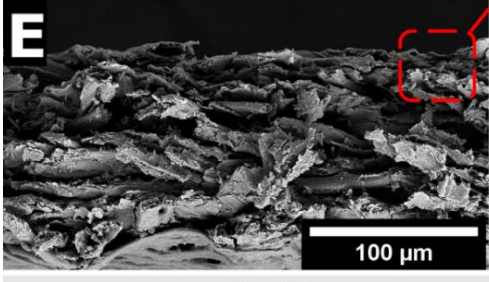
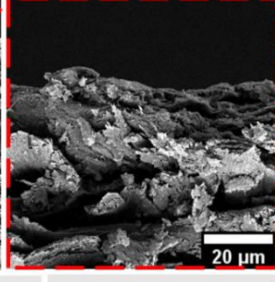
The continuity or discontinuity of the coating on kraftliner paper influences the physical and barrier properties of the package (Yang *et al.*, 2022). The paper coated with cationic starch

and glycerol (S) showed film continuity. However, the paper fibers could be seen underneath the barrier, suggesting a high permeability to water, water vapor, oil, and gases of the coating (Figure 2C).

No formation of a wax layer over the paper coated with carnauba and polysorbate (W) was seen; the wax likely melted and got absorbed by the paper fibers during the drying process (Zhang *et al.*, 2019). The lack of film formation on the paper for the carnauba wax sample directly influences the barrier properties. On the other hand, the S1:1W coated paper presents a continuous film on the surface with a certain roughness, which can modify the interaction with water. Other authors have associated similar roughness to tiny particles of wax crystals (Cheng *et al.*, 2023; Diyana *et al.*, 2021; Rodrigues *et al.*, 2014; Muscat *et al.*, 2013).

SEM cross-section allowed the estimation of the coating' thickness and the density of samples, including the film and part of the kraftliner paper. We estimated that cationic starch-coated paper (S) has the highest thickness, with 0.147mm, while carnauba wax samples the lowest, with 0.134 mm (Figures 3C and 3E). Density calculations of the paper-fiber and coating area showed instead carnauba coated samples (W) having the highest with 0.757 g/cm³ and cationic starch-coated samples with the lowest, 0.693 g/cm³. The high viscosity of cationic starch at low solids content generates a low paper density; the cationic starch suspension does not penetrate the paper due to its high viscosity and the gelatinized cationic starch, with non-aligned amorphous regions, favors the formation of a coating with greater volume than those observed by the mixtures coated papers. In addition, fast drying at 103±2 °C prevented the polymer from adjusting on the paper's surface, decreasing its density. Only some of the cationic starch appears to have penetrated the paper.

Figure 3 - Scanning electron microscopy of coated papers' cross-section, thickness, and density characteristics.

| | | | |
|---|--|---|--|
|  |  | <p>C1</p> <p>Thickness: ^d 0.125 ± 0.001 mm</p> <p>Density: ^c 0.691 ± 0.002 g/cm³</p> | |
|  |  | <p>C2</p> <p>Thickness: ^d 0.124 ± 0.002 mm</p> <p>Density: ^c 0.689 ± 0.003 g/cm³</p> | |
|  |  | <p>S</p> <p>Thickness: ^a 0.147 ± 0.003 mm</p> <p>Density: ^c 0.693 ± 0.014 g/cm³</p> | |
|  |  | <p>S1:1W</p> <p>Thickness: ^b 0.140 ± 0.002 mm</p> <p>Density: ^b 0.725 ± 0.007 g/cm³</p> | |
|  |  | <p>W</p> <p>Thickness: ^c 0.134 ± 0.002 mm</p> <p>Density: ^a 0.757 ± 0.032 g/cm³</p> | |
| <p>S3:1W</p> <p>Thickness: ^b 0.138 ± 0.002 mm</p> <p>Density: ^b 0.736 ± 0.005 g/cm³</p> | | <p>S1:3W</p> <p>Thickness: ^b 0.140 ± 0.004 mm</p> <p>Density: ^b 0.727 ± 0.031 g/cm³</p> | |

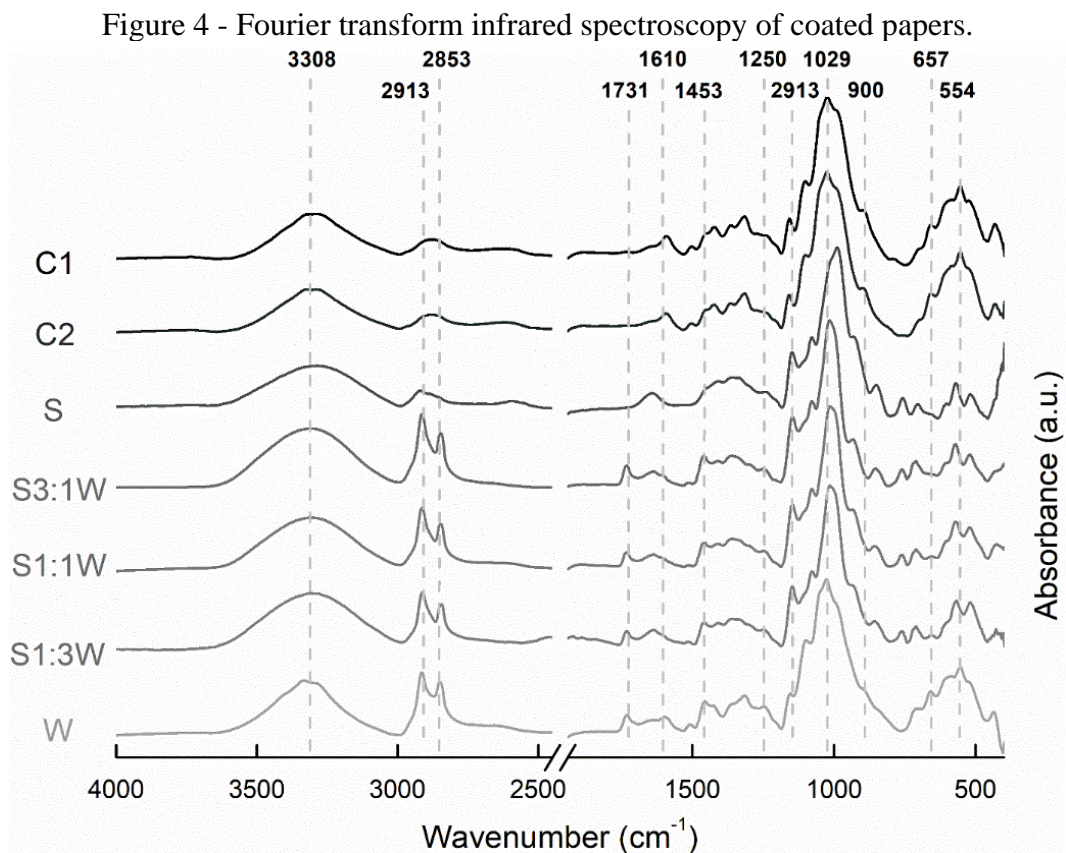
The same letters for each characteristic do not differ according to the Scott-Knott test at 5% significance. Average value ± standard deviation. Control treatments with no coating - C1 (A) and double wet-and-dry coating - C2 (B). Treatments with complementary proportions (m:m) of 1:0 (C), 3:1, 1:1 (D), 1:3, and 0:1 (E) of cationic starch (S) and carnauba wax (W).

Source: From the author (2023).

As illustrated in Figure 3D, the S1:1W mixture show a homogeneous coating, suggesting good interfacial interaction, which is directly related to the performance of the multilayer paper. In addition, the better contact surface between the wax and the cationic starch and the insertion of the plasticizer and emulsifier contributed to a homogeneous dispersion (Liu *et al.*, 2022). As a result, the mixture showed moderate thickness and density.

3.3 Fourier transform infrared spectroscopy and Raman spectroscopy

The FT-IR spectra helped to understand the chemical interactions at the surface of the coated mixture papers and to compare it to the uncoated paper. For C1 and C2 kraftliner papers (Figure 4), the FT-IR spectra of functional groups are attributed to the O-H stretching of hydroxyl groups at $3,308\text{ cm}^{-1}$. They are in water molecules, cellulose, hemicelluloses, and even glycerol (Chen *et al.*, 2016). Peaks between the $1,610\text{ cm}^{-1}$ and $1,250\text{ cm}^{-1}$ bands are present in lignins and hemicelluloses and are characteristic of uronic ester groups and ester bonds of the carboxylic group of ferulic and p-coumaric acid (Miao, Lin, and Bian, 2020; Bian *et al.*, 2019).



Control treatments with no coating (C1) and double wet-and-dry coating (C2). Treatments with complementary proportions (m:m) of 1:0, 3:1, 1:1, 1:3, and 0:1 of cationic starch (S) and carnauba wax (W).

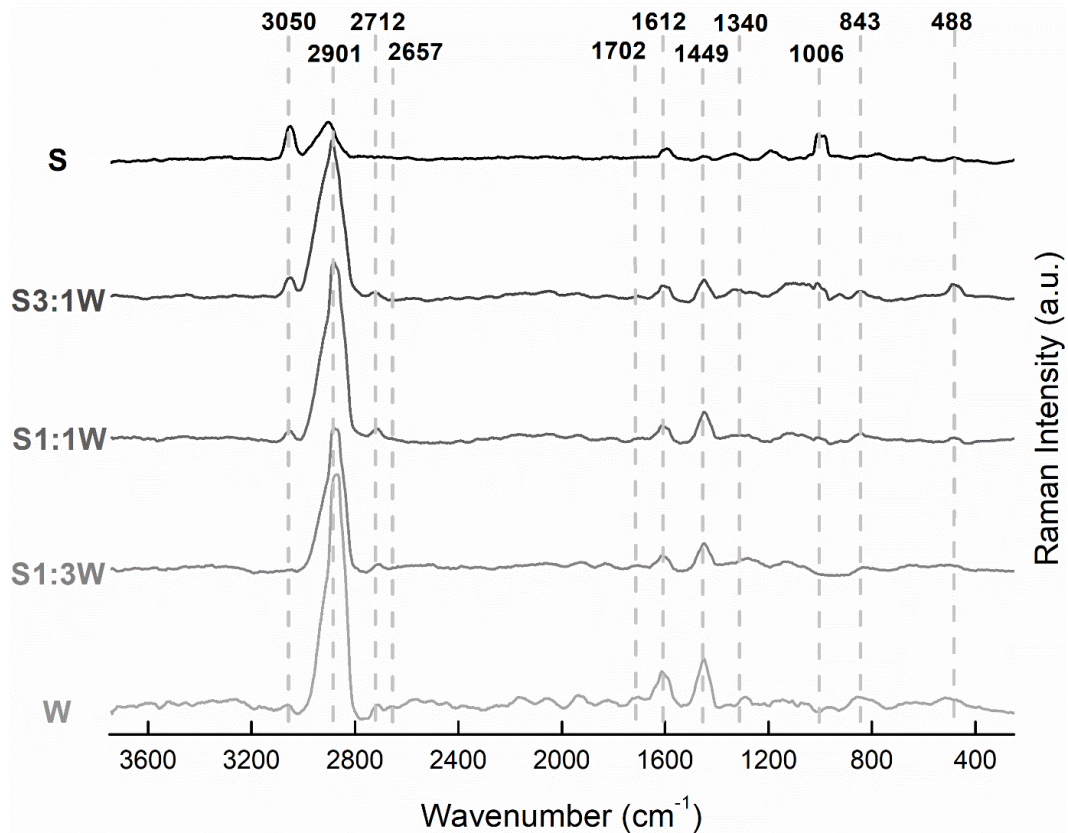
Source: From the author (2023).

Accessible hydroxyls are abundant in cationic starch chains performing intra- and intermolecular bonds; they are responsible for restricting chain movement (Liu *et al.*, 2022; Gao *et al.*, 2012). The peak at $3,308\text{ cm}^{-1}$ represents the stretching vibration of the O-H bond. This peak for the cationic starch sample is broader than that presented by the control kraftliner papers and the carnauba wax. In addition, this broader peak is also observed in the cationic starch-based mixtures, even in smaller amounts, such as S1:3W. The large quantity of O-H increased this bond's electron density, causing this peak to intensify.

Carnauba wax showed characteristic FT-IR peaks at $1,731$, $1,453$, and $1,029\text{ cm}^{-1}$, referring to $\nu\text{C}=\text{O}$ of carbonyl ester, δCH of $-\text{CH}_2-$, and C-O-C, respectively. The C-O-C vibration peak for starch is more intense and shifted to 990 cm^{-1} (Zhu *et al.*, 2022). According to Abdulla *et al.* (2018), this region represents the crystalline fraction of starch in its natural form. The absorption peaks at $2,913$ and $2,853\text{ cm}^{-1}$ represent the asymmetric stretching of the C-H bond of carnauba wax (Liu *et al.*, 2022; Muscat *et al.*, 2014).

Analyzing the mixture FT-IR spectra, no new peaks are present compared to the spectra of cationic starch or carnauba wax. That suggests no formation of new IR sensitive chemical bonds-interactions. Raman spectra were obtained to detect any eventual difference (Figure 5).

Figure 5 - Raman spectroscopy characterization of cationic starch and carnauba wax composite films.



Treatments with complementary proportions (m:m) of 1:0, 3:1, 1:1, 1:3, and 0:1 of cationic starch (S) and carnauba wax (W).

Source: From the author (2023).

The Raman scattering of light is given by the changes in polarizability of chemical bonds and functional groups present in a surface's material which has been illuminated with monochromatic light. Such bonds have different polarizabilities and produce different Raman shifts. Unlike FT-IR, Raman presents the obstacle of the analysis being unfeasible in the presence of too intense autofluorescence. Kraftliner-coated papers produced autofluorescence which hid the Raman signal (Sá, Miranda, and José, 2015). Therefore, it was decided not to analyze the papers of the samples C1 and C2.

Typical peaks in the Raman spectra of starch correlate to their helical structures (Zheng *et al.*, 2021; Guo *et al.*, 2019), such as single helix, amylose double helix, or amylopectin double helix. This starch helical structures' order correlates with their properties (Lu, Tian, and Ma, 2023). Raman bands at 3,050 and 2,901 cm^{-1} in cationic starch can assess the degree of cationic starch retrogradation. These bands are related to C-H stretching, conformationally altered by the formation of amylopectin double helices. The peak at 2,901 cm^{-1} is directly dependent on the change of these double helices (Hu *et al.*, 2017; Bulkin and Kwak, 1987). The peak at 1,006

cm^{-1} is associated with the ether group, present in the cationic portion of the starch (Wyan, 2019). According to Guo *et al.* (2019), the peak at $1,340 \text{ cm}^{-1}$ is attributed to the angular movement of the C-O-H bond caused by the spiralization of single helical amylose.

Carnauba wax is a material with a complex chemical nature. Following the work of Edwards and Falk (1997), carnauba wax is characterized by high-intensity bands at $2,901$, $1,612$, and $1,449 \text{ cm}^{-1}$ representing symmetrical CH_3 , CCH, and CH_2 , respectively. With bands of lower intensity, $3,050$, $2,712$, and $2,657 \text{ cm}^{-1}$ represent olefinic $\text{C}=\text{CH}$, $\text{CH}_3\text{-CH}$, and CH-CH_3 , respectively. The presence of carbonyl groups is confirmed by the band close to $1,702 \text{ cm}^{-1}$, methyl groups in the bands $1,340$ and 843 cm^{-1} , and, finally, $\text{d}(\text{CCC})$ confirmed by band 488 cm^{-1} . Note the absence of the $2,712 \text{ cm}^{-1}$ band in the cationic starch sample.

The O-H band of hydroxyl groups usually appears between $3,170$ and $3,650 \text{ cm}^{-1}$ (Salmén and Bergström, 2009), but unlike in IR-spectroscopy, hydroxyls are not a Raman active group and are mainly visible in the moist state. In fact, apart from the 100% Carnauba wax sample, we do not observe any peak in this range. That is probably because the films are completely dry and the naturally occurring hydroxyls are not abundant enough to produce a Raman scattering that is visible in the spectra. The bands $1,612$ and $1,702 \text{ cm}^{-1}$ are related to chemical bonds C-H and $\text{C}=\text{C}$, respectively (Alves *et al.*, 2016). The increase in intensity at the peak of $2,901 \text{ cm}^{-1}$ with the addition of carnauba wax to the mixture may have occurred due to the increase of carbonic chains, C-H bonds, present in the wax.

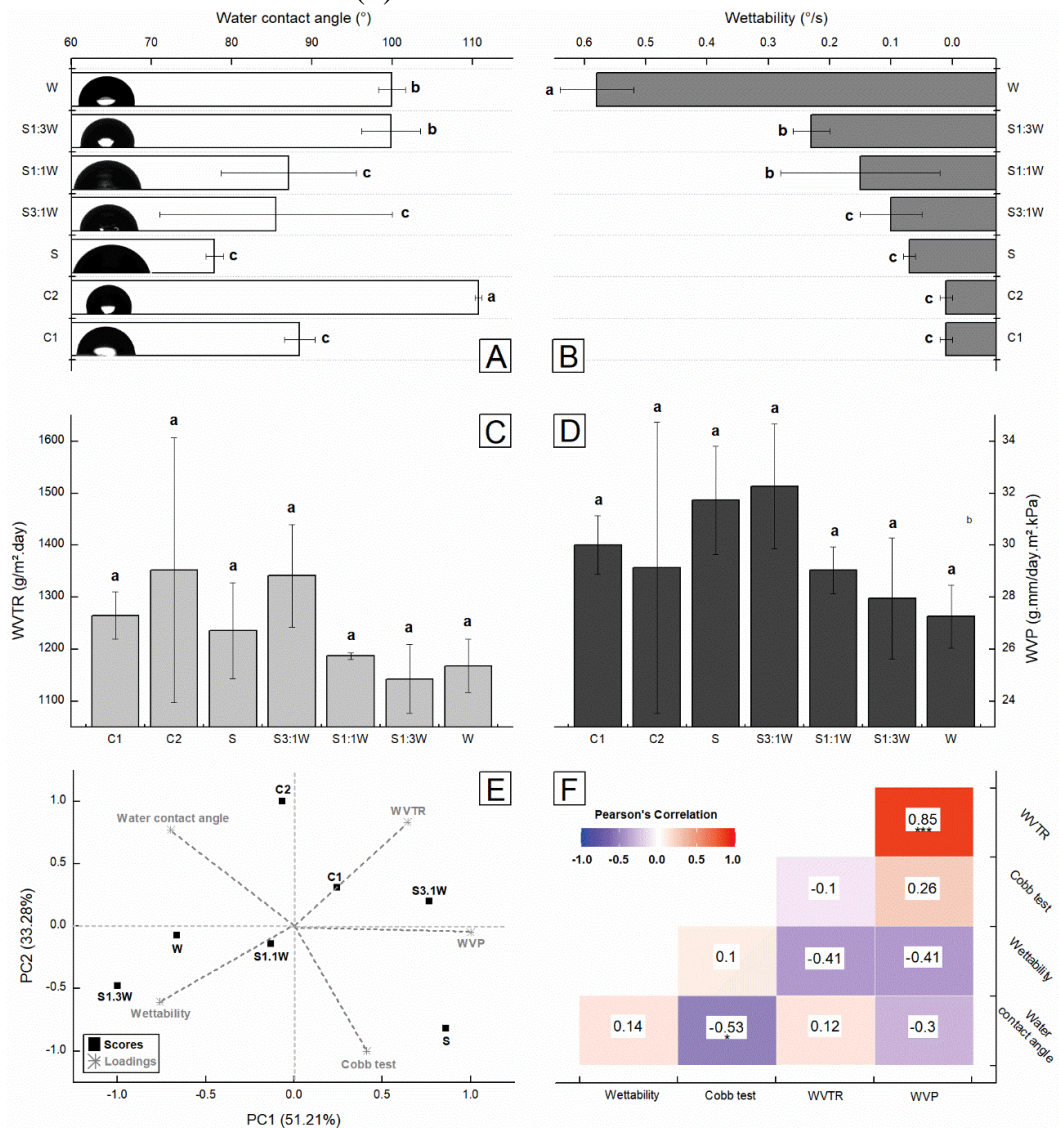
The Raman spectra of the mixture films (S1:3W, S1:1W, S3:1W) are dominated by the spectrum of carnauba wax, especially by looking at the peaks at $2,901 \text{ cm}^{-1}$ and $1,449 \text{ cm}^{-1}$. The peak at $3,050 \text{ cm}^{-1}$, associated with retrogradation of cationic starch, is proportionally varying together with the concentration of cationic starch in the different coatings.

3.4 Water and oil barrier

The coated paper barrier properties can be derived from the water contact angle, wettability, water vapor permeability (Figures 6A-D), and for the water barrier through the Cobb test (Table 2). Usually, water contact angles above 90° indicate hydrophobicity (Bačovská *et al.*, 2016), which depends on the material's surface chemistry and roughness, paper porosity, among others. Controlled by these factors, the surface determines a specific angle between the water drop and the surface (Saji, 2020). Some surfaces may retain a thin air layer at the interface (Zhao *et al.*, 2019; Ferrari and Benedetti, 2015). Alternatively, it is possible

for the material to absorb water. Principal component analysis and Pearson's correlation coefficient for correlation among the water barrier properties are shown in Figure 6E and 6F.

Figure 6 - Water contact angle (A), wettability (B), water vapor transmission rate – WVTR (C), and water vapor permeability – WVP (D) property of coated papers and their correlation analyzed by the principal component analysis (E) and Pearson's correlation coefficient (F).



The same letters for each property do not differ according to the Scott-Knott test at 5% significance.

Control treatments with no coating (C1) and double wet-and-dry coating (C2). Treatments with complementary proportions (m:m) of 1:0, 3:1, 1:1, 1:3, and 0:1 of cationic starch (S) and carnauba wax (W).

Source: From the author (2023).

Table 2 - Water absorbance and oil resistance of coated papers.

| Treatment | Cobb test (g/m ²) | Oil kit test- Surface* | Oil kit test - Fold* |
|-----------|-------------------------------|------------------------|----------------------|
| C1 | 37 ± 1 ^e | 0 | 0 |
| C2 | 36 ± 1 ^e | 0 | 0 |
| S | 189 ± 2 ^a | 10 | 0 |
| S3:1W | 73 ± 1 ^c | 9 | 0 |
| S1:1W | 57 ± 5 ^d | 8 | 0 |
| S1:3W | 56 ± 6 ^d | 5 | 0 |
| W | 91 ± 4 ^b | 6 | 0 |

* Oil kit test number according to T 559 cm-12 (TAPPI, 2012). Average value ± standard deviation. The same letters in the columns do not differ according to the Scott-Knott test at 5% significance. Control treatments with no coating (C1) and double wet-and-dry coating (C2). Treatments with complementary proportions (m:m) of 1:0, 3:1, 1:1, 1:3, and 0:1 of cationic starch (S) and carnauba wax (W).

Source: From the author (2023).

The highest contact angles were observed for samples C2, W, and S1:3W with $111\pm 1^\circ$, $100\pm 2^\circ$, and $100\pm 4^\circ$, respectively (Figure 6A). The high water contact angle of C2 might be induced by the double wet-and-dry procedure, which caused the hornification of paper (Mascarenhas *et al.*, 2022), hindering the access of hydroxyl groups to water molecules. Another reason might be the water tension release after drying (Vaezi, Asadpour, and Sharifi, 2019). According to Ferreira *et al.* (2017), a piece of the cell wall collapses when water is removed from fibers, increasing interfibrillar contact and forming hydrogen bonds that are both irreversible and partially reversible. Also, a thin layer of air may have formed on the paper fiber's surface, making it more hydrophobic (Samyn, 2013). For W and S1:3W samples, the coating composition explains their performance; due to their nonpolar chemical nature, waxes are the most affordable hydrophobic compounds (Basson and Reynhardt, 1988), generating high contact angles compared to cationic starch. For the S1:3W mixture, as suggested in Section 3.2, the micro, meso and macro roughness on the coating surface may also have contributed to the high angle. In turn, the high amount of hydroxyl in the cationic starch coated paper (S) resulted in a low contact angle with water of $78\pm 1^\circ$.

On the other hand, wettability, which indicates the water spread over the surface, was lower for the control treatments C1 and C2 with $0.01\pm 0.01^\circ/\text{s}$ (Figure 6B). The high wettability of carnauba wax ($0.58\pm 0.06^\circ/\text{s}$) can be explained by the insertion of the emulsifier polysorbate 80, making the material more hydrophilic, spreading the water drop in the coating. The addition of cationic starch to the wax caused the wettability of the coating to decrease, reaching $0.10\pm 0.05^\circ/\text{s}$ for S3:1W.

Wang *et al.* (2016) sprayed different liquid solutions of carnauba wax or beeswax to glass substrates. They found that the contact angle of the liquids was more than 150° when their surface free energy was more significant than 45 mN/m. Wang, He, and Zhao (2017) reached a 140° contact angle of a water/diesel drop in a TiO_2 + carnauba wax surface.

The WVTR and WVP values were similar for all treatments tested (Figures 6C and 6D). The water vapor, being a small molecule, passed through the paper's pores and the coating. Generally, porous materials and amorphous polysaccharides are highly susceptible to gas transport (Chi and Catchmark, 2018).

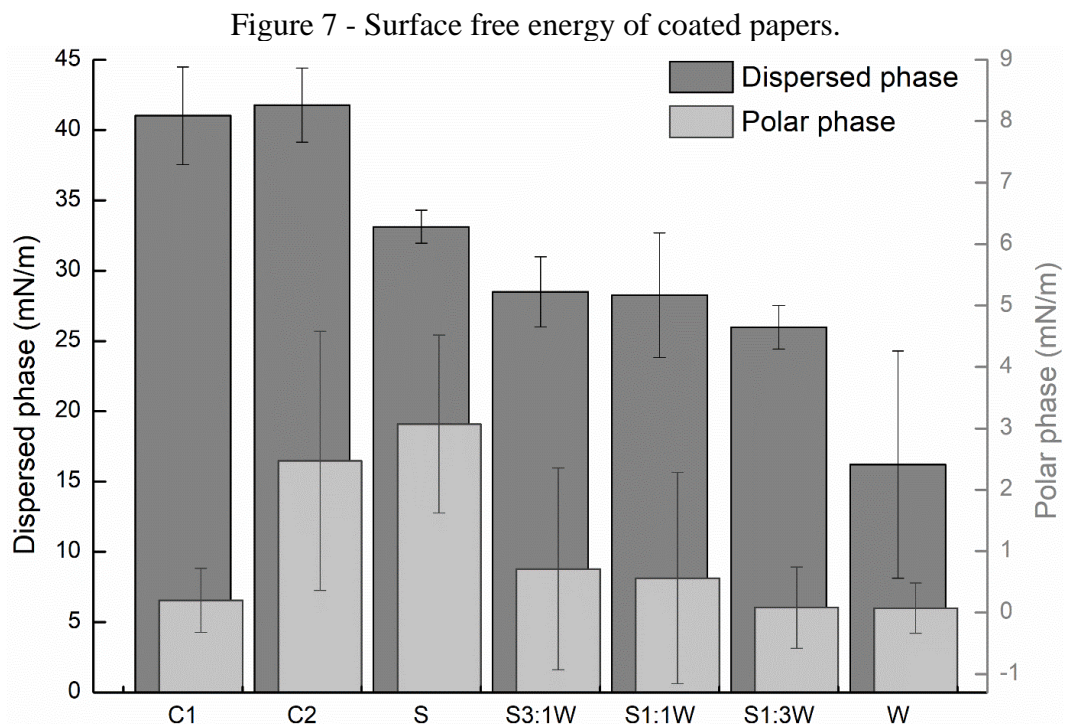
Evaluating the water absorption by the coated paper, the Cobb test indicated high absorption by the cationic starch with 189 ± 2 g/m² followed by the carnauba wax with 90.7 ± 3.6 g/m² (Table 2). The porosity of the papers and the number of available hydroxyls of the cationic starch promoted water absorption and swelling of the coating (Chi, Wang, and Catchmark, 2020). The samples formed by the mixtures presented lower Cobb values than the individual cationic starch and wax, confirming good synergism; however, they were still higher than the controls.

With the sum of the principal component analysis equal to 84.49%, the dimensional perceptual map (Figure 6E) is suitable for assessing the relationship between the studied variables. A strong dynamic between TPVA and PVA (Pearson's $r=0.85$) can be observed (Figure 6F). The positive value indicates the simultaneous increase of the correlated variables that present results on water vapor diffusion through the sample. Between the Cobb test and contact angle (Pearson's $r = -0.53$), the observed dynamics imply that one variable increases with the decrease of the other; in this way, when the contact angle reduces, indicating greater hydrophilicity of the material, its Cobb increases indicating greater absorption of water. With probabilities close to zero, the other variables studied showed weak correlations.

Coated papers demonstrated some oil barrier because of polymers and wax's polarity and cohesive energy (Table 2). Paper is a porous material that readily absorbs oil, which lowers its oil barrier. Tests were run on folds and multilayer paper surfaces to mimic packaging use. The cationic starch offered the kit oil n. 10 resistance, being kit n. 12 the maximum. The papers reduced the oil resistance to n. 5 for S1:3W when carnauba wax was added to cationic starch. The presence of more nonpolar C-C bonds and fewer polar C-O bonds may have contributed to it. None of the samples showed a barrier to oil when folded.

The barrier characteristics of multilayer sheets are also related to the surface free energy. Higher surface free energy supports more effective ink dispersion in coated paper, lowering the consumption of paint and, as a result, removing the need for corona charge treatment

(Mascarenhas *et al.*, 2022; Lopes *et al.*, 2018). In addition, the presence of accessible polar groups, such as hydroxyls, is expressed by the polar phase of the surface free energy. The samples with more significant wax contents, W and S1:3W, had the lowest values of the polar phase, measuring 0.08 and 0.07 mN/m, respectively (Figure 7). The rise in the polar phase of free energy for cationic starch, which reached 3.07 mN/m, is influenced by its hydrophilic functional groups. Żołek-Tryznowska and Holica (2020) discovered that the scattered phase was much higher than the polar phase for all samples.



Control treatments with no coating (C1) and double wet-and-dry coating (C2). Treatments with complementary proportions (m:m) of 1:0, 3:1, 1:1, 1:3, and 0:1 of cationic starch (S) and carnauba wax (W).

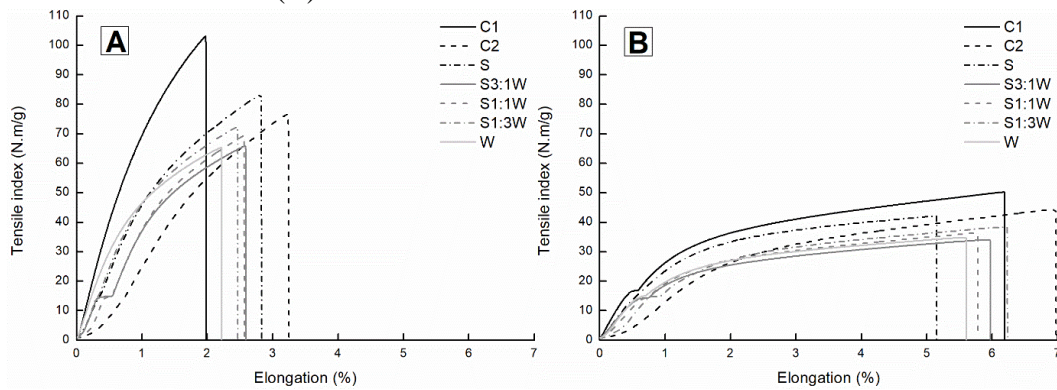
Source: From the author (2023).

3.5 Mechanical characterization

Paper is an anisotropic material, caused by fiber orientation (Alzweighi *et al.*, 2021), with mechanical properties that differ in the MD and CD directions. They are generally more rigid and resistant in MD, with lower elongation (Seth and Page, 1974), a behavior also observed for the multilayer papers (Figure 8, Table 3, and Table 4). Double wet-and-dry paper (C2) decreased the tensile strength and tensile index by 25% on MD papers and 10% on CD. The parallel separation of the fibers by humidity and the hornification by drying caused the impediment of interactions between fibers, decreasing their strength (Rhim, 2010; Parker,

Bronlund, and Mawson, 2006). Coatings based on cationic starch and carnauba wax have high water contents, as seen in early sections, directly influencing their application on paper and mechanical strength. The coating did not affect the fibers' orientation but changed their bonds (Lin *et al.*, 2017; Zhang, Xiao, and Qian, 2014), decreasing up to 25% tensile strength for MD in the S3:1W sample and 20% for CD, similarly found by W sample. Furthermore, a high hydrocarbon content in wax can favor the deterioration of the tensile strength (Liu *et al.*, 2019). Additionally, inserting glycerol into the mixture sample formula may decrease the tensile stress (Nordin *et al.*, 2020). Even with such a decrease, the papers have adequate tensile strength and now have barrier properties to oil, pencil hardness, and a higher water contact angle.

Figure 8 - Tensile properties of coated papers in the machine direction - MD (A) and the cross direction - CD (B).



Control treatments with no coating (C1) and double wet-and-dry (C2). Treatments with complementary proportions (m:m) of 1:0, 3:1, 1:1, 1:3, and 0:1 of cationic starch (S) and carnauba wax (W).

Source: From the author (2023).

Table 3 - Tensile properties of multilayer paper in the machine direction (MD).

| Sample | Tensile strength (kN/m) | Tensile Index (N.m/g) | Tensile energy absorption (J/m ²) | Tensile stiffness (kN/m) | Elongation (%) |
|--------|-------------------------|--------------------------|---|----------------------------|------------------------|
| C1 | 8.9 ± 0.1 ^a | 103.3 ± 1.5 ^a | 11.1 ± 0.4 ^b | 744.4 ± 29.2 ^a | 2.0 ± 0.1 ^d |
| C2 | 6.7 ± 0.5 ^c | 77.4 ± 5.3 ^c | 11.5 ± 2.3 ^b | 233.4 ± 36.0 ^c | 3.2 ± 0.4 ^a |
| S | 8.2 ± 0.2 ^b | 80.9 ± 2.1 ^b | 15.0 ± 1.1 ^a | 517.9 ± 107.1 ^b | 2.8 ± 0.1 ^b |
| S3:1W | 6.7 ± 0.2 ^c | 65.6 ± 2.3 ^e | 10.0 ± 0.8 ^c | 525.1 ± 133.6 ^b | 2.5 ± 0.1 ^c |
| S1:1W | 7.1 ± 0.2 ^b | 70.2 ± 1.5 ^d | 11.0 ± 0.6 ^b | 512.0 ± 44.6 ^b | 2.5 ± 0.1 ^c |
| S1:3W | 6.9 ± 0.5 ^b | 67.5 ± 4.5 ^e | 9.2 ± 2.1 ^c | 472.9 ± 142.1 ^b | 2.1 ± 0.3 ^d |
| W | 6.7 ± 0.2 ^c | 65.8 ± 1.6 ^e | 9.3 ± 1.1 ^c | 693.6 ± 27.6 ^a | 2.1 ± 0.2 ^d |

Average value ± standard deviation. The same letters in the columns do not differ according to the Scott-Knott test at 5% significance. Control treatments with no coating (C1) and double wet-and-dry (C2). Treatments with complementary proportions (m:m) of 1:0, 3:1, 1:1, 1:3, and 0:1 of cationic starch (S) and carnauba wax (W).

Source: From the author (2023).

Table 4 - Tensile properties of multilayer paper in the cross direction (CD).

| Sample | Tensile strength (kN/m) | Tensile Index (N.m/g) | Tensile energy absorption (J/m ²) | Tensile stiffness (kN/m) | Elongation (%) |
|--------|----------------------------|--------------------------|--|-----------------------------|------------------------|
| C1 | 4.4 ± 0.2 ^a | 50.5 ± 2.4 ^a | 19.5 ± 3.4 ^a | 336.9 ± 10.9 ^a | 5.9 ± 0.8 ^b |
| C2 | 4.0 ± 0.1 ^c | 46.0 ± 1.1 ^b | 20.7 ± 2.0 ^a | 144.5 ± 10.7 ^d | 7.7 ± 0.6 ^a |
| S | 4.2 ± 0.3 ^b | 40.9 ± 2.7 ^c | 17.7 ± 3.9 ^b | 286.0 ± 17.0 ^b | 5.5 ± 0.9 ^c |
| S3:1W | 3.5 ± 0.1 ^e | 34.1 ± 0.5 ^f | 13.9 ± 1.1 ^d | 252.3 ± 37.2 ^b | 5.3 ± 0.3 ^c |
| S1:1W | 3.7 ± 0.1 ^d | 36.5 ± 1.2 ^e | 16.6 ± 2.6 ^c | 275.1 ± 18.7 ^b | 5.8 ± 0.8 ^b |
| S1:3W | 3.9 ± 0.1 ^c | 38.0 ± 1.2 ^d | 18.2 ± 1.3 ^b | 249.6 ± 35.9 ^c | 6.2 ± 0.3 ^b |
| W | 3.5 ± 0.1 ^e | 34.5 ± 1.2 ^f | 15.9 ± 1.6 ^c | 275.1 ± 38.2 ^b | 5.8 ± 0.5 ^b |

Average value ± standard deviation. The same letters in the columns do not differ according to the Scott-Knott test at 5% significance. Control treatments with no coating (C1) and double wet-and-dry (C2). Treatments with complementary proportions (m:m) of 1:0, 3:1, 1:1, 1:3, and 0:1 of cationic starch (S) and carnauba wax (W).

Source: From the author (2023).

In addition to the tensile strength, the drying cycle negatively affected the tensile stiffness of the papers, decreasing 69% in MD and 57% in CD. The replacement of the intermolecular interactions between the hydroxyls of the fibers by the water molecule followed by double drying generated stiffer papers (Sørensen and Hoffmann, 2003; Bandyopadhyay, Ramarao, and Ramaswamy, 2002). On the other hand, Hassani *et al.* (2022) evaluated a crosslinked cationic starch coating on bleached papers and found a 103% increase in Young's modulus through interfacial adhesion. However, Bandyopadhyay, Ramarao, and Ramaswamy (2002) suggested that Young's modulus generally decreases in humid environments.

The elongation property, on the other hand, increased with water application when comparing C1 and C2. As fiber interactions decrease, for the reasons already mentioned, the slipping between them grows, increasing the paper's elasticity. However, when applying the coating with the mixtures, the samples with higher cationic starch content favored elongation, while those with higher wax content maintained the elongation of the C1 control treatment. The interaction between wax and cationic starch increases the flexibility and extensibility of the films, influencing the elongation of the multilayer paper (Liu *et al.*, 2022). In addition, Follain *et al.* (2005) suggested that the late retrogradation of starch causes increased elongation due to the introduction of structural defects by crosslinking.

The addition of carnauba wax into a cationic starch matrix for coating on kraftliner paper shown significant promise as barrier layers with good mechanical strength. Modifications to increase their hydrophobicity might provide a potential replacement in terms of lowering non-renewable material, so contributing to the manufacture of green packaging.

4. CONCLUSION

The mixture of cationic starch biopolymer and the natural carnauba wax showed good compatibility, confirmed by FT-IR and Raman spectroscopy. The mixture increased the wax's melting temperature, not penetrating entirely into the paper's pores but forming a layer over it. Carnauba wax incorporated into cationic starch increased the water contact angle and decreased the dispersed and polar phases of the surface free energy of the coated papers. On the other hand, cationic starch reduced the wettability caused by the wax and increased its resistance to oil. However, the water vapor permeability rate was not altered, with the insertion of glycerol and polysorbate 80 being a probable cause. The cationic starch/wax interaction still generated lower water absorption than the individual polymers; however, they were not inferior to those found in the control kraftliner papers C1 and C2. Regarding the mechanical strength, water in the suspensions seems to have been primarily responsible for the decreased tensile strength and Young's modulus of the coated papers caused by hornification under drying. Better formulations seeking excellent barriers still need to be explored and there is still a long way to find a biodegradable material from an affordable renewable resource, aiming at high-quality packaging. We hope to have contributed to improving the understanding of wax and cationic starch mixtures, seeking a healthy human–environment relationship.

ACKNOWLEDGMENT

This study was financed in part by the Coordenação de Aperfeiçoamento de Pessoal de Nível Superior – Brasil (CAPES) – Finance Code 001. The authors are grateful for the support of the Laboratory BioNano from the Federal University of Pelotas - UFPel, the Laboratory of Electron Microscopy and Analysis of Ultrastructural from the Federal University of Lavras - UFLA, and FINEP, FAPEMIG, CNPq, Rede RELIGAR and CAPES for supplying the equipment and technical support for experiments involving electron microscopy. The authors are also thankful for the Wood Science and Technology graduate program at the Federal University of Lavras – UFLA, the Forest, Nature, and Biomass section, and the department of Chemistry at the University of Copenhagen - UCPH. Likewise, Klabin S/A for supplying commercial kraft paper and some characterization.

REFERENCES

- ABADIAS, G.; CHASON, E.; KECKES, E. *et al.* Stress in thin films and coatings: Current status, challenges, and prospects. **Journal of Vacuum Science and Technology A**, v. 36, n. 2, p.020801, 2018.
- ABDULLA, A.H.D.; PUDJIRAHAR, S.; KARINA, M. *et al.* Fabrication and characterization of sweet potato starch-based bioplastics plasticized e work reported in this p with glycerol. **Journal of Biological Sciences**, v. 19, p. 57–64, 2018.
- ABNT NBR 8877 (2020) Adhesives - Determination of solids content. **Associação Brasileira de Normas Técnicas**, São Paulo, SP, 2020.
- ABNT NBR 9277 (2020) Adesivos - Determinação da viscosidade - Método do viscosímetro Brookfield, **Associação Brasileira de Normas Técnicas**, São Paulo, SP, 2020.
- ALVES, A. P. P.; OLIVEIRA, L. P. Z.; CASTRO, A. A. N. *et al.* The structure of different cellulosic fibres characterized by Raman spectroscopy. **Vibrational Spectroscopy**, v. 86, p. 324–330, 2016.
- ALZWEIGHI, M.; MANSOUR, R.; LAHTI, J. *et al.* The influence of structural variations on the constitutive response and strain variations in thin fibrous materials. **Acta Materialia**, v. 203, p. 116460, 2021.
- ASTM D3363-22 (2022) Standard Test Method For Film Hardness By Pencil Test. **ASTM International**, West Conshohocken, PA, 2022.
- ASTM D646-13 (2013) Standard Test Method for Grammage of Paper and Paperboard (Mass Per Unit Area). **ASTM International**, West Conshohocken, PA, 2013.
- ASTM D724-99 (2003) Standard Test Method For Surface Wettability Of Paper (Angle-Of-Contact Method). **ASTM International**, West Conshohocken, PA, 2003.
- ASTM D828-22 (2022) Standard Test Method For Tensile Properties Of Paper And Paperboard Using Constant-Rate-Of-Elongation Apparatus. **ASTM International**, West Conshohocken, PA, 2022.
- ASTM E104-02 (2012) Standard Practice For Maintaining Constant Relative Humidity By Means Of Aqueous Solutions. **ASTM International**, West Conshohocken, PA, 2002.
- ASTM E96 / E96M-16 (2016) Standard Test Methods for Water Vapor Transmission of Materials. **ASTM International**, West Conshohocken, PA, 2016.
- ASTM T 458 cm-04 (2004) Surface Wettability Of Paper (Angle Of Contact Method). **ASTM International**, West Conshohocken, PA, 2004.
- BAČOVSKÁ, R.; WISIAN-NEILSON, P.; ALBERTI, M. *et al.* Phenyl-methyl phosphazene derivatives for preparation and modification of hydrophobic properties of polymeric nonwoven textiles. **Reactive and Functional Polymers**, v. 100, p. 53-63, 2016.

BANDYOPADHYAY, A.; RAMARAO, B. V.; RAMASWAMY, S. Transient moisture diffusion through paperboard materials. **Colloids and Surfaces A: Physicochemical and Engineering Aspects**, v. 206, n.1-3, p. 455-467, 2002.

BASIAK, E.; LENART, A.; DEBEAUFORT, F. How Glycerol and Water Contents Affect the Structural and Functional Properties of Starch-Based Edible Films. **Polymers**, v. 10, n. 4, p. 412, 2018.

BASSON, I.; REYNHARDT, E. C. An investigation of the structures and molecular dynamics of natural waxes. I. Beeswax. **Journal of Physics D: Applied Physics**, v. 21, p. 1421–1428, 1988.

BETTAIEB, F.; KHIARI, R.; DUFRESNE, A. *et al.* Mechanical and thermal properties of *Posidonia oceanica* cellulose nanocrystal reinforced polymer. **Carbohydrate Polymer**, v. 123, p. 99–104, 2015.

BIAN, H., GAO, Y., LUO, J. *et al.* Lignocellulosic nanofibrils produced using wheat straw and their pulping solid residue: from agricultural waste to cellulose nanomaterials. **Waste Management**, v. 91, p. 1–8, 2019.

BULKIN, B.; KWAK, Y. Retrogradation kinetics of waxy-corn and potato starches: A rapid, Raman-spectroscopic study. **Carbohydrate Research**, v. 160, p. 95–112, 1987.

CHEN, L.; SUN, X.; HANG, J. *et al.* Large-Scale Fabrication of Robust Superhydrophobic Coatings with High Rigidity and Good Flexibility. **Advanced materials interfaces**, v. 3, p. 1500718, 2016.

CHENG, Y.; ZHAI, X.; WU, U. *et al.* Effects of natural wax types on the physicochemical properties of starch/gelatin edible films fabricated by extrusion blowing. **Food Chemistry**, v. 401, p. 134081, 2023.

CHI, K.; CATCHMARK, J. M. Improved eco-friendly barrier materials based on crystalline nanocellulose/chitosan/carboxymethyl cellulose polyelectrolyte complexes. **Food Hydrocolloids**, v. 80, p. 195-205, 2018.

CHI, K.; WANG, H.; CATCHMARK, J. M. Sustainable starch-based barrier coatings for packaging applications. **Food Hydrocolloids**, v. 103, p. 105696, 2020.

CHIUMARELLI, M.; HUBINGER, M. D. Evaluation of edible films and coatings formulated with cassava starch, glycerol, carnauba wax and stearic acid. **Food Hydrocolloids**, v. 38, p. 20-27, 2014.

CHIUMARELLI, M.; HUBINGER, M. D. Stability, solubility, mechanical and barrier properties of cassava starch – Carnauba wax edible coatings to preserve fresh-cut apples. **Food Hydrocolloids**, v. 28, n. 1, p. 59-67, 2012.

CIANNAMEA, E. M.; CASTILLO, L. A.; BARBOSA, S. E. *et al.* Barrier properties and mechanical strength of bio-renewable, heat-sealable films based on gelatin, glycerol and soybean oil for sustainable food packaging. **Reactive and Functional Polymers**, v. 125, p. 29–36, 2018.

DESPOND, S.; ESPUCHE, E.; CARTIER, N. *et al.* Barrier properties of paper-chitosan and paper-chitosan-carnauba wax films. **Journal of Applied Polymer Science**, v. 98, p. 704–710, 2005.

DEVI, L. S.; KALITA, S.; MUKHERJEE, A. *et al.* Carnauba wax-based composite films and coatings: recent advancement in prolonging postharvest shelf-life of fruits and vegetables. **Trends in Food Science and Technology**, v. 129, p. 296–305, 2022.

DICKINSON, E. D. Towards more natural emulsifiers. **Trends in Food Science and Technology**, v. 10, p. 330–334, 1993.

DILKES-HOFFMAN, L. S.; PRATT, S.; LANT, P. A. *et al.* 19 - The Role of Biodegradable Plastic in Solving Plastic Solid Waste Accumulation. In: AL-SALEM, S. M. *Plastics to Energy*. **William Andrew Publishing**, p. 469-505, 2019.

DIYANA, Z. N.; JUMAIDIN, R.; SELAMAT, M. Z. *et al.* Thermoplastic starch/beeswax blend: Characterization on thermal mechanical and moisture absorption properties. **International Journal of Biological Macromolecules**, v. 190, p. 224–232, 2021.

EBNESAJJAD, S. *Handbook of Biopolymers and Biodegradable Plastics: Properties, Processing and Applications*. **Elsevier Science**, 1204 p., 2012.

EDWARDS, H. G. M.; FALK, M. J. P. Fourier-transform Raman spectroscopic study of unsaturated and saturated waxes. **Spectrochimica Acta Part A**, v. 53, p. 2685–2694, 1997.

ESPINOSA, E.; DOMÍNGUEZ-ROBLES, J.; SÁNCHEZ, R. *et al.* The effect of pre-treatment on the production of lignocellulosic nanofibers and their application as a reinforcing agent in paper. **Cellulose**, v. 24, p. 2605–2618, 2017.

FDA - Food and Drugs Administration, 2012. Chapter I - Food and drug administration, department of health and human services (continued), part 184, direct food substances affirmed as generally recognized as safe, Sec. 184.1978 - carnauba wax. **Title 21 – Food and drugs**. <https://www.govinfo.gov/app/details/CFR-2012-title21-vol3/CFR-2012-title21-vol3-sec184-1978> (Accessed October 7th, 2022), 2012.

FERRARI, M.; BENEDETTI, A. Superhydrophobic surfaces for applications in seawater. **Advances in Colloid and Interface Science**, v. 222, p. 291–304, 2015.

FERREIRA, D. F. Sisvar: a Guide for its Bootstrap procedures in multiple comparisons. **Ciência e agrotecnologia**, v. 38, n.2, 2014.

FERREIRA, S. R.; SILVA, F. A.; LIMA, P. R. L. *et al.* Effect of hornification on the structure, tensile behavior and fiber matrix bond of sisal, jute and curaua´ fiber cement based composite systems. **Construction and Building Materials**, v. 139, p. 551–561, 2017.

FIROOZMAND, H.; MURRAY, B. S.; DICKINSON, E. Microstructure and rheology of phase-separated gels of gelatin + oxidized starch. **Food Hydrocolloids**, v. 23, p. 1081–1088, 2009.

FOLLAIN, N.; JOLY, C.; DOLE, P. *et al.* Properties of starch based blends. Part 2. Influence of poly vinyl alcohol addition and photocrosslinking on starch based materials mechanical properties. **Carbohydrate Polymers**, v. 60, n. 2, p. 185-192, 2005.

FORSMAN, N.; JOHANSSON, L.; KOIVULA, H.; *et al.* Open coating with natural wax particles enables scalable, non-toxic hydrophobation of cellulose-based textiles. **Carbohydrate Polymers**, v. 227, n. 1, p. 115363, 2020.

GADHAVE, R.V.; MAHANWAR, P.A.; GADEKAR, P.T. Effect of glutaraldehyde on thermal and mechanical properties of starch and polyvinyl alcohol blends. **Designed Monomers and Polymers**, v. 22, p. 164–170, 2019.

GAO, W.; DONG, H.; HOU, H. *et al.* Effects of clays with various hydrophilicities on properties of starch–clay nanocomposites by film blowing. **Carbohydrate Polymers**, v. 88, n. 1, p. 321-328, 2012.

GAO, W.; WU, W.; LIU, P. *et al.* Preparation and evaluation of hydrophobic biodegradable films made from corn/octenylsuccinated starch incorporated with different concentrations of soybean oil. **International Journal of Biological Macromolecules**, v. 142, p. 376-383, 2020.

GUIMARÃES JR., M.; BOTARO, V.R.; NOVACK, K.M. *et al.* Preparation of cellulose nanofibrils from bamboo pulp by mechanical defibrillation for their applications in biodegradable composites. **Journal of Nanoscience and Nanotechnology**, v. 15, p. 6751–6768, 2015.

GUO, Z.; JIA, X.; LIN, X. *et al.* Insight into the formation, structure and digestibility of lotus seed amylose-fatty acid complexes prepared by high hydrostatic pressure. **Food and Chemical Toxicology**, v. 128, p. 81–88, 2019.

HASSANI, S. A.; SALIM, F. Z.; KASSAB, M. H. *et al.* Crosslinked starch-coated cellulosic papers as alternative food-packaging materials. **RSC Advances**, v. 12, n. 14, p. 8536-8546, 2022.

HU, X.; SHI, J.; ZHANG, F. *et al.* Determination of retrogradation degree in starch by mid-infrared and Raman spectroscopy during storage. **Food Analytical Methods**, v. 10, n. 11, p. 3694–3705, 2017.

ISO 534:2011 (2011) Paper And Board - Determination Of Thickness, Density And Specific Volume. **International Organization for Standardization**, Washington, DC, 2011.

JAKUBOWSKA, E.; GIERSZEWSKA, M.; SZYDŁOWSKA-CZERNIAK, a. *et al.* Development and characterization of active packaging films based on chitosan, plasticizer, and quercetin for repassed oil storage. **Food Chemistry**, v. 399, p. 133934, 2023.

KORHONEN, O., FORSMAN, N., ÖSTERBERG, M., *et al.* Eco-friendly surface hydrophobization of all-cellulose composites using layer-by-layer deposition. **Express Polymer Letters**, v. 14, n. 10, p. 896-907, 2020.

- KRUK, J.; TKACZEWSKA, J.; SZUWARZYŃSKI, M. *et al.* Influence of storage conditions on functional properties of multilayer biopolymer films based on chitosan and furcellaran enriched with carp protein hydrolysate. **Food Hydrocolloids**, v. 135, p. 108214, 2023.
- LAGO, R. C.; OLIVEIRA, A. L. M.; SANTOS, A. A. *et al.* Addition of wheat straw nanofibrils to improve the mechanical and barrier properties of cassava starch-based bionanocomposites. **Industrial Crops and Products**, v. 170, p. 113816, 2021.
- LAROTONDA, F. D. S.; MATSUI, K. N.; SOBRAL, P. J. A. *et al.* Hygroscopicity and water vapor permeability of Kraft paper impregnated with starch acetate. **Journal of Food Engineering**, v. 71, n. 4, p. 394-402, 2005.
- LIN, D.; KUANG, Y. CHEN, G. *et al.* Enhancing moisture resistance of starch-coated paper by improving the film forming capability of starch film. **Industrial Crops and Products**, v. 100, p. 12-18, 2017.
- LIU, B.; XUE, C.; AN, Q. *et al.* Fabrication of superhydrophobic coatings with edible materials for super-repelling non-newtonian liquid foods. **Chemical Engineering Journal**, v. 371, p. 833–841, 2019.
- LIU, S.; LIU, L.; LI, B. *et al.* Size effect of carnauba wax nanoparticles on water vapor and oxygen barrier properties of starch-based film. **Carbohydrate Polymers**, v. 296, p. 119935, 2022.
- LOPES, T. A.; BUFALINO, L.; CLARO, P. I. C. *et al.* The effect of surface modifications with corona discharge in Pinus and Eucalyptus nanofibril films. **Cellulose**, v. 25, p. 5017–5033, 2018.
- LU, H.; TIAN, Y.; MA, R. Assessment of order of helical structures of retrograded starch by Raman spectroscopy. **Food Hydrocolloids**, v. 134, p. 108064, 2023.
- MA, S.; KOVASH JR., C.S.; WEBSTER, D.C. Effect of solvents on the curing and properties of fully bio-based thermosets for coatings. **Journal of Coatings Technology and Research**, v. 14, p. 367–375, 2017.
- MATOS, L.C; ROMPA, V.D.; DAMÁSIO, R.A.P. *et al.* Incorporação de nanomateriais e emulsão de ceras no desenvolvimento de papéis multicamadas. **Scientia Forestalis**, v. 47, n. 122, p. 1-15, 2019.
- MASCARENHAS, A. R. P.; SCATOLINO, M. V.; DIAS, M. C. *et al.* Association of cellulose micro/nanofibrils and silicates for cardboard coating: Technological aspects for packaging. **Industrial Crops and Products**, v. 188, n. 1, p. 115667, 2022.
- MCCLEMENTS, D. J. Critical review of techniques and methodologies for characterization of emulsion stability. **Critical Reviews in Food Science and Nutrition**, v. 47, p. 611-649, 2007.
- MIAO, X.; LIN, J.; BIAN, F. Utilization of discarded crop straw to produce cellulose nanofibrils and their assemblies. **Journal of Bioresources and Bioproducts**, v. 5, p. 26–36, 2020.

MIRANDA, M.; RIBEIRO, M. M. M.; SPRICIGO, P. C. *et al.* Carnauba wax nanoemulsion applied as an edible coating on fresh tomato for postharvest quality evaluation. **Heliyon**, v. 8, p. e09803, 2022.

MUSCAT, D.; ADHIKARI, R.; MCKNIGHT, S. *et al.* The physicochemical characteristics and hydrophobicity of high amylose starch–glycerol films in the presence of three natural waxes. **Journal of Food Engineering**, v. 119, p. 205–219, 2013.

MUTHU, S.S. Environmental Footprints of Packaging. **Springer Singapore**, v. 1, n. 1, 192 p. 2016.

NAM, S.; FRENCH, A.; CONDON, B. *et al.* Segal crystallinity index revisited by the simulation of X-ray diffraction patterns of cotton cellulose I β and cellulose II. **Carbohydrate Polymers**, v. 135, p. 1–9, 2016.

NOÈ, C.; TONDA-TURO, C.; CARMAGNOLA, I. *et al.* UV-Cured Biodegradable Methacrylated Starch-Based Coatings. **Coatings**, v. 11, p. 127, 2021.

NORDIN, N.; OTHMAN, S.H.; RASHID, S.A. *et al.* Effects of Glycerol and Thymol on Physical, Mechanical, and Thermal Properties of Corn Starch Films. **Food Hydrocolloids**, v. 106, p. 105884, 2020.

NILSEN-NYGAARD, J.; FERNÁNDEZ, E. N.; RADUSIN, T. *et al.* Current status of biobased and biodegradable food packaging materials: Impact on food quality and effect of innovative processing technologies. **Comprehensive Reviews in Food Science and Food Safety**, v. 20, p. 1333-1380, 2021.

OLIVEIRA FILHO, J. G.; ALBIERO, B. R.; CALISTO, I. H. *et al.* Bio-nanocomposite edible coatings based on arrowroot starch/cellulose nanocrystals/carnauba wax nanoemulsion containing essential oils to preserve quality and improve shelf life of strawberry. **International Journal of Biological Macromolecules**, v. 219, p. 812–823, 2022.

OLIVEIRA FILHO, J. G.; BEZERRA, C. C. O. N.; ALBIERO, B. R. *et al.* New approach in the development of edible films: The use of carnauba wax micro- or nanoemulsions in arrowroot starch-based films. **Food Packaging and Shelf Life**, v. 26, p. 100589, 2020.

OLIVOTO, T.; LÚCIO, A. D. Metan: An R package for multi-environment trial analysis. **Methods in Ecology and Evolution**, v. 11, p. 783-789, 2020.

OLSSON, E.; MENZEL, C.; JOHANSSON, C. *et al.* The effect of pH on hydrolysis, cross-linking and barrier properties of starch barriers containing citric acid. **Carbohydrate Polymers**, v. 98, n. 2, p. 1505-1513, 2013.

PARKER, M.E.; BRONLUND, J.E; MAWSON, A.J. Moisture sorption isotherms for paper and paperboard in food chain conditions. **Packaging Technology and Science**, v. 19, p. 193-209, 2006.

PETERSEN, K.; NIELSEN, P.V.; BERTELSEN, G. *et al.* Potential of biobased materials for food packaging. **Trends in Food Science and Technology**, v. 10, p. 52-68, 1999.

- PODSHIVALOV, A.; ZAKHAROVA, M.; GLAZACHEVA, E. *et al.* Gelatin/potato starch edible biocomposite films: Correlation between morphology and physical properties. **Carbohydrate Polymers**, v. 157, p. 1162–1172, 2017.
- REICHERT, C. L.; BUGNICOURT, E.; COLTELLI, M. B. *et al.* Bio-Based Packaging: Materials, Modifications, Industrial Applications and Sustainability. **Polymers**, v. 12, n. 7, p. 1558, 2020.
- RHIM, JW. Effect of moisture content on tensile properties of paper-based food packaging materials. **Food Science and Biotechnology**, v. 19, p. 243–247, 2010.
- RODRIGUES, D. C.; CACERES, C. A.; RIBEIRO, H. L. *et al.* Influence of cassava starch and carnauba wax on physical properties of cashew tree gum-based films. **Food Hydrocolloids**, v. 38, p. 147-151, 2014.
- ROJAS-LEMA, S.; NILSSON, K.; LAGTON, M. *et al.* The effect of pine cone lignin on mechanical, thermal and barrier properties of faba bean protein films for packaging applications. **Journal of Food Engineering**, v. 339, p. 111282, 2023.
- SÁ, R. M.; MIRANDA, C. S.; JOSÉ, N. M. Preparation and characterization of Nanowhiskers cellulose from fiber arrowroot (*Maranta arundinacea*). **Materials Research**, v. 18, p. 225–229, 2015.
- SAJI, V. S. Wax-based Artificial Superhydrophobic Surfaces and Coatings. **Colloids and Surfaces A: Physicochemical and Engineering Aspects**, v. 602, p. 125132, 2020.
- SAKKARA, S.; NATARAJ, D.; VENKATESH, K. *et al.* Effect of pH on the physicochemical properties of starch films. **Journal of Applied Polymer Science**, p. 48563-48563, 2020.
- SALMÉN, L.; BERGSTRÖM, E. Cellulose structural arrangement in relation to spectral changes in tensile loading FT-IR. **Cellulose**, v. 16, p. 975–982, 2009.
- SAMYN, P. Wetting and hydrophobic modification of cellulose surfaces for paper applications. **Journal of Material Science**, v. 48, p. 6455–6498, 2013.
- SANTOS, A. M. P.; YOSHIDA, M. P. Embalagens. Recife: **Edufre**, 152p. ISBN 978-85-7946-090-6, 2011.
- SETH, R. S.; PAGE, D. J. Fracture resistance of paper. **Journal of Materials Science**, v. 9, p. 1745-1753, 1974.
- SØRENSEN, G.; HOFFMANN, J. Moisture sorption in moulded fibre trays and effect on static compression strength. **Packaging Technology and Science**, v. 16, p. 159-169, 2003.
- TAPPI T 559 cm-12 (2012) Grease Resistance Test for Paper and Paperboard. **Technical Association of the Pulp and Paper Industry**, Peachtree Corners, GA, United States, 2012.

TAPPI T441 om-13 (2013) Water absorptiveness of sized (non-bibulous) paper, paperboard, and corrugated fiberboard (Cobb test). **Technical Association of the Pulp and Paper Industry**, Peachtree Corners, GA, United States, 2013.

TINTO, W. F.; ELUFIOYE, T. O.; ROACH, J. Waxes In Pharmacognosy – Fundamentals, Applications and Strategies. BADAL, S.; DELGODA, R. **Elsevier**, p. 443–455, 2017.

TODOROVA, D.; YAVOROV, N.; LASHEVA, V. Improvement of barrier properties for packaging applications. **Sustainable Chemistry and Pharmacy**, v. 27, p. 100685, 2022.

TOMASIK, P.; SCHILLING, C.H. Chemical modification of starch. **Advances in Carbohydrate Chemistry and Biochemistry**, v. 59, p. 175-403, 2004.

TORRES, F.I.; DA SILVA, J.C.; VIEIRA, O. *et al.* Eukalinertm: the first 100% hardwood kraftliner in the world. In: 53RD ABTCP INTERNATIONAL PULP AND PAPER CONGRESS AND EXHIBITION AND 9TH. 2020. São Paulo, **Anais [...]** São Paulo: ABCTP, 2020.

TRINH, B. M.; SMITH, M.; MEKONNEN, T. H. A nanomaterial-stabilized starch-beeswax Pickering emulsion coating to extend produce shelf-life. **Chemical Engineering Journal**, v. 431, p. 133905, 2022.

VAEZI, K.; ASADPOUR, G.; SHARIFI, S. H. Effect of coating with novel bio nanocomposites of cationic starch/cellulose nanocrystals on the fundamental properties of the packaging paper. **Polymer Testing**, v. 80, p. 106080, 2019.

WANG, W.; LOCKWOOD, K.; BOYD, L. M. *et al.* Superhydrophobic Coatings with Edible Materials. **ACS Applied Materials and Interfaces**, v. 8, n. 29, p. 18664–18668, 2016.

WANG, Y.; HE, B.; ZHAO, L. Fabrication of hydrophobic coating on filter paper from selfemulsifying carnauba wax-alcohol emulsions with nano-TiO₂ particles for water/diesel separation. **BioResources**, v. 12, p. 7774–7783, 2017.

WYAN, L. **Analysis of Over-the-Counter Antihistamines Through Raman Spectroscopy and Density Functional Theory Calculations**. Honors College Theses – Pace University, New York, 264 p., 2019.

YANG, J.; ZHAO, K.; WANG, G. *et al.* Influence of coating thickness on microstructure, mechanical and LBE corrosion performance of amorphous AlCrFeTiNb high-entropy alloy coatings. **Surface and Coatings Technology**, v. 441, p. 128502, 2022.

ZHANG, R.; WANG, W.; ZHANG, H. *et al.* Effects of hydrophobic agents on the physicochemical properties of edible agar/maltodextrin films. **Food Hydrocolloids**, v. 88, p. 283–290, 2019.

ZHANG, W.; XIAO, H.; QIAN, L. Enhanced water vapour barrier and grease resistance of paper bilayer-coated with chitosan and beeswax. **Carbohydrate Polymers**, v. 101, p. 401-406, 2014.

ZHAO, Y.; LIU, E.; FAN, J. *et al.* Superhydrophobic PDMS/wax coated polyester textiles with self-healing ability via inlaying method. **Progress in Organic Coatings**, v. 132, p. 100-107, 2019.

ZHENG, Y.; OU, Y.; ZHANG, C. *et al.* The impact of various exogenous type starch on the structural properties and dispersion stability of autoclaved lotus seed starch. **International Journal of Biological Macromolecules**, v. 175, p. 49–57, 2021.

ZHU, M.; YING, D.; ZHANG, H. Self-healable hydrophobic films fabricated by incorporating natural wax into cellulose matrix. **Chemical Engineering Journal**, v. 446, p. 136791, 2022.

ŻOŁEK-TRYZNOWSKA, Z.; HOLICA, J. Starch films as an environmentally friendly packaging material: Printing performance. **Journal of Cleaner Production**, v. 276, p. 124265, 2020.

FOURTH PART

Addition of bentonite to cationic starch matrix for coating on kraftliner paper to improve grease resistance

Allan de Amorim dos Santos^{ab*}, Lays Camila Matos^a, Maressa Carvalho Mendonça^{ac}, Marcelo Coelho dos Santos Muguet^c, Andrea Ponzecchi^b, Anand Ramesh Sanadi^b, Gustavo Henrique Denzin Tonoli^a.

^a Department of Forest Science, University of Lavras, University Campus, P.O. Box 3037, 37200-000, Lavras, MG, Brazil.

^b Department of Geosciences and Natural Resource Management, University of Copenhagen, Rolighedsvej 23 – 1958, Frederiksberg, Denmark.

^c Klabin, Technology Center, Industrial R&D+I, Fazenda Monte Alegre, St. Harmonia, 84275-000, Telêmaco Borba, PR, Brazil.

* Corresponding author: *allan.santos1@estudante.ufla.br*

Paper published at Nordic Pulp and Paper Research Journal
<https://doi.org/10.1515/npprj-2022-0104>

Received December 15, 2022;

accepted March 5, 2023;

published online March 17, 2023.

ABSTRACT

In this work, we aimed to analyze suspensions of cationic starch by adding 5 wt%, 7 wt%, and 10 wt% of bentonite as a bilayer coating on kraftliner paper (85 g/m²). The controls were doubly-wet-and-dry and uncoated kraftliner paper. In a coating machine, the formulations were applied until reaching a grammage of 15 g/m² and then dried at 103 ± 2 °C. The test was carried out about pH, solids content, and viscosity of the suspensions. The physical characteristics of the coated papers were evaluated, as well as their ability to block water, water vapor, and oil/grease. We also analyzed with scanning electron microscopy, Raman spectroscopy, and Fourier transform infrared spectroscopy. The packaging, having a water contact angle of up to 78° and 189 g/m² for Cobb, showed a low resistance to water, which is further responsible for decreased mechanical resistance. Nevertheless, the coating did not change the permeability to water vapor, however, bentonite promoted a decrease in wettability

and Cobb value of the paper. The addition of 7 wt% bentonite to the cationic starch matrix promoted high oil resistance with 12 for kit-oil, while 10 wt% bentonite promoted greater pencil hardness, with a value of 8H. Bentonite strength and cationic starch showed good interaction, increasing oil resistance.

Keywords: Bentonite clay. Green packaging. Kraft paper. Montmorillonite. Multilayer packaging.

1. INTRODUCTION

Using renewable materials as barriers for consumer products in place of synthetic, petroleum-based polymers is a hotly debated research topic (Dey *et al.*, 2022; Todorova *et al.*, 2022; Wang *et al.*, 2022; Zhu *et al.*, 2022). Starch is one potential substituent as a coating on paper, functioning well as a biopolymer for creating films due to the angulation of the glucose unit bonds and the extension of the amylopectin chain. These films have a low mechanical strength, moderate oil and gas barrier, and low moisture barrier, but they also have a high yield and availability. Starch and plasticizers can be mixed to increase the strength of the films. The most popular low molecular mass plasticizer addition for starch is glycerol, which is safe and ideal for packaging that comes into contact with food (Basiak *et al.*, 2018). Starch is very hydrophilic due to the abundance of primary and secondary hydroxyl groups at carbons 2, 3, and 6. These hydroxyl groups are susceptible to the addition or modification of cations and anions (Tomasik and Schilling, 2004).

Due to their potential to enhance barrier qualities, combining clay minerals from various origins into polymeric matrices, such as starch, has also been the subject of numerous investigations in recent years. The clay minerals strengthen the starch matrix for coatings and films, including talc (Castillo *et al.*, 2019), montmorillonite (Olsson *et al.*, 2014a; Wang and Jing, 2017), kaolinite (Méité *et al.*, 2022), halloysite (Dang *et al.*, 2020), sepiolite (Olivato *et al.*, 2017), and bentonite (Breen *et al.*, 2019; Clegg *et al.*, 2019; Vaysi and Vaghari, 2021; Oliveira *et al.*, 2022). The mechanical, barrier, thermal, and antibacterial properties of paper products can be improved by clay/starch nanocomposites.

According to Nielsen (1967), the formation of a tortuous pathway that lengthens the effective distance for gas molecules to diffuse through a material is the cause of barrier properties. Increasing the particle aspect ratio lowers aggregation and improves particle alignment, which lowers permeability. Moreover, the addition of clay minerals to a polymeric matrix can reduce the mobility of the polymeric phase in the film immediately adjacent to the

surface of the particles, thereby reducing the mobility of penetrant molecules in this area and reducing the diffusion of small molecules through the structure (Drozdov *et al.*, 2003). Furthermore, paper is primarily filled with and coated with nanoclays. A nanoclay enhances printability and the appearance of the paper, characterized by gloss, smoothness, brightness, and opacity. Nanoclays also stretch the fiber in paper (Bundy and Ishley, 1991). They are hydrated aluminum silicates formed by silicon, aluminum or magnesium, oxygen, and hydroxyl groups linked to cations. Their structures are found in layers that are irregularly spaced and have a large surface area (Gul *et al.*, 2016).

Bentonite is a phyllo-silicate clay mineral with tetrahedral and octahedral structures coordinated into 2:1 layers in a nanoscale dimension that can expand. Bentonite has attracted great attention from the nanoclay community and is already employed as a filler to boost maximum tensile strength, even in small quantities. In addition, bentonite assists in filling the porosity of the papers and helps in the printability and brightness of the papers (Romer, 1978) and can considerably enhance the moisture barrier qualities of sustainable starch coatings for paper and board by lowering the water vapor permeability, according to research by Breen *et al.* (2019). The authors showed that bentonites with a layer charge of 0.4 electrons per formula unit could tolerate starch in the interlayer space and consistently offered the best water vapor barrier when added to the coating. The water vapor permeability values for comparable coatings made using the higher-charge bentonites were three to four times higher. In contrast, bentonites with a layer charge of >0.4 electrons per formula unit could not accept starch in the interlayer region.

According to Olsson *et al.* (2014 a,b) and Johansson *et al.* (2012), the water vapor barrier properties of the base paper, which depend on a maximum dispersion of the platelets in the water-based coating, can be significantly reduced by the incorporation of high aspect ratio Na-bentonite into starch plasticizer coatings. Additionally, bentonite is a perfect substrate for incorporating and managing the release of antimicrobials.

In their study, Vaysi and Vaghari (2021) demonstrated that adding bentonite and cationic starch to recyclable paper boosted the paper's rip, tensile, burst, and ring crush strengths while decreasing its Cobb 60 and thickness. Khairuddin *et al.* (2019) noted that adding bentonite clay to the starch matrix improved the water vapor barrier up to 23 wt%. However, the addition of bentonite caused a decrease in the oil barrier. When bentonite was added, the lignocellulosic nanofibrillated specific Young's modulus of the films increased to levels higher than the levels of the clean nanofibril films (Horseman *et al.*, 2017).

Oliveira *et al.* (2022) studied the impact of spray coating papers with layers of cellulose micro/nanofibrils and bentonite on the mechanical and barrier qualities of packaging bags in papers with three different grammages. The greater the number of layers is, the greater the barrier property. The authors found that papers coated with micro/nanofibrils and bentonite increased the barrier to water vapor and hydrophilicity, in addition to reducing the surface porosity of the papers.

Although there have been several studies on applying starch and nanoclays with a barrier function (Monteiro *et al.*, 2018; Rihayat *et al.*, 2018; Lendvai *et al.*, 2019; Ahmed *et al.*, 2021; Sarkar *et al.*, 2021; Shanmathy *et al.*, 2021; Zamrud *et al.*, 2021; Behera *et al.*, 2022; Oliveira *et al.*, 2022), the application of bentonite to a high viscosity cationic starch matrix on kraftliner paper is still scarce. By assessing and analyzing the paper's physical, chemical, mechanical, and barrier properties, this work sought to determine the impact of adding bentonite (5 wt%, 7 wt%, and 10 wt%) as reinforcement to a starch/glycerol cationic matrix for the development of multilayer barrier paper, as a possible replacement for single-use plastic.

2. MATERIALS AND METHODS

2.1 Material

Both kraftliner paper ($86 \pm 1 \text{ g/m}^2$) and cationic starch (95 wt%, amylose content 42%, and degree of substitution 0.243) were obtained from Klabin S/A (Paraná, Brazil), glycerol ($\geq 99\%$) from Êxodo Científica (São Paulo, Brazil), and bentonite (B), a nanoclay type ($\text{Al}_2\text{O}_3 \cdot 4(\text{SiO}_2) \cdot \text{H}_2\text{O}$) from Sigma-Aldrich Inc. (Missouri, EUA).

2.1.1 Preparation of suspensions

Following the recommendations of Gao *et al.* (2019), 4.0 wt% cationic starch was prepared by completely solubilizing the starch at room temperature (23 °C, 400 rpm) for 30 min, heating it to complete gelatinization at 60 °C (500 rpm) and then adding 20 wt% glycerol.

Bardet *et al.* (2015) suggested that for nanoclay preparation, the suspension is subjected to a 750 W ultrasonic treatment with 60% amplitude after agitation at 400 rpm for 24 h in deionized water (Ultronique Disruptor, Brazil). The nanoclay is exfoliated so that its characteristics are increased rather than agglomerating.

Samples with cationic starch (S) were produced incorporating 5 wt%, 7 wt%, and 10 wt% bentonite (B). The concentration was defined according to Zafar *et al.* (2021) and Chiumarelli and Hubinger (2014) and pre-tests considering the cationic starch viscosity. Mechanical agitation was used to mix each sample for 10 min at 400 rpm. Additionally, two control treatments were applied for comparison: C1 is the kraftliner paper alone with no coating, and C2 is a coating with only water for two times. There was a total of six treatments, each with its solid content (NBR 8877 – ABNT, 2020), pH measurement (W38 Bel Engineering, Brazil), and viscosity (NBR 9277 – ABNT, 2020) parameters, as shown in Table 1.

Table 1 - Suspensions produced by cationic starch and bentonite and their pH, solids content, and viscosity characteristics.

| Sample | Description | pH | Solid content (%) | Viscosity (cP) |
|--------|------------------------------------|-----------------|-------------------|--------------------|
| C1 | Control 1 - without coating | - | - | - |
| C2 | Control 2 – water coating | - | - | - |
| S | Cationic starch | 7.8 ± 0.1^a | 4.2 ± 0.1^b | 4707.7 ± 3.1^a |
| S.B5 | Cationic starch + 5 wt% bentonite | 8.0 ± 0.1^a | 4.4 ± 0.1^a | 42.7 ± 0.6^c |
| S.B7 | Cationic starch + 7 wt% bentonite | 8.1 ± 0.1^a | 4.5 ± 0.1^a | 49.3 ± 4.5^b |
| S.B10 | Cationic starch + 10 wt% bentonite | 8.3 ± 0.1^a | 4.6 ± 0.1^a | 47.7 ± 0.3^b |

Average value \pm standard deviation. The same letters in the columns do not differ according to the Scott-Knott test at 5% of significance.

Source: From the author (2023).

2.1.2 Kraftliner paper coating

A coating machine running at 4 m/min was used to apply the suspension layer by layer to a kraftliner paper measuring 297×210 mm. The solid content determined how much it is needed to disperse the suspension evenly so that the first layer's grammage was 7.5 ± 0.5 g/m² using grooved coating bar n° 220 (0.22 mm) (D646-13, ASTM, 2013). The coated paper was then dried for 5 min at 102 ± 1 °C. A second layer, totaling 15.0 ± 0.5 g/m², was applied under the same circumstances but with a grooved coating n. 100 (0.1 mm) and dried at same conditions. While the second layer evened out the surface and created a continuous film, the first layer filled in the paper's roughness and some porosity. The application followed the fiber direction within the paper's machine direction (MD).

2.2 Methods

2.2.1 Physical properties of coated paper

The thickness and density of multilayer packaging were measured in accordance with ISO 534:2011 (ISO 534:2011, 2011) using a Regmed micrometer (ESP/SA-10, Brazil).

Scanning electron microscopy (SEM) was evaluated using a Zeiss microscope (LEO EVO 40XVP, Thornwood, NY, USA) for the paper surface and cross-section. Using a spray coating method, gold was applied to the samples (SCD 050).

2.2.2 Pencil hardness

Following the ASTM D 3363-22 pencil test (ASTM, 2022a), the pencil's hardness was measured using a Wolf Wilborn durometer (TKB Erichsen Commercial e Técnica LTDA, São Paulo, Brazil). The device is dragged while a softer pencil (10B, 9B, 8B, 7B, 6B, 5B, 4B, 3B, 2B, B, HB) is fastened at a 45° angle to the paper. If there are no indications that the coating has been damaged after dragging, the test is repeated using a pencil with a harder grade (F, H, 2H, 3H, 4H, 5H, 6H, 7H, 8H, 9H, or 10H). Hardness is represented by the pencil number that does not damage the coating.

2.2.3 Attenuated total reflectance Fourier transform infrared (ATR-FTIR) spectroscopy.

To determine the chemical composition of the coating and potential interactions between its constituent parts, Fourier transform infrared spectroscopy was used with coated kraftliner paper samples positioned with the coating directed towards the infrared laser. A Nicolet 6700 FTIR fitted with a Pike Technologies GladiATR diamond spectrometer (Thermo Scientific, Waltham, MA, USA) was used to acquire the spectra in an average of 60 scans at a resolution of 4 cm⁻¹ in the range of 4,000 to 500 cm⁻¹ at room temperature of 23 °C.

2.2.4 Raman spectroscopy

A confocal Raman microscope (alpha 300, WITec GmbH, Ulm, Germany) fitted with a 10× air objective (NA = 0.25, Carl Zeiss GmbH, Jena, Germany) was used to collect Raman

spectra in triplicate. A diffraction-limited spot size of 0.61 NA was targeted using a linearly polarized laser with a power of 10 mW and a wavelength of 532 nm (Crysta Laser, Reno, NV, USA). Each Raman spectrum was the mean of 10 accumulations collected with an exposure time of 0.1 s. With a spectral resolution of 6 cm⁻¹, a backlit, air-cooled charge-coupled device (CCD) detector (DV401 BV, Andor, Belfast, UK) was used to detect Raman scattered light. The spectra were baseline corrected and smoothed using Origin Pro 8.5 software (OriginLab, USA). The investigation was limited to composite films since kraftliner paper displayed too strong autofluorescence. The films were first created by casting them on Petri dishes with a 50 mm diameter. Then, 10 mL of the suspension (1.0 wt%) was dried for 48 h at 45 °C in a circulating oven (Solab SL-100, Brazil).

2.2.5 Mechanical properties of coated paper

Following the ASTM D828-22 (ASTM, 2022) requirements, the tensile strength test is carried out using a Shimadzu testing apparatus (AGS-X, Japan) with a distance between the claws of 122.0 mm, a speed of 25.4 mm/min, and a 10 kN load cell. For each treatment, ten 25.4 × 254.0 mm samples were examined. The maximum force that may be given to a specimen without causing failure is its tensile strength. Tensile index is the tensile strength divided by the grammage of the sample and tensile energy absorption is the amount of work done when a specimen is forced to rupture under tension. Tensile stiffness, which denotes the elastic property of multilayer paper, is the tangent of the linear section of a tensile strength-strain curve (Santos and Yoshida, 2011). When a stress is applied, the specimen's reaction is the elongation, which causes the specimen to expand. Anisotropic kraftliner paper presents differing qualities in the paper sheet's machine direction (MD) and cross direction (CD). Version 1.5.4 of Trapezium Software was used to analyze the data.

2.2.6 Water barrier properties of coated paper

The Krüss Drop Shape Analyzer–Goniometer DSA25 (Hamburg, Germany) was used to measure the contact angle of the water with the coated papers in triplicate. Deionized water is applied to the sample's surface 20 mm above the surface using a syringe. The average contact angle between the water drop and the paper surface at room temperature (23 °C) is calculated using the Advance Software. The analysis is carried out in the first second after water contacts the sample. Ten average angles are used to measure it.

In addition, ASTM 458 cm-04 (ASTM, 2004) recommended procedures to determine the wettability of multilayer packaging. This technique entails measuring the angle in triplicate at 5 s and 60 s after contact with the coated paper surface. The angle during the analysis might get smaller, indicating that the paper is more wettable. Equation (1) is used to determine the wettability (°/s).

$$\text{Wettability} = \frac{(A-a)}{55} \quad (1)$$

Where ‘A’ represents the contact angle with water in 5 s, in °, ‘a’ represents the contact angle with the water after 60 s, in °, and 55 represents the time, in seconds, for the paper to absorb the water.

For water vapor permeance, Guimarães *et al.*, (2015) used an adaption of the ASTM E96/E96M–16 standard method (ASTM, 2016) for measuring water vapor transmission rate (WVTR) and water vapor permeability (WVP). 16 mm diameter samples were attached to silica-filled permeation cells. These cells were kept in a 38 °C, 90% relative humidity (RH) environment for eight days while being weighed daily. According to ASTM E104-02 (ASTM E104-02, 2002), a desiccator filled with a saturated saline solution produces a 90% RH environment. Following equations (2) and (3), WVTR (g/m²/day) and WVP (g mm/day m²/kPa) are calculated:

$$\text{WVTR} = \frac{(M/t)}{A} \quad (2)$$

$$\text{WVP} = \text{WVTR} \cdot \frac{\text{Th}}{S} \cdot (R^1 - R^2) \quad (3)$$

‘M’ is the mass (g), ‘t’ is the time (d), ‘M/t’ is the angular coefficient from the linear regression of day (d) and mass gain (g), and ‘A’ is the test area (m²). ‘Th’ is the paper thickness (µm), ‘S’ is the saturation vapor pressure at the test temperature (kPa), ‘R¹’ is the relative humidity in the desiccator (90%), and ‘R²’ is the relative humidity of the test environment (0%). All samples were tested in triplicate.

The water absorption test (Cobb test), which was conducted after TAPPI T441 om-13 (TAPPI, 2013), is another water barrier feature. 100 mL of deionized water is placed into a ring instrument for 120 s after the 15 × 15 cm samples have been produced. The “wet samples” are pressed between two absorbent papers with a 10 kg roller, in order to release any trapped water.

Both before and after the process, the sample is weighed. The Cobb test depicts the relationship between the wetted area (g/m^2) and the mass of water that is absorbed by the multilayer paper.

2.2.7 Oil/grease barrier property of coated packaging

T 559 cm-12 (TAPPI, 2012) was used to evaluate oil resistance. With oil kit solutions ranging from 1 to 12, which include precise ratios of the three reagents castor oil, toluene, and n-heptane, multilayer paper samples were examined. The kit test with the highest surface energy is kit test 12, which is a mixture of toluene and n-heptane, as opposed to kit test 1, which contains solely castor oil. On the paper's surface, a drop of the kit test is applied at a 13 mm height. Extra oil is removed after 15 s. The kit test for the sample is recorded as the kit test if it remains on the paper's surface and is not absorbed by the paper. A paper with kit test number 12 reveals a coating that is more oil/grease resistant.

A crease made on the sample using the same methods was subjected to the same kit test process. In order to simulate a possible discontinuity of the thin coating when folding the multilayer paper, the paper is folded repeatedly to create the crease.

The sessile drop technique described by Owens and Wendt (1969), Kaelble (1970), and Rabel (1971) was utilized for surface free energy analysis. The contact angles created in the samples by five different solvents were determined by Advance Software at room temperature ($23\text{ }^\circ\text{C}$) using the values of the polar and dispersive surface energies. Deionized water, glycerol, diiodomethane, ethylene glycol, and 1-bromonaphthalene, all expressed in mN/m , were the solvents utilized. The ratio of the estimated polar components to the paper's total surface energy was used to determine polarity.

2.3 Statistical analysis

To evaluate the qualities of multilayer paper and uncoated kraftliner paper, the findings were subjected to one-way analysis of variance (ANOVA) and the Scott-Knott test, both with a 5% level of significance. Data processing was done using Sisvar 5.6 (Ferreira, 2014).

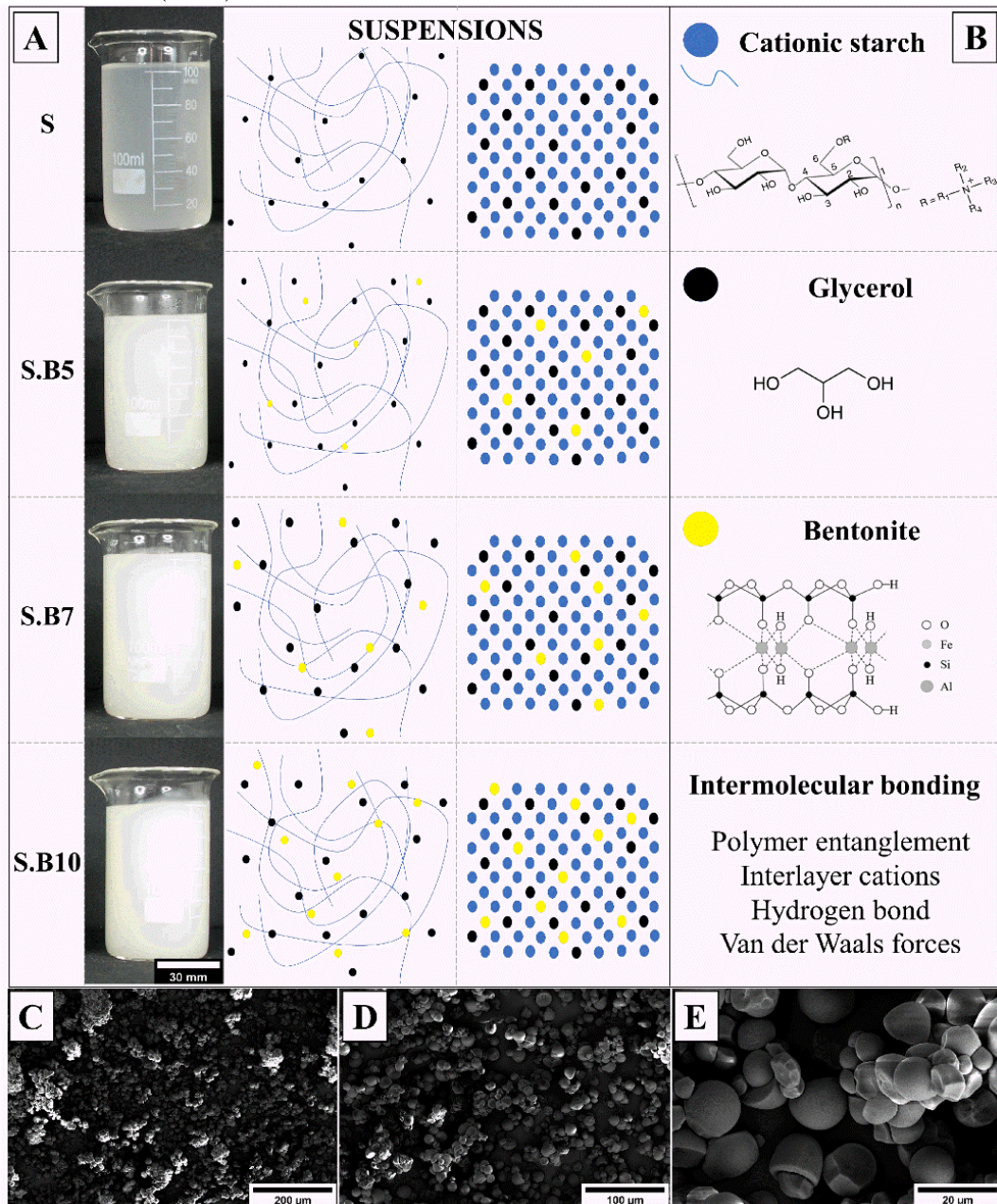
3. RESULTS AND DISCUSSION

3.1 Suspension investigation

Bentonite and cationic starch interact in an aqueous suspension, as seen in the literature (Alekseeva *et al.*, 2017). Bentonite has a good molecular size that causes it to connect with starch composite lattices tangibly, demonstrating its ability to function well with various particles in composite film networks.

In suspension, there is simultaneous interaction between water, cationic starch, glycerol, and bentonite by secondary bonds (Figure 1). Bentonite has an octahedral structure composed of aluminum, iron, or magnesium linked to the tetrahedral structure by six oxygen molecules. Tetrahedral structures are composed of silica-oxygen. At the same time, starch possesses several hydroxyl groups on the amylose and amylopectin chains. Between the starch and the intercalated layered arrangement of bentonite, interactions of interlayer cations form, as well as van der Waals forces, and hydrogen bonds (Rhim *et al.*, 2006; Natália and Cristina, 2010; Liu *et al.*, 2017; Uddin, 2018; Zamrud *et al.*, 2021). In addition, cationic starch polymer chains are physically entangled (Tian *et al.*, 2017).

Figure 1 - Illustration of suspensions of cationic starch and bentonite in deionized water (A) and their interaction (B). Cationic starch granules in a scale of 200 μ (C), 100 μ (D), and 20 μ (E). Cationic starch (S) with the addition of 5 wt% (.B5), 7 wt% (.B7), and 10 wt% (.B10) of bentonite.



Source: From the author (2023).

The solids content of all suspensions did not change as the addition of bentonite to the starch matrix was small. In suspensions of pH higher than 4.0 with cure at temperatures below 105 °C, starch hydrolysis is limited (Olsson *et al.*, 2013). This pH range is observed in this experiment. Cationic starch has high viscosity even with low solids content (Radosta *et al.*, 2004).

There is a significant decrease in the viscosity of the suspensions when incorporating any percentage of bentonite into the cationic starch matrix, as seen in Table 1, with the lowest viscosity observed for S.B5 sample. More aggregated clay minerals have been shown to have a reduced viscosity at low bentonite concentrations, which can be explained by a decline in the hydrated layer and, consequently, in the effective particle volume fraction (Van Olphen, 1957). Additionally, agitation of the suspensions for 24 h to exfoliate the bentonite may have generated retrogradation of the starch, aligning its polymeric chain and decreasing the viscosity.

3.2 Physical and morphological characterization

The coating deposition on the paper directly affected the packaging thickness and density through suspension penetration, changing the interaction among fibers or film formation (Table 2). The S.B5 packaging sample presented the lowest thickness and the highest density at 0.141 ± 0.002 mm and 0.719 ± 0.002 g/cm³, respectively. S.B5 formed a thinner layer over the paper caused by low viscosity, and suspension filled the paper's porous (Figure 2), promoting decreased thickness. Low viscosity may result in better suspension absorption by the kraftliner paper, directly influencing film formation and potentially impacting the barrier properties (Thébault *et al.*, 2017; Yang *et al.*, 2022). The barrier properties of packages depend on the minimum thickness of continuous films to achieve their potential (Brodin *et al.*, 2014).

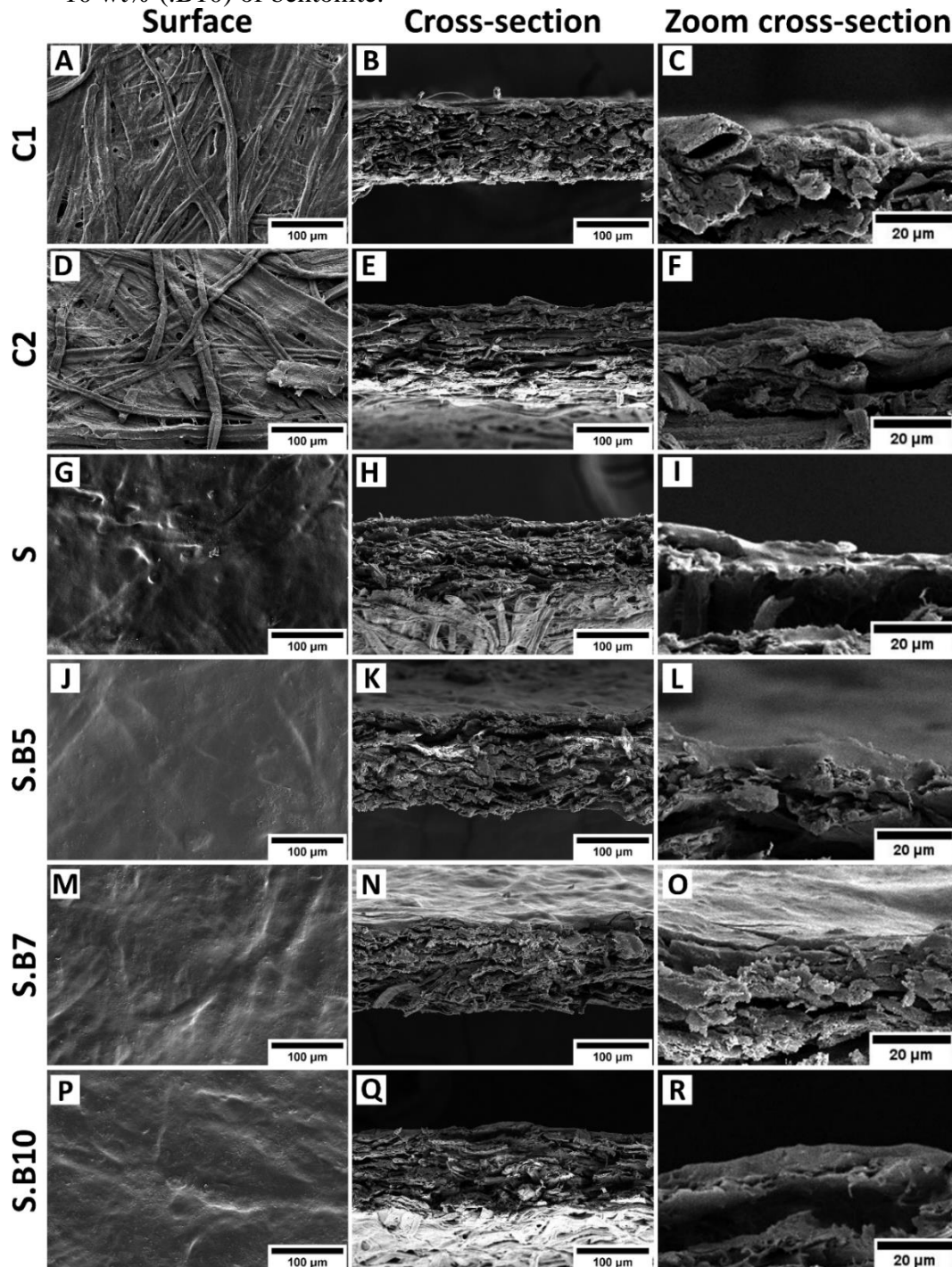
Table 2 - Characterization of the thickness, density, and hardness of multilayer paper.

| Sample | Packaging thickness (mm) | Packaging density (g/cm ³) | Pencil Hardness* |
|--------|--------------------------------|--|------------------|
| C1 | 0.125 ± 0.001 ^c | 0.691 ± 0.002 ^b | - |
| C2 | 0.124 ± 0.002 ^c | 0.689 ± 0.003 ^b | - |
| S | 0.147 ± 0.003 ^a | 0.693 ± 0.014 ^b | 6H |
| S.B5 | 0.141 ± 0.002 ^b | 0.719 ± 0.002 ^a | 3H |
| S.B7 | 0.145 ± 0.003 ^a | 0.700 ± 0.007 ^b | 2H |
| S.B10 | 0.148 ± 0.009 ^a | 0.685 ± 0.003 ^b | 8H |

*Following ASTM D 3363-20 standard (ASTM, 2022a). Average value \pm standard deviation. The same letters in the columns do not differ according to the Scott-Knott test at 5% of significance. Control treatments with no coating (C1) and water coating (C2). Cationic starch (S) with the addition of 5 wt% (.B5), 7 wt% (.B7), and 10 wt% (.B10) of bentonite.

Source: From the author (2023).

Figure 2 - Surface and cross-sectional images of multilayer packaging captured using standard scanning electron microscopy. Control treatments with no coating (C1) and water coating (C2). Cationic starch (S) with the addition of 5 wt% (.B5), 7 wt% (.B7), and 10 wt% (.B10) of bentonite.



Source: From the author (2023).

Along its entire length, the kraftliner paper's network of flattened threads generates porous structures (Figure 2A–F). These pores allow for the passage of gases, oil, water, and water vapor through the paper (Zhang *et al.*, 2014). For the C2 sample, it is also feasible to see an expansion of the paper's pores. Water and gases can be displaced through the paper more

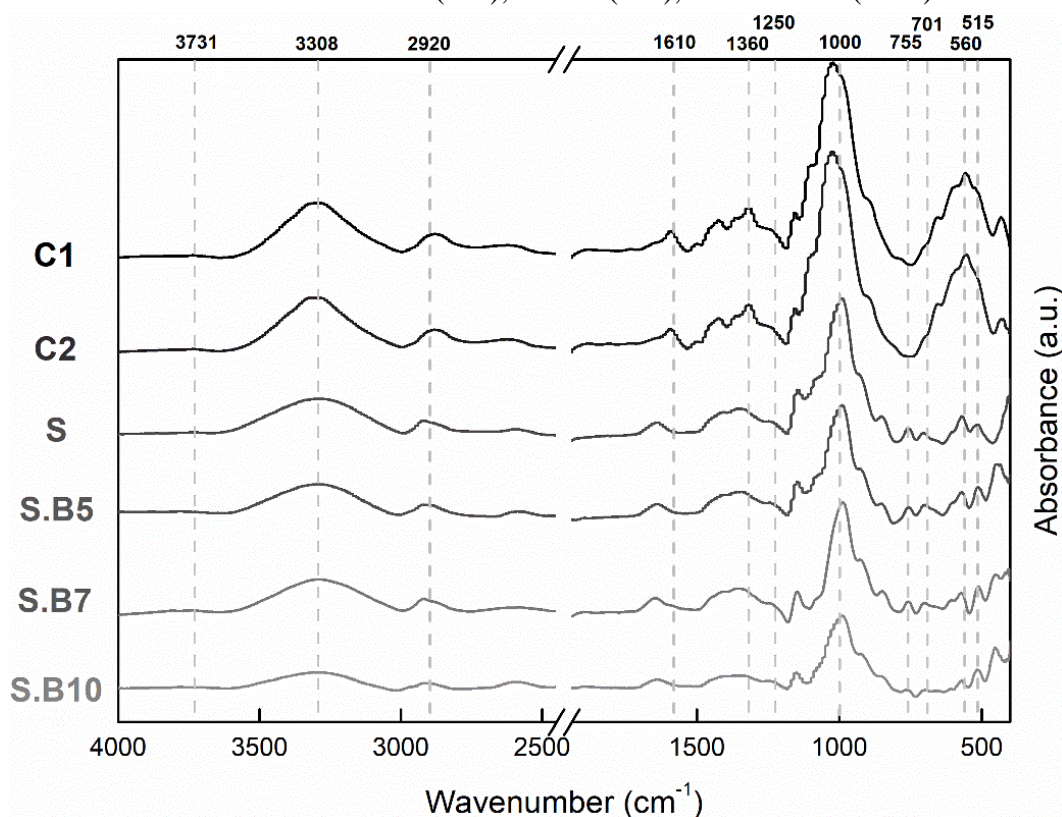
easily due to the heterogeneity of the pores and the surface. In contrast, fiber entanglement increases mechanical strength, favoring its use in packing.

The continuity of the films formed on the kraftliner paper can be observed by the SEM images shown in Figure 2G–R. On the kraftliner paper, pure cationic starch and composite suspensions created a homogeneous coating with a low thickness standard deviation at a similar grammage. Figure 2G shows that the starch film's surface is more uneven and discontinuous. It is possible to visualize the fibers underneath the coating, suggesting a reduced barrier property, differently observed by the samples containing bentonite (Figure 2J, M, and P). A similar behavior was found by Monteiro *et al.* (2018). However, Wang and Jing (2017) noticed in their SEM images that adding nanoclay montmorillonite to a chitosan matrix impaired film formation on kraft paper when compared to paper coated with only chitosan. A film with superior homogeneity and no discontinuity was produced due to the interaction between the starch and bentonite's nanometric structures, also affecting their pencil hardness. While the pencil hardness of the samples containing 5 wt% and 7 wt% was lower than the pencil hardness of the 6H starch, only the S.B10 sample displayed a pencil hardness higher than the pencil hardness of starch, with an 8H pencil. The flexibility of the coating chains and the interactions among their inner components, which represent adhesion to the paper, determine the hardness of the pencil (Gadhav *et al.*, 2019).

3.3 ATR-FTIR spectroscopy and Raman spectroscopy

ATR-FTIR was used to compare the surface chemistry of coated paper to that of uncoated paper. The peak at $3,308\text{ cm}^{-1}$ is responsible for the O–H stretching from water molecules and functional hydroxyl groups present in the material. The peak is visible in the FTIR spectra of lignocellulosic material C1 and C2 (Figure 3), but also exists in glycerol, cellulose, hemicelluloses, lignin, bentonite, and water molecules (Chen *et al.*, 2016; Sarkar *et al.*, 2021). Lignin and hemicellulose have peaks between the $1,610\text{ cm}^{-1}$ and $1,250\text{ cm}^{-1}$, assigned to uronic ester groups and ester bonds of the carboxylic group of ferulic and p-coumaric acid (Bian *et al.*, 2019; Miao *et al.*, 2020).

Figure 3 - Multilayer packing characterization by Fourier-transform infrared spectroscopy. Control treatments with no coating (C1) and water coating (C2). Cationic starch (S) with the addition of 5 wt% (.B5), 7 wt% (.B7), and 10 wt% (.B10) of bentonite.



Source: From the author (2023).

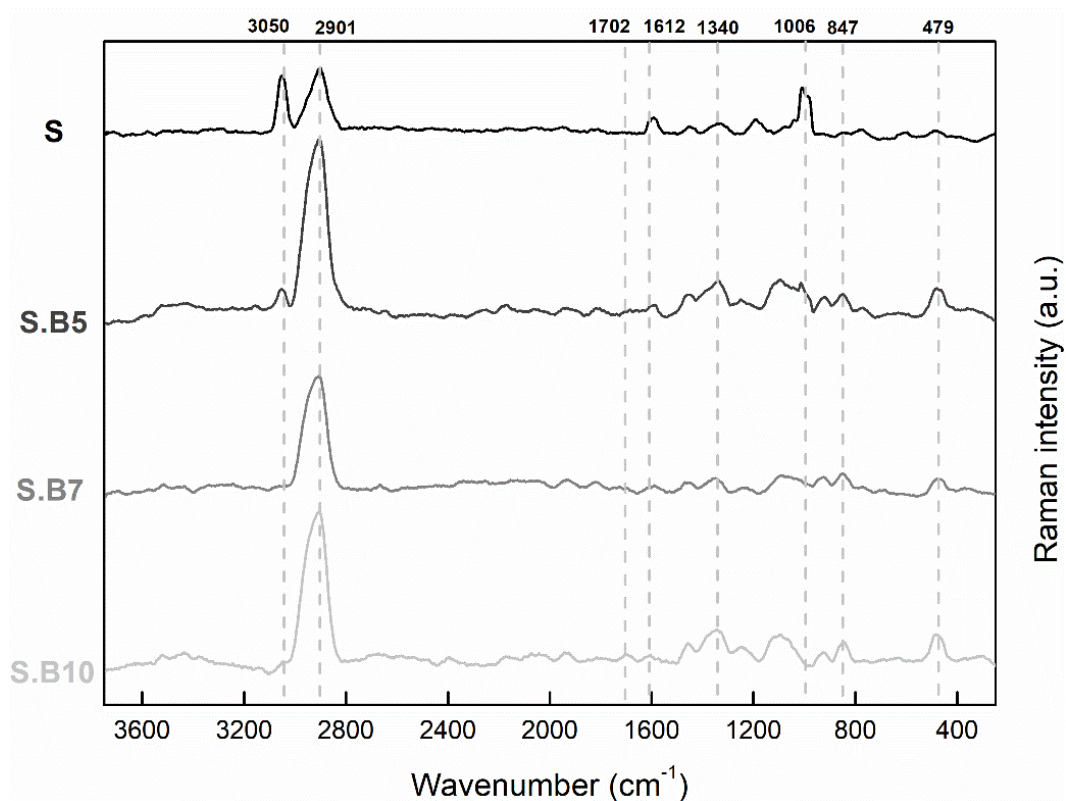
Starch chains with exposed hydroxyl groups frequently form intra- and intermolecular interactions that prevent the chain from moving (Gao *et al.*, 2012; Liu *et al.*, 2022). Even at lower quantities, such as in S.B5, the O–H peak is wider for the cationic starch sample than for the kraftliner papers and the bentonite-starch composites. The O–H peak band expands as a result of the higher amount of free O–H groups and water molecules in the sample. The narrower O–H peak in bentonite-starch composite than the cationic starch samples can be because of a high intermolecular interaction between clay, starch and glycerol, which reduces the amount of free O–H groups and the amount of water molecules (Tan and Thomas, 2016). Glycerol causes the starch film to break down the intramolecular and intermolecular contacts, as well as the internal hydrogen bonds that have formed between the chains of the biopolymer (Nordin *et al.*, 2020). That might be the cause of more intermolecular interactions in bentonite-starch composites.

For starch, the C–O–C vibration peak is stronger and displaced to 990 cm^{-1} (Zhu *et al.*, 2022). This region, according to Abdulla *et al.* (2018), represents the crystalline portion of starch in its unprocessed state. For bentonite, the peaks that in the FTIR spectra correspond to

Si–O–Al, S–O–Mg, and Al–Al–OH stretching, are, respectively, at 701, 755, and 3,731 cm^{-1} (Alghunaim, 2016) and to C–H wagging and CH_2 stretching are at 1,360 and 2,920 cm^{-1} (Sarkar *et al.*, 2021). Bentonite's Si–O–Si functional group becomes more noticeable as its concentration rises to 1,000 cm^{-1} (Foletto *et al.*, 2003). The interaction between the Al from the bentonite and the OH group from the glycerol and cationic starch and glycerol is indicated by the decrease in the frequency of OH bonding following the addition of bentonite to starch matrices. Similar behavior was found by Behera *et al.* (2022) and Abdullah and Dong (2019).

A complementary analysis to IR spectroscopy, which depends on the change of molecule's dipole moment, is Raman spectroscopy, which depends on the change in polarizability of a molecule. When a surface is irradiated with monochromatic light, the chemical bonds and functional groups of the material's surface scatter this light differently, depending on their polarizability. These backscattered and shifted light can be visualized in a Raman spectrum. Different functional groups cause different intensities and shifts to the back scattered Raman light. Raman spectroscopy faces the challenge of analysis being impractical in the presence of excessive autofluorescence. According to Sá *et al.* (2015), kraftliner-coated papers created autofluorescence that covered up the Raman signal. For this reason, Raman spectroscopy was performed on only the films of the composites, while not on the samples C1 and C2 (Figure 4).

Figure 4 - Characterization of cationic starch and bentonite films using Raman spectroscopy. Cationic starch (S) with the addition of 5 wt% (.B5), 7 wt% (.B7), and 10 wt% (.B10) of bentonite.



Source: From the author (2023).

Raman bands in cationic starch at $3,050$ and $2,901\text{ cm}^{-1}$ are associated with C–H stretching. In amylopectin, the formation of double helices is reflected in the intensity of the peak at $2,901\text{ cm}^{-1}$ (Bulkin and Kwak, 1987; Hu *et al.*, 2017). Instead, Guo *et al.* (2019) claimed that the peak at $1,340\text{ cm}^{-1}$ is due to the angular displacement of the C–O–H bond as a result of the spiralization of single helical amylose. Besides that, the ether group, which is likely present in the cationic starch, is linked to the peak at $1,006\text{ cm}^{-1}$ (Wyan, 2019).

For the bentonite composite samples, the silica structure Si–O–Si is responsible for the peak at 847 cm^{-1} (Galeener and Geissberger, 1983). The stretching oxygen atom in the silica framework of bentonite is represented by the 479 cm^{-1} peak in the Raman spectra (Ahmed *et al.*, 2021). For S.B10, the bentonite peak intensity at $1,340\text{ cm}^{-1}$ increased and moved to a lower value. Galeener and Geissberger (1983) and Ahmed *et al.* (2021) attribute this to the insertion and intercalation of starch by the CH₂ twisting vibrational mode within the bentonite layers.

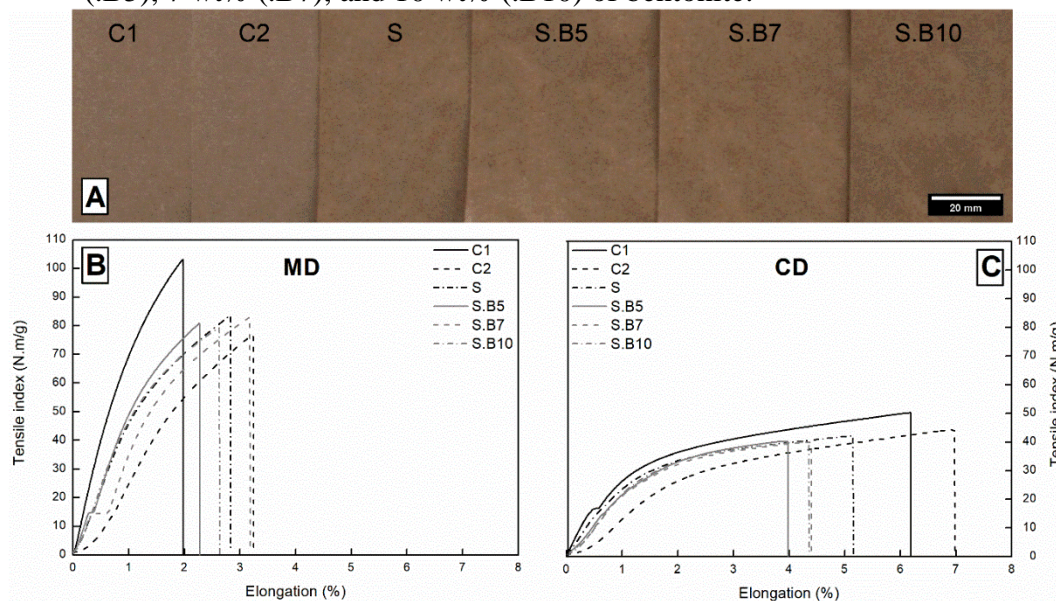
According to Salmén and Bergström (2009), the O–H band of hydroxyl groups typically appears between $3,170$ and $3,650\text{ cm}^{-1}$, although unlike in IR spectroscopy, hydroxyls are not Raman active groups and are mostly evident in the moist state. Chemical linkages C–H and

C=C are connected to the bands at $1,612$ and $1,702\text{ cm}^{-1}$, respectively (Alves *et al.*, 2016), with the C=C being more evident for S.B10. With the addition of bentonite to the composite, the intensity of the peak at $2,901\text{ cm}^{-1}$ increased, possibly as a result of the insertion of additional C–H bonds into the tetrahedral structure.

3.4 Mechanical characterization

As a material with anisotropy, paper has mechanical characteristics that vary in the MD and CD directions (Alzweighi *et al.*, 2021). They are typically more rigid and resistant in MD, with less elongation (Seth and Page, 1974), as shown in Figure 5, Table 3, and Table 4.

Figure 5 - Tensile index x elongation curves of multilayer packaging (A) in their machine direction – MD (B) and cross direction – CD (C). Control treatments with no coating (C1) and water coating (C2). Cationic starch (S) with the addition of 5 wt% (.B5), 7 wt% (.B7), and 10 wt% (.B10) of bentonite.



Source: From the author (2023).

Table 3 - Mechanical properties of multilayer paper in their machine direction (MD).

| Sample | Tensile strength (kN/m) | Tensile Index (N.m/g) | Tensile energy absorption (J/m ²) | Tensile stiffness (kN/m) | Elongation (%) |
|--------|----------------------------|--------------------------|--|-----------------------------|------------------------|
| C1 | 8.9 ± 0.1 ^a | 103.3 ± 1.5 ^a | 11.1 ± 0.4 ^b | 744.4 ± 29.2 ^a | 2.0 ± 0.1 ^c |
| C2 | 6.7 ± 0.5 ^c | 77.4 ± 5.3 ^c | 11.5 ± 2.3 ^b | 233.4 ± 36.0 ^c | 3.2 ± 0.4 ^a |
| S | 8.2 ± 0.2 ^b | 80.9 ± 2.1 ^b | 15.0 ± 1.1 ^a | 517.9 ± 107.1 ^b | 2.8 ± 0.1 ^b |
| S.B5 | 8.2 ± 0.5 ^b | 81.2 ± 4.9 ^b | 14.3 ± 2.8 ^a | 459.4 ± 85.6 ^b | 2.8 ± 0.3 ^b |
| S.B7 | 8.5 ± 0.5 ^b | 83.9 ± 4.7 ^b | 15.6 ± 2.2 ^a | 463.5 ± 71.0 ^b | 3.0 ± 0.2 ^a |
| S.B10 | 7.9 ± 0.3 ^c | 77.6 ± 2.5 ^c | 13.6 ± 0.4 ^a | 434.7 ± 98.6 ^b | 2.7 ± 0.2 ^b |

Average value ± standard deviation. The same letters do not differ according to the Scott-Knott test at 5% of significance. Control treatments with no coating (C1) and double wet-and-dry (C2). Cationic starch (S) with the addition of 5 wt% (.B5), 7 wt% (.B7), and 10 wt% (.B10) of bentonite.

Source: From the author (2023).

Table 4 - Mechanical properties of multilayer paper in their cross direction (CD).

| Sample | Tensile strength (kN/m) | Tensile Index (N.m/g) | Tensile energy absorption (J/m ²) | Tensile stiffness (kN/m) | Elongation (%) |
|--------|----------------------------|--------------------------|--|-----------------------------|------------------------|
| C1 | 4.4 ± 0.2 ^a | 50.5 ± 2.4 ^a | 19.5 ± 3.4 ^a | 336.9 ± 10.9 ^a | 5.9 ± 0.8 ^b |
| C2 | 4.0 ± 0.1 ^b | 46.0 ± 1.1 ^b | 20.7 ± 2.0 ^a | 144.5 ± 10.7 ^d | 7.7 ± 0.6 ^a |
| S | 4.2 ± 0.3 ^b | 40.9 ± 2.7 ^c | 17.7 ± 3.9 ^a | 286.0 ± 17.0 ^b | 5.5 ± 0.9 ^b |
| S.B5 | 4.1 ± 0.2 ^b | 40.4 ± 2.1 ^c | 13.4 ± 3.4 ^b | 241.0 ± 39.8 ^c | 4.4 ± 0.8 ^c |
| S.B7 | 4.0 ± 0.1 ^b | 39.7 ± 0.8 ^c | 12.1 ± 2.4 ^b | 208.4 ± 74.4 ^c | 4.2 ± 0.5 ^c |
| S.B10 | 4.1 ± 0.2 ^b | 40.3 ± 1.5 ^c | 15.5 ± 3.9 ^b | 222.4 ± 26.7 ^c | 5.0 ± 1.0 ^c |

Average value ± standard deviation. The same letters do not differ according to the Scott-Knott test at 5% of significance. Control treatments with no coating (C1) and double wet-and-dry (C2). Cationic starch (S) with the addition of 5 wt% (.B5), 7 wt% (.B7), and 10 wt% (.B10) of bentonite.

Source: From the author (2023).

The tensile strength of double wet and dry paper (C2) dropped by 25% on MD papers and 10% on CD. The obstruction of interactions between the fibers produced by humidity-induced separation and hornification caused by drying reduced the paper strength (Parker *et al.*, 2006; Rhim, 2010). As already mentioned in earlier sections, coatings made of starch and bentonite have large water content, which has a direct impact on how well they adhere to the paper and how strong they interconnect. The coating affected the fiber bonding rather than the orientation of the fibers (Zhang *et al.*, 2014; Lin *et al.*, 2017), causing a decrease in tensile strength of up to 11% for MD in the S.B10 sample and 10% for CD in the S.B7 sample. Oliveira *et al.* (2022) coated sack kraft paper with cellulose micro/nanofibrils, and bentonite also noticed a decrease in all multilayer papers when compared to an uncoated paper. Additionally, adding glycerol to the recipe for the composite samples may reduce tensile stress (Nordin *et al.*, 2020).

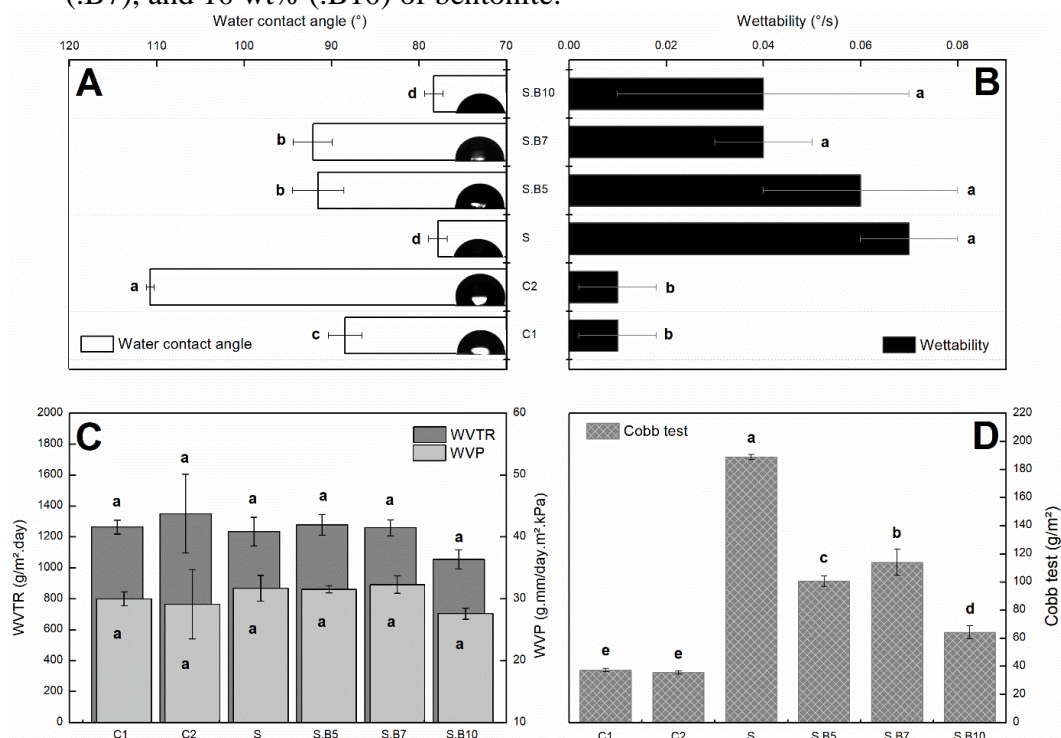
The drying cycle also had a significant impact on the papers' tensile stiffness, which dropped by 69% and 57% in MD and CD, respectively. Stiffer papers might be produced by replacing the intermolecular connections between the fibers' hydroxyls with water molecules, followed by twofold drying (Sørensen and Hoffmann, 2003; Bandyopadhyay *et al.*, 2002). However, Hassani *et al.* (2022) reported a 103% increase in Young's modulus due to interfacial adhesion when they studied the crosslinked starch coating on bleached papers. In addition, according to Bandyopadhyay *et al.* (2002), humid environment typically results in a drop in Young's modulus.

When comparing C1 and C2, the elongation property, however, is enhanced with water application. As fiber contacts weaken, more slippage occurs between them, increasing the paper's elasticity. For CD, it is noticed that the presence of bentonite to the starch matrix resulted in a reduction in elongation, which occurred as result of the development of clay layers that limit the extensibility and reduce the elongation of the paper, as discovered by Oliveira *et al.* (2022) and Gabr *et al.* (2013). Additionally, Follain *et al.* (2005) hypothesized that the introduction of structural flaws by crosslinking during late retrogradation of starch results in greater elongation.

3.5 Water and oil barrier

Through the water contact angle, wettability, water vapor permeability, and water barrier Cobb test (Figure 6), it is possible to determine the suitability of coated paper. According to Bačovská *et al.* (2016), hydrophobicity is often shown by water contact angles above 90° and is influenced by the surface chemistry and roughness of the material. These elements influence how the surface chooses what angle the water drop makes with it (Saji, 2020). A thin air layer may continue to exist between some surfaces (Ferrari and Benedetti, 2015; Zhao *et al.*, 2019), or even the ability of the substance to absorb water.

Figure 6 - Properties of multilayer packaging for water contact angle (A), wettability (B), water vapor transmission rate (WVTR), water vapor permeability (WVP) (C), and water absorption (Cobb test) (D). The same letters in the columns do not differ according to the Scott-Knott test at 5% of significance. Control treatments with no coating (C1) and water coating (C2). Cationic starch (S) with the addition of 5 wt% (.B5), 7 wt% (.B7), and 10 wt% (.B10) of bentonite.



Source: From the author (2023).

Sample C2 had the highest contact angles, measuring $111 \pm 1^\circ$, followed by sample S.B5 and S.B7, measuring $92 \pm 3^\circ$ and $92 \pm 2^\circ$, respectively (Figure 6A). The hydroxyl groups of the fibers may have been damaged by the double wet-and dry process, increasing the water contact angle by horrifaction. Ferreira *et al.* (2017) claim that when water is removed from fibers, a portion of the cell wall collapses, boosting interfibrillar interactions and creating hydrogen bonds that are both irreversible and partially reversible. In addition, the surface of the paper fiber may have developed a thin air layer, increasing its hydrophobicity (Samyn, 2013). Because cationic starch has a large number of hydroxyl groups, it exhibits a low water contact angle of $78 \pm 1^\circ$, boosting its hydrophilicity.

However, the control treatments C1 and C2 had less wettability, which measures how much water has spread across the surface, at 0.01 ± 0.01 °/s (Figure 6B). The addition of the plasticizer glycerol, which makes the polymer even more hydrophilic, explains why cationic starch has a high wettability (0.07 ± 0.01 °/s). The wettability of the coating decreased as result of the bentonite addition to the starch matrix, reaching 0.04 ± 0.01 °/s for S.B7, when comparing to S sample.

Coatings that have bentonite in their composition tend to have low WVTR and WVP (Oliveira *et al.*, 2022). However, high humidity can interfere with this result. The water vapor permeability analysis condition used in this work (90% RH, 38 °C) was superior to most of the literature, trying to reach extreme conditions to which packages can be submitted (Figure 6C). It is possible to see many differences in the literature when mixing starch with nanoclays. At 54% RH and 24 °C, Park *et al.* (2002) found that adding 5 wt% clay to a mixture of 100 pph potato starch + 60 pph glycerol reduced the water vapor permeability by 50%. Mueller *et al.* (2011) found a comparable decrease in WVP following the addition of 5 wt% montmorillonite to a 100 pph cassava starch + 25 pph glycerol matrix, but under the conditions of 75% RH and 25 °C. At 75% RH and 25 °C, the Tang *et al.* (2008) method of adding 9 wt% montmorillonite to 100 pph potato starch + 15 pph glycerol succeeded in reducing the WVP by only 55%. In addition, Ning *et al.* (2009) found that dispersing 9 wt% montmorillonite in maize starch and 30% glycerol decreased the WVP by 60% at 75% RH and 24 °C. In this work, the ability of the coatings to function as a water vapor barrier, however, was unaffected by the addition of bentonite, as similarly found by Clegg *et al.* (2019) under the environmental conditions of 50% RH and 23 °C. Amorphous polysaccharides and porous materials, such as starch and kraftliner paper, are quite vulnerable to gas movement (Chi and Catchmark, 2018). Additionally, the surface roughness and porosity of the films formed in the kraftliner paper may increase the rate at which water vapor binds to them (Hu *et al.*, 2009).

When evaluating the water absorption of the coated paper, the Cobb test showed that the cationic starch had the highest absorption with 189 g/m², followed by the S.B7 composite sample with 114 g/m² (Figure 6D). The number of accessible hydroxyl groups in the starch and the porosity of the sheets encouraged the ability of the coating to absorb water and swell (Chi *et al.*, 2020). Cobb was lower in the composite samples than in the individual starch samples, indicating good synergism, but they still outperformed the controls.

Because of the polarity and cohesive energy of starch, coated papers showed some oil barrier. The oil barrier of the paper for C1 and C2 is lowered since it is a porous substance that readily absorbs oil. The paper's porous nature and high oil penetration rate lower the quality of the package (Zhang *et al.*, 2014). To simulate the use of packaging, tests were conducted on folds and multilayer paper surfaces (Table 5). None of the samples displayed an oil barrier when folded. Paper coated with cationic starch showed an oil resistance of 10 at kit oil. For S.B5 and S.B10, the papers decreased the oil resistance to kit n. 6 and 4, respectively. When 7 wt% bentonite was added to the starch matrix, the oil barrier did, however, rise to number 12 of the oil kit.

Table 5 - Cationic starch and bentonite multilayer paper properties of oil resistance and surface free energy.

| Sample | Oil kit test* | | Surface free energy (mN/m) | |
|--------|---------------|------|----------------------------|-----------------|
| | Surface | Fold | Polar phase | Dispersed phase |
| C1 | 0 | 0 | 0.2 ± 0.5 | 41.0 ± 3.5 |
| C2 | 0 | 0 | 2.5 ± 2.1 | 41.8 ± 2.6 |
| S | 10 | 0 | 3.1 ± 1.5 | 33.1 ± 1.2 |
| S.B5 | 6 | 0 | 1.2 ± 1.2 | 36.4 ± 2.7 |
| S.B7 | 12 | 0 | 2.8 ± 2.4 | 34.5 ± 1.1 |
| S.B10 | 4 | 0 | 1.4 ± 1.1 | 38.6 ± 2.0 |

* Oil kit test number according to T 559 cm-12 (TAPPI, 2012). Average value ± standard deviation. Control treatments with no coating (C1) and double wet-and-dry (C2). Cationic starch (S) with the addition of 5 wt% (.B5), 7 wt % (.B7), and 10 wt % (.B10) of bentonite.

Source: From the author (2023).

Good dispersion of bentonite intercalated in a cationic polymeric matrix provides improved properties of nanocomposites, as observed by Xu *et al.* (2018). Bentonite is a semi crystalline material that assumes a layered structure in optimal concentrations in the surrounding matrix. In addition, the proper exfoliation of bentonite platelets helps in their organization, forming a physical barrier layer (Aulin *et al.*, 2012). If the bentonite platelets in an optimal concentration are intercalated by the polymeric chains of the cationic starch without breaking their spatial periodicity, the barrier property is enhanced. This characteristic is observed for adding 7wt% of bentonites to the starch matrix (S.B7), as it showed a higher barrier to oil. On the other hand, barrier properties are negatively affected if the platelet's spatial periodicity is lost due to agglomeration by an excessive amount of bentonite (Romo-Uribe, 2022), as implied by S.B10. In addition, the barrier property is also diminished if there is a separation and random organization of the nanoplatelets due to the insufficient number of platelets (Romo-Uribe, 2022), as indicated by S.B5.

The surface free energy is connected to the barrier properties of multilayer sheets. The polar phase of the surface free energy indicates the presence of accessible polar groups, such as hydroxyl groups (Shahbazi *et al.*, 2017). The S sample presented the highest polar phase, indicating its high OH availability, followed by S.B7 packaging. The C2 paper, despite having also presented a high value of the polar phase of the surface free energy, also presented a high standard deviation, indicating that some regions of this paper have more hydroxyl groups available than other regions, which can be caused by the dual conditions of being wet and dry. The dispersed phase was significantly higher than the polar phase for all samples, which was also reported by Żołek-Tryznowska and Holica (2020).

4. CONCLUSION

Bentonite and cationic starch suspensions worked well together, demonstrating good synergy. Starch retrogradation from the prolonged mixing process may have contributed to the reduction in suspension viscosity that occurred with the addition of bentonite to the starch matrix. High pencil hardness was demonstrated using papers coated with cationic starch and cationic starch + 10 wt% bentonite. Additionally, the coatings demonstrated strong bonding to the paper, as demonstrated by SEM images and pencil hardness, with no interface gaps while filling the pores of the kraftliner paper in the coating area. Due to the hydrophilic properties of both starch and nanoclay, coated sheets demonstrated minimal water resistance in tests for wettability, water contact angle, and the Cobb test. However, when 7 wt% of bentonite was added to starch, the multilayer sheets displayed resistance to oil/grease and lost some of their wettability. The distribution between 7 wt% of bentonite positioned uniformly their platelets in the cationic starch matrix that physically blocked oil molecules and led to a maximum oil resistance by the coated paper. The mechanical strength of the paper was found to be predominantly affected by the water coating and drying process, whereas the starch demonstrated an increase in the ability of the coated sheets to elongate. Packaging produced from composites of bentonite and cationic starch on kraftliner paper showed a low barrier to water and water vapor. However, due to its oil barrier, adequate pencil hardness, tensile strength, and lower wettability, the S.B7 package may be a possible material for use in food/fat product packaging. For multilayer packaging for non-wetted products, coatings made of cationic starch, glycerol, and bentonite showed tremendous promise by increasing for up to 8H on pencil hardness, serving as a physical barrier between the environment and the product inside with a maximum oil barrier (n. 12 of oil kit test). More research is still needed to better understand how biodegradable and renewable materials interact to create waterproof affordable packaging or using a second hydrophobic layer to circumvent such interaction with water.

ACKNOWLEDGEMENT

This study was financed in part by the Coordenação de Aperfeiçoamento de Pessoal de Nível Superior – Brasil (CAPES) – Finance Code 001. The authors are grateful for the support of the Laboratory BioNano from the Federal University of Pelotas – UFPel, the Laboratory of Electron Microscopy and Analysis of Ultrastructural from the Federal University of Lavras – UFLA, and FINEP, FAPEMIG, CNPq, Rede RELIGAR, and CAPES for supplying the

equipment and technical support for experiments involving electron microscopy. The authors are also thankful for the Wood Science and Technology graduate program at the Federal University of Lavras – UFLA, and the Forest, Nature, and Biomass section at the University of Copenhagen – UCPH. Likewise, Klabin S/A for supplying commercial kraft paper and some characterization.

REFERENCES

- ABDULLA, A. H. D.; PUDJIRAHAR, S.; KARINA, M. *et al.* Fabrication and characterization of sweet potato starch-based bioplastics plasticized e work reported in this p with glycerol. **Journal of Biological Sciences**, v. 19, p. 57–64, 2018.
- ABDULLAH, Z. W.; DONG, Y. Biodegradable and water resistant poly(vinyl) alcohol (PVA)/starch (ST)/glycerol (GL)/halloysite nanotube (HNT) nanocomposite films for sustainable food packaging. **Frontiers in Materials**, v. 6, n. 58, 2019.
- ABNT NBR 8877 (2020) Adhesives - Determination of solids content. **Associação Brasileira de Normas Técnicas**, São Paulo, SP, 2020.
- ABNT NBR 9277 (2020) Adesivos - Determinação da viscosidade - Método do viscosímetro Brookfield, **Associação Brasileira de Normas Técnicas**, São Paulo, SP, 2020.
- AHMED, H. E.; BETIHA, M. A.; EL-DARDIR, M. *et al.* High-Performance Rheology Modifiers And Fluid Loss Of Starch-Bentonite System Based Mud Fluids: Experimental And Optimization Study. **Egyptian Journal of Chemistry**, v. 64, n. 4, p. 1653-1664, 2021.
- ALEKSEEVA, O. V.; RODIONOVA, A. N.; BAGROVSKAYA, N. A. *et al.* Effect of the organobentonite filler on structure and properties of composites based on hydroxyethyl cellulose. **Journal of Chemistry**, v. 11, 2017.
- ALGHUNAIM, N. S. Optimization and spectroscopic studies on carbon nanotubes/PVA nanocomposites. **Results in Physics**, v. 6, p. 56–60, 2016.
- ALVES, A. P. P.; OLIVEIRA, L. P. Z.; CASTRO, A. A. N. *et al.* The structure of different cellulosic fibres characterized by Raman spectroscopy. **Vibrational Spectroscopy**, v. 86, p. 324–330, 2016.
- ALZWEIGHI, M.; MANSOUR, R.; LAHTI, J. *et al.* The influence of structural variations on the constitutive response and strain variations in thin fibrous materials. **Acta Materialia**, v. 203, p. 116460, 2021.
- ASTM D3363-22 (2022) Standard Test Method For Film Hardness By Pencil Test, **ASTM International**, West Conshohocken, PA, 2022.
- ASTM D646-13 (2013) Standard Test Method for Grammage of Paper and Paperboard (Mass Per Unit Area), **ASTM International**, West Conshohocken, PA, 2013.

ASTM T 458 cm-04 (2004) Surface Wettability Of Paper (Angle Of Contact Method), **ASTM International**, West Conshohocken, PA, 2004.

ASTM D828-22 (2022) Standard Test Method for Tensile Properties of Paper and Paperboard Using Constant-Rate-of-Elongation Apparatus, **ASTM International**, West Conshohocken, PA, 2022.

ASTM E104-02 (2002) Standard Practice For Maintaining Constant Relative Humidity By Means Of Aqueous Solutions, **ASTM International**, West Conshohocken, PA, 2002.

ASTM E96 / E96M-16 (2016) Standard Test Methods for Water Vapor Transmission of Materials, **ASTM International**, West Conshohocken, PA, 2016.

AULIN, C.; GÄLLSTEDT, M.; LINDSTRÖM, T. Oxygen and oil barrier properties of microfibrillated cellulose films and coatings. **Cellulose**, v. 17, p. 559–574, 2010.

BAČOVSKÁ, R.; WISIAN-NEILSON, P.; ALBERTI, M. *et al.* Phenyl-methyl phosphazene derivatives for preparation and modification of hydrophobic properties of polymeric nonwoven textiles. **Reactive and Functional Polymers**, v. 100, p. 53-63, 2016.

BANDYOPADHYAY, A.; RAMARAO, B. V.; RAMASWAMY, S. Transient moisture diffusion through paperboard materials. **Colloids and Surfaces A: Physicochemical and Engineering Aspects**, v. 206, n.1-3, p. 455-467, 2002.

BARDET, R.; REVERDY, C.; BELGACEM, N. *et al.* Substitution of nanoclay in high gas barrier films of cellulose nanofibrils with cellulose nanocrystals and thermal treatment. **Cellulose**, v. 22, n. 2, p. 1227-1241, 2015.

BASIAK, E.; LENART, A.; DEBEAUFORT, F. How Glycerol and Water Contents Affect the Structural and Functional Properties of Starch-Based Edible Films. **Polymers**, v. 10, n. 4, p. 412, 2018.

BEHERA, L.; MOHANTA, M.; THIRUGNANAM, A. Intensification of yam-starch based biodegradable bioplastic film with bentonite for food packaging application. **Environmental Technology and Innovation**, v. 25, p. 102180, 2022.

BIAN, H., GAO, Y., LUO, J. *et al.* Lignocellulosic nanofibrils produced using wheat straw and their pulping solid residue: from agricultural waste to cellulose nanomaterials. **Waste Management**, v. 91, p. 1–8, 2019.

BREEN, C.; CLEGG, F.; THOMPSON, S. *et al.* Exploring the interactions between starches, bentonites and plasticizers in sustainable barrier coatings for paper and board. **Applied Clay Science**, v. 183, p. 105272, 2019.

BRODIN, F. W.; GREGERSEN Ø. W.; SYVERUD, K. Cellulose nanofibrils: challenges and possibilities as a paper additive or coating material - a review. **Nordic Pulp and Paper Research Journal**, v. 29, p. 156–166, 2014.

BULKIN, B.; KWAK, Y. Retrogradation kinetics of waxy-corn and potato starches: A rapid, Raman-spectroscopic study. **Carbohydrate Research**, v. 160, p. 95–112, 1987.

- BUNDY, W. M.; ISHLEY, J. N. Kaolin in paper filling and coating. **Applied Clay Science**, v. 5, p. 397-420, 1991.
- CASTILLO, L. A.; LÓPEZ, O. V.; GARCÍA, M. A. *et al.* Crystalline morphology of thermoplastic starch/talc nanocomposites induced by thermal processing. **Heliyon**, v. 5, n. 6, p. e01877, 2019.
- CHEN, L.; SUN, X.; HANG, J. *et al.* Large-Scale Fabrication of Robust Superhydrophobic Coatings with High Rigidity and Good Flexibility. **Advanced materials interfaces**, v. 3, p. 1500718, 2016.
- CHI, K.; CATCHMARK, J. M. Improved eco-friendly barrier materials based on crystalline nanocellulose/chitosan/carboxymethyl cellulose polyelectrolyte complexes. **Food Hydrocolloids**, v. 80, p. 195-205, 2018.
- CHI, K.; WANG, H.; CATCHMARK, J. M. Sustainable starch-based barrier coatings for packaging applications. **Food Hydrocolloids**, v. 103, p. 105696, 2020.
- CHIUMARELLI, M.; HUBINGER, M. D. Evaluation of edible films and coatings formulated with cassava starch, glycerol, carnauba wax and stearic acid. **Food Hydrocolloids**, v. 38, p. 20–27, 2014.
- CLEGG, F.; BREEN, C.; MURANYI, P. *et al.* Antimicrobial, starch based barrier coatings prepared using mixed silver/sodium exchanged bentonite. **Applied Clay Science**, v. 179, p. 105144, 2019.
- DANG, K. M.; YOKSAN, R.; POLLET, E. *et al.* Morphology and properties of thermoplastic starch blended with biodegradable polyester and filled with halloysite nanoclay. **Carbohydrate Polymers**, v. 242, p. 116392, 2020.
- DEY, N.; VICKRAM, S.; THANIGAIVEL, S. *et al.* Nanomaterials for transforming barrier properties of lignocellulosic biomass towards potential applications – A review. **Fuel**, v. 316, p. 123444, 2022.
- DROZDOV, A. D.; CHRISTIANSEN, J. D.; GUPTA, R. K. *et al.* Model for anomalous moisture diffusion through a polymer–clay nanocomposite. **Journal of Polymer Science Part B: Polymer Physics**, v.41, p. 476–492, 2003.
- FERRARI, M.; BENEDETTI, A. Superhydrophobic surfaces for applications in seawater. **Advances in Colloid and Interface Science**, v. 222, p. 291–304, 2015.
- FERREIRA, D. F. Sisvar: a Guide for its Bootstrap procedures in multiple comparisons. **Ciência e agrotecnologia**, v. 38, n.2, 2014.
- FERREIRA, S. R.; SILVA, F. A.; LIMA, P. R. L. *et al.* Effect of hornification on the structure, tensile behavior and fiber matrix bond of sisal, jute and curauá fiber cement based composite systems. **Construction and Building Materials**, v. 139, p. 551–561, 2017.

FOLETTI, E. L.; VOLZONE, C.; PORTO, L. M. Performance of an argentinian acid-activated bentonite in the bleaching of soybean oil. **Brazilian Journal of Chemical Engineering**, v. 20, n. 2, 2003.

FOLLAIN, N.; JOLY, C.; DOLE, P. *et al.* Properties of starch based blends. Part 2. Influence of poly vinyl alcohol addition and photocrosslinking on starch based materials mechanical properties. **Carbohydrate Polymers**, v. 60, n. 2, p. 185-192, 2005.

GABR, M. H.; PHONG, N. T.; ABDELKAREEM, M. A. *et al.* Mechanical, thermal, and moisture absorption properties of nano-clay reinforced nano-cellulose biocomposites. **Cellulose**, v. 20, p. 819–826, 2013.

GADHAVE, R.V.; MAHANWAR, P.A.; GADEKAR, P.T. Effect of glutaraldehyde on thermal and mechanical properties of starch and polyvinyl alcohol blends. **Designed Monomers and Polymers**, v. 22, p. 164–170, 2019.

GALEENER, F. L.; GEISSBERGER, A. E. Vibrational dynamics in isotopically substituted vitreous GeO₂. **Physical Review B - Condensed matter**, v. 27, p. 6199, 1983.

GAO, W.; DONG, H.; HOU, H. *et al.* Effects of clays with various hydrophilicities on properties of starch–clay nanocomposites by film blowing. **Carbohydrate Polymers**, v. 88, n. 1, p. 321-328, 2012.

GAO, W.; WU, W.; LIU, P. *et al.* Preparation and evaluation of hydrophobic biodegradable films made from corn/octenylsuccinated starch incorporated with different concentrations of soybean oil. **International Journal of Biological Macromolecules**, 2019.

GUIMARÃES JR., M.; BOTARO, V.R.; NOVACK, K.M. *et al.* Preparation of cellulose nanofibrils from bamboo pulp by mechanical defibrillation for their applications in biodegradable composites. **Journal of Nanoscience and Nanotechnology**, v. 15, p. 6751–6768, 2015.

GUL, S.; KAUSAR, A.; MUHAMMAD, B. *et al.* Research progress on properties and applications of Polymer/Clay nanocomposite. **Polymer-Plastics Technology and Engineering**, v. 55, p. 684-703, 2016.

GUO, Z.; JIA, X.; LIN, X. *et al.* Insight into the formation, structure and digestibility of lotus seed amylose-fatty acid complexes prepared by high hydrostatic pressure. **Food and Chemical Toxicology**, v. 128, p. 81–88, 2019.

HASSANI, S. A.; SALIM, F. Z.; KASSAB, M. H. *et al.* Crosslinked starch-coated cellulosic papers as alternative food-packaging materials. **RSC Advances**, v. 12, n. 14, p. 8536-8546, 2022.

HORSEMAN, T.; TAJVIDI, M.; DIOP, C. I. K. *et al.* Preparation and property assessment of neat lignocellulose nanofibrils (LCNF) and their composite films. **Cellulose**, v. 24, p. 2455–2468, 2017.

HU, X.; SHI, J.; ZHANG, F. *et al.* Determination of retrogradation degree in starch by mid-infrared and Raman spectroscopy during storage. **Food Analytical Methods**, v. 10, n. 11, p. 3694–3705, 2017.

HU, Z.; ZEN, X.; GONG, J. *et al.* Water resistance improvement of paper by superhydrophobic modification with microsized CaCO₃ and fatty acid coating. **Colloids and Surfaces A: Physicochemical and Engineering Aspects**, v. 351, n. 1–3, p. 65–70, 2009.

ISO 534:2011 (2011) Paper And Board - Determination Of Thickness, Density And Specific Volume. **International Organization for Standardization**, Washington, DC, 2011.

JOHANSSON, C.; BRA, J.; MONDRAGON, I. *et al.* Renewable Fibres and Biobased Materials for packaging applications - a review of recent developments. **Bioresources**, v. 7, p. 2506–2552, 2012.

KAELBLE, D. H. Dispersion-polar surface tension properties of organic solids. **The Journal of Adhesion**, v. 2, p. 66–81, 1970.

KHAIRUDDIN, K.; NURHAYATI, N. D.; SHODIK, I. S. J. *et al.* Water vapour and grease resistance properties of paper coating based starch-bentonite clay. **Journal of Physics: Conference Series**, v. 1153, p. 012090, 2019.

LENDVAI, L.; SAJÓ, I.; KARGER-KOCSIS, J. Effect of Storage Time on the Structure and Mechanical Properties of Starch/Bentonite Nanocomposites. **Starch – Stärke**, v. 71, p. 1800123, 2019.

LIN, D.; KUANG, Y. CHEN, G. *et al.* Enhancing moisture resistance of starch-coated paper by improving the film forming capability of starch film. **Industrial Crops and Products**, v. 100, p. 12-18, 2017.

LIU, H.; XIE, B.; QIN, Y. Effect of bentonite on the pelleting properties of iron concentrate. **Journal of Chemistry**, p. 1–6, 2017.

LIU, S.; LIU, L.; LI, B. *et al.* Size effect of carnauba wax nanoparticles on water vapor and oxygen barrier properties of starch-based film. **Carbohydrate Polymers**, v. 296, p. 119935, 2022.

MÉITÉ, N.; KONAN, L. K.; TOGNONVI, M. T. *et al.* Effect of metakaolin content on mechanical and water barrier properties of cassava starch films. **South African Journal of Chemical Engineering**, v. 40, p. 186-194, 2022.

MIAO, X.; LIN, J.; BIAN, F. Utilization of discarded crop straw to produce cellulose nanofibrils and their assemblies. **Journal of Bioresources and Bioproducts**, v. 5, p. 26–36, 2020.

MONTEIRO, M. K. S.; OLIVEIRA, V. R. L.; SANTOS, F. K. G. *et al.* Incorporation of bentonite clay in cassava starch films for the reduction of water vapor permeability. **Food Research International**, v. 105, p. 637–644, 2018.

- MUELLER, C. M. O.; LAURINDO, J. B.; YAMASHITA, F. Effect of nanoclay incorporation method on mechanical and water vapor barrier properties of starch-based films. **Industrial Crops and Products**, v. 33, p. 605–610, 2011.
- NATÁLIA, F. M.; CRISTINA, T. A. Calcium bentonite as reinforcing nanofiller for thermoplastic starch. **Journal of the Brazilian Chemical Society**, v. 21, p. 202–208, 2010.
- NIELSEN, L. E. Models for the permeability of filled polymer systems. **Journal of Macromolecular Science: Part A - Chemistry**, v.1, n. 5, p. 929–942, 1967.
- NING, W.; XINGXIANG, Z.; NA, H. *et al.* Effect of citric acid and processing on the performance of thermoplastic starch/montmorillonite nanocomposites. **Carbohydrate Polymers**, v. 76, p. 68–73, 2009.
- NORDIN, N.; OTHMAN, S.H.; RASHID, S.A. *et al.* Effects of Glycerol and Thymol on Physical, Mechanical, and Thermal Properties of Corn Starch Films. **Food Hydrocolloids**, v. 106, p. 105884, 2020.
- OLIVATO, J. B.; YAMASHITA, F.; POLLET, E. *et al.* Sepiolite as a promising nanoclay for nano-biocomposites based on starch and biodegradable polyester. **Materials Science and Engineering: C**, v. 70, n. 1, p. 296-302, 2017.
- OLIVEIRA, M. L. C.; MIRMEHDI, S.; SCATOLINO, M. V. *et al.* Effect of overlapping cellulose nanofibrils and nanoclay layers on mechanical and barrier properties of spray-coated papers. **Cellulose**, v. 29, p. 1097–1113, 2022.
- OLSSON, E.; JOHANSSON, C.; JÄRNSTRÖM, L. *et al.* Montmorillonite for starch-based barrier dispersion coating—Part 1: The influence of citric acid and poly(ethylene glycol) on viscosity and barrier properties. **Applied Clay Science**, v. 97–98, p. 160–166, 2014a.
- OLSSON, E.; JOHANSSON, C.; LARSSON, J. *et al.* Montmorillonite for starch based barrier dispersion coating – part 2: pilot trials and PE-lamination. **Applied Clay Science**, v. 97–98, p. 167–173, 2014b.
- OLSSON, E.; MENZEL, C.; JOHANSSON, C. *et al.* The effect of pH on hydrolysis, cross-linking and barrier properties of starch barriers containing citric acid. **Carbohydrate Polymers**, v. 98, n. 2, p. 1505-1513, 2013.
- OWENS, D. K.; WENDT, R. C. Estimation of the surface free energy of polymers. **Journal of Applied Polymer Science**, v. 13, p. 1741–1747, 1969.
- PARK, H.; LI, X.; JIN, C. *et al.* Preparation and properties of biodegradable thermoplastic starch/clay hybrids. **Macromolecular Materials and Engineering**, v. 287, p. 553–558, 2002.
- PARKER, M.E.; BRONLUND, J.E; MAWSON, A.J. Moisture sorption isotherms for paper and paperboard in food chain conditions. **Packaging Technology and Science**, v. 19, p. 193-209, 2006.

- RABEL, W. Einige Aspekte der Benetzungstheorie und ihre Anwendung auf die Untersuchung und Veränderung der Oberflächeneigenschaften von Polymeren. **Farbe und Lack**, v. 77, p. 997–1005, 1971.
- RADOSTA, S.; VORWERG, W.; ELBERT, A. *et al.* Properties of Low-substituted Cationic Starch Derivatives Prepared by Different Derivatisation Processes. **Starch**, v. 56, p. 277–287, 2004.
- RHIM, J.W. Effect of moisture content on tensile properties of paper-based food packaging materials. **Food Science and Biotechnology**, v. 19, p. 243–247, 2010.
- RHIM, J. W.; HONG, S. I.; PARK, H. M. *et al.* Preparation and characterization of chitosan-based nanocomposite films with antimicrobial activity. **Journal of Agricultural and Food Chemistry**, v. 54, p. 5814–5822, 2006.
- RIHAYAT, T.; SURYANI, S.; SATRIANANDA, S. *et al.* Poly lactic acid (PLA)/chitosan/bentonite nanocomposites based on cassava starch for materials in biomedical applications. **The 3rd International Seminar on Chemistry AIP Conference Proceedings**, v. 2049, p. 020021-1–020021-6, 2018.
- ROMER, C. T. A study of bentonite as an additive for starch size press treatment. **Paper Engineering Senior Theses**, P. 394. Western Michigan University, 1978.
- ROMO-URIBE, A. Wide-angle X-ray diffraction and small-angle X-ray scattering studies of elastomer blends and nanocomposites. In: Rangappa, S.K., Parameswaranpillai, J., Siengchin, S., and Ozbakkaloglu, T. (Eds.). *Elastomers, blends and composites*. Elsevier, Amsterdam, 2022.
- SÁ, R. M.; MIRANDA, C. S.; JOSÉ, N. M. Preparation and characterization of Nanowhiskers cellulose from fiber arrowroot (*Maranta arundinacea*). **Materials Research**, v. 18, p. 225–229, 2015.
- SAJI, V. S. Wax-based Artificial Superhydrophobic Surfaces and Coatings. **Colloids and Surfaces A: Physicochemical and Engineering Aspects**, v. 602, p. 125132, 2020.
- SALMÉN, L.; BERGSTRÖM, E. Cellulose structural arrangement in relation to spectral changes in tensile loading FT-IR. **Cellulose**, v. 16, p. 975–982, 2009.
- SAMYN, P. Wetting and hydrophobic modification of cellulose surfaces for paper applications. **Journal of Material Science**, v. 48, p. 6455–6498, 2013.
- SANTOS, A. M. P.; YOSHIDA, M. P. Embalagens. Recife: **Edufre**, 152p. ISBN 978-85-7946-090-6, 2011.
- SARKAR, A.; BISWAS, D. R.; DATTA, S. C. *et al.* Preparation of novel biodegradable starch/poly(vinyl alcohol)/bentonite grafted polymeric films for fertilizer encapsulation. **Carbohydrate Polymers**, v. 259, p. 117679, 2021.
- SETH, R. S.; PAGE, D. J. Fracture resistance of paper. **Journal of Materials Science**, v. 9, p. 1745-1753, 1974.

SHAHBAZI, M.; RAJABZADEH, G.; SOTOODEH, S. Functional characteristics, wettability properties and cytotoxic effect of starch film incorporated with multi-walled and hydroxylated multi-walled carbon nanotubes. **International Journal of Biological Macromolecules**, v. 104, n. 1, p. 597-605, 2017.

SHANMATHY, M.; MOHANTA, M.; THIRUGNANAM, A. Development of biodegradable bioplastic films from Taro starch reinforced with bentonite. **Carbohydrate Polymer Technologies and Applications**, v. 2, p. 100173, 2021.

SØRENSEN, G.; HOFFMANN, J. Moisture sorption in moulded fibre trays and effect on static compression strength. **Packaging Technology and Science**, v. 16, p. 159-169, 2003.

TAN, B.; THOMAS, N. L. A review of the water barrier properties of polymer/clay and polymer/grapheme nanocomposites. **Journal of Membrane Science**, v. 514, p. 595–612, 2016.

TANG, X.; ALAVI, S.; HERALD, T. J. Effects of plasticizers on the structure and properties of starch-clay nanocomposite films. **Carbohydrate Polymers**, v. 74, p. 552–558, 2008.

TAPPI T 559 cm-12 (2012) Grease Resistance Test for Paper and Paperboard. **Technical Association of the Pulp and Paper Industry**, Peachtree Corners, GA, United States, 2012.

TAPPI T441 om-13 (2013) Water absorptiveness of sized (non-bibulous) paper, paperboard, and corrugated fiberboard (Cobb test). **Technical Association of the Pulp and Paper Industry**, Peachtree Corners, GA, United States, 2013.

THÉBAULT, M.; KANDELBAUER, A.; MÜLLER, U. *et al.* Factors influencing the processing and technological properties of laminates based on phenolic resin impregnated papers. **European Journal of Wood and Wood Products**, v. 75, p. 785–806, 2017.

TIAN, H.; YAN, J.; RAJULU, A. V. *et al.* Fabrication and properties of polyvinyl alcohol/starch blend films: Effect of composition and humidity. **International Journal of Biological Macromolecules**, v. 96, p. 518-523, 2017.

TODOROVA, D.; YAVOROV, N.; LASHEVA, V. Improvement of barrier properties for packaging applications. **Sustainable Chemistry and Pharmacy**, v. 27, p. 100685, 2022.

TOMASIK, P.; SCHILLING, C.H. Chemical modification of starch. **Advances in Carbohydrate Chemistry and Biochemistry**, v. 59, p. 175-403, 2004.

UDDIN, F. Montmorillonite: an introduction to properties and utilisation. Current topics in the utilisation of clay in industrial and medical applications. **IntechOpen**, p. 3–20, 2018.

VAN OLPHEN, H. Surface conductance of various ion forms of bentonite in water and the electrical double layer. **Journal of Physical Chemistry**, v. 61, p. 1276–1280, 1957.

VAYSI, R.; VAGHARI, K. The effect of using cationic starch, long fiber and nano-clay on physical and mechanical properties of recycled pulp. **Iranian Journal of Wood and Paper Science Research**, v. 36, n. 4, 2021.

WANG, S.; JING, Y. Effects of formation and penetration properties of biodegradable montmorillonite/chitosan nanocomposite film on the barrier of package paper. **Applied Clay Science**, v. 138, p. 74–80, 2017.

WANG, F.; WANG, L.; ZHANG, X. *et al.* Study on the barrier properties and antibacterial properties of cellulose-based multilayer coated paperboard used for fast food packaging. **Food Bioscience**, v. 46, p. 101398, 2022.

WYAN, L. **Analysis of Over-the-Counter Antihistamines Through Raman Spectroscopy and Density Functional Theory Calculations**. Honors College Theses – Pace University, New York, 264 p., 2019.

XU, D.; QIN, H.; REN, D. Prolonged preservation of tangerine fruits using chitosan/montmorillonite composite coating. **Postharvest Biology and Technology**, v. 143, p. 50–57, 2022.

YANG, J.; ZHAO, K.; WANG, G. *et al.* Influence of coating thickness on microstructure, mechanical and LBE corrosion performance of amorphous AlCrFeTiNb high-entropy alloy coatings. **Surface and Coatings Technology**, v. 441, p. 128502, 2022.

ZAFAR, N.; NIAZI, M. B. K.; SHER, F.; *et al.* Starch and polyvinyl alcohol encapsulated biodegradable nanocomposites for environment friendly slow release of urea fertilizer. **Chemical Engineering Journal Advances**, v. 7, p. 100123, 2021.

ZAMRUD, Z.; NG, W. M.; SALLEH, H. M. Effect of bentonite nanoclay filler on the properties of bioplastic based on sago starch. **IOP Conf. Series: Earth and Environmental Science**, v. 765, p. 012009, 2021.

ZHANG, W.; XIAO, H.; QIAN, L. Enhanced water vapour barrier and grease resistance of paper bilayer-coated with chitosan and beeswax. **Carbohydrate Polymers**, v. 101, p. 401–406, 2014.

ZHAO, Y.; LIU, E.; FAN, J.; *et al.* Superhydrophobic PDMS/wax coated polyester textiles with selfhealing ability via inlaying method. **Progress in Organic Coatings**, v. 132, p.100–107, 2019.

ZHU, R.; FU, X.; JIN, S. *et al.* Water and oil-resistant paper materials based on sodium alginate/hydroxypropyl methylcellulose/polyvinyl butyral/nano-silica with biodegradable and high barrier properties. **International Journal of Biological Macromolecules**, 2022.

ŻOŁEK-TRYZNOWSKA, Z.; HOLICA, J. Starch films as an environmentally friendly packaging material: Printing performance. **Journal of Cleaner Production**, v. 276, p. 124265, 2020.

FIFTH PART

Kraftliner paper coated with cationic starch/glycerol and poly(vinyl alcohol) blends to generate water vapor and O₂ barriers

Allan de Amorim dos Santos^{ab*}, Lays Camila Matos^a, Alisson Farley Soares Durães^a, Maressa Carvalho Mendonça^a, Marcelo Coelho dos Santos Muguet^c, Anand Ramesh Sanadi^b, Gustavo Henrique Denzin Tonoli^a.

^a Department of Forest Science/ESAL, University of Lavras, University Campus, PO Box 3037, 37200-000, Lavras, MG, Brazil.

^b Department of Geosciences and Natural Resource Management, University of Copenhagen, Rolighedsvej 23 – 1958, Frederiksberg, Denmark.

^c Klabin, Technology Center, Industrial R&D+I, Fazenda Monte Alegre, St. Harmonia, 84275-000, Telêmaco Borba, PR, Brazil.

*Corresponding author: *allan.santos1@estudante.ufla.br*

The manuscript can be modified according to the suggestions of the journal's reviewers.

ABSTRACT

This work aimed to evaluate blend formulations with cationic starch/glycerol and poly(vinyl alcohol) for applications as a kraftliner paper coating. Blends of both polymers in 5 different proportions were tested in formulations. Uncoated kraftliner paper and double wet-and-dry paper were used as controls. The formulations were applied in two layers of 15.0 ± 0.5 g/m² on 86 ± 1 g/m² paper with a coating machine. Suspension characterization and the physical properties of the coated papers were evaluated, as well as the barrier to water, water vapor, oxygen, and oil/grease, scanning electron microscopy, and Fourier transform infrared spectroscopy following standard methods. The papers coated with cationic starch showed low water resistance. However, the blends formed with poly(vinyl alcohol) presented oxygen and water vapor barriers, reaching values lower than 10 cc/(mm².day) and 586 ± 23 g/m².day, respectively. Combining materials can improve the barrier properties of coated papers to create biodegradable and renewable formulations, promoting sustainable packaging.

Keywords: Eco-friendly coating. Oxygen barrier. Renewable packaging.

1. INTRODUCTION

Oxygen plays a vital role in the food we eat, as its presence causes food to deteriorate through lipid and vitamin oxidation and might favor mold growth. In addition, through acting on enzymes, oxygen can change the color of fruits and drinks, cause unpleasant flavors, decrease the nutritional value of food, and reduce the shelf life, thus causing a risk to consumers (Giuseppe *et al.*, 2022; Dey and Neogi, 2019). Therefore, oxygen contributes to increased food losses and causes economic damage; therefore, controlling the presence of oxygen in packaging is an essential factor.

A viable strategy is using packaging, such as glass and aluminum, that blocks the entry of oxygen and prevents oxygen from contacting food. In addition to generating an oxygen barrier, these materials also provide an oil/grease and water vapor barrier. Aluminum packaging also blocks light. However, using these materials can involve some disadvantages. The weight of glass can increase transportation costs, and aluminum packaging involves complex recycling issues (Xu *et al.*, 2022; Vinci *et al.*, 2019). Plastic packaging met this demand, as its use and application are versatile. However, plastic packaging exhibits several disadvantages, as the material is not biodegradable, persists for a long time in the environment, and releases toxic substances in soil and water (Kan and Miller, 2022; Bassi *et al.*, 2020). Paper and cardboard play a significant role in replacing plastic packaging. These materials originate from renewable resources, are biodegradable, exhibit good mechanical properties, utilize traditional production technology and are inexpensive (Petersen *et al.*, 1999; Conti, 1997). Kraftliner is a flexible, durable, tensile-resistant, and suitable type of printable kraft paper that exhibits high performance and superior presentation (Torres *et al.*, 2020; Bierman, 1996). However, due to its fibrous structure and high porosity content, kraftliner is highly permeable to moisture and gases, making its use unfeasible for packaging certain food products, i.e., those with a high water content or those requiring low translocation of gases. Therefore, the technology of coating potential biodegradable polymers and biopolymers on paper can add barrier properties to the high mechanical property of paper packaging (Dilkes-Hoffman *et al.*, 2019; Muthus, 2016).

As a polymer susceptible to biodegradation (Byerne *et al.*, 2021), poly(vinyl alcohol) (PVOH) is a good coating for paper due to its ability to form thin films with an oil/grease barrier, low water vapor permeability, and high oxygen barrier, with oxygen transmission rates close to 0.4 mL/m²/day (Patil *et al.*, 2022; Suhag *et al.*, 2022; Ge, Lansing, and Lewis, 2021; Roy and Rhim, 2021; Hay and Lyon, 1967). The angulation of glucose unit bonds and the extension of the amylopectin chain make starch a good film-forming biopolymer. These films

have a moderate oil and gas barrier, a low moisture barrier, and low mechanical strength but also exhibit a high yield and availability. Plasticizers are combined with starch to improve the strength properties of films. Glycerol, which is nontoxic and suitable for packaging that contacts food, is the most common low molecular weight plasticizer additive for starch (Basiak *et al.*, 2018).

The starch chain contains numerous primary and secondary hydroxyl groups at carbons 2, 3, and 6, making starch highly hydrophilic. Such hydroxyl groups favor their transformation (Tomasik and Schilling, 2004). The modification of starch can improve its adhesion as a blend, increasing its barrier properties (Guo *et al.*, 2022; Hakke *et al.*, 2022; Dang *et al.*, 2021; Patil *et al.*, 2021). Cationic starch, for example, improves the mechanical strength and barrier of starch by providing a positive charge, which is easily attracted by the negative charges from cellulose fiber or other polymers used as a blend (Wang *et al.*, 2022; You *et al.*, 2022). Thus, the combination of PVOH and starch expands barrier functions (Garavand *et al.*, 2022; Kochkina, Butikova, and Lukin, 2022; Wu *et al.*, 2021; Khazael *et al.*, 2021; Kumar *et al.*, 2021; Lee *et al.*, 2021; Liu *et al.*, 2021; Yao *et al.*, 2021).

Christophliemk *et al.* (2017) investigated the addition of modified poly(vinyl alcohol) on the performance of corn and potato starch coatings. The authors showed that up to 70 wt.% starch, as a renewable polymer, was effective in maintaining the oxygen barrier of PVOH. Gómez-Alpada *et al.* (2020) evaluated mixtures in different proportions of PVOH and starch regarding the effect on water adsorption, water vapor permeability, and mechanical and thermal properties for biodegradable alternatives to food packaging and for synthetic packaging materials. Mittal, Garg, and Bajpai (2020) studied starch and PVOH films reinforced with grafted barley husks as substitutes for synthetic films in paper packaging. Patil *et al.* (2021) found that incorporating PVOH into the starch polymer resulted in composite films with better mechanical and barrier performances, decreasing water vapor permeability by 52% (25 °C, 85% RH). Qin *et al.* (2021) added anthocyanin-loaded nanocomplexes to a starch/PVOH blend and noticed denser microstructures with stronger intermolecular interactions, blocking by water vapor 75% (at 20 °C, 90% RH).

Even with a diverse amount of research related to using blends of PVOH and starch with barrier function, studies on the application of high-viscosity cationic starch in such a mixture on kraftliner paper remained to be better explored and elucidated. There is still a lack of information and details in the literature about the application (suspensions and bar coating) and performance (chemical interactions, surface energy, thermomechanical, microstructure, and permeabilities) of high-viscosity cationic starch:PVOH blends as a paper coating for different

paper barriers (oil/grease, water vapor, and O₂). Our hypothesis is that cationic starch:PVOH blends are able to provide important barrier properties for coated papers, which depends on, and are related to the ratio of the components in those blends. More detailed information about the chemical interactions of cationic starch and PVOH, microstructure, and performance of the ensuing coated papers are valuable for optimizations and theoretical studies about renewable and biodegradable polymers. In this context, this work aimed to evaluate the influence of the addition of cationic starch to PVOH (1:0, 3:1, 1:1, 1:3, and 0:1 – m/m) on physical, chemical, mechanical, and barrier properties of the ensuing kraftliner coated barrier papers.

2. EXPERIMENTAL

2.1 Material

Klabin S/A (Paraná, Brazil) provided kraftliner paper (kappa number 100, 86 ± 1 g/m²), cationic starch (95 wt.%, amylose content 42%, degree of substitution 0.243), and PVOH (M_w 89,000 g/mol, degree of hydrolysis 98 mol%). Glycerol ($\geq 99\%$) was obtained from Êxodo Científica (São Paulo, Brazil).

2.1.1 Preparation of suspensions

The preparation of 4.0 wt.% cationic starch followed Gao *et al.* (2020) suggestions with complete starch solubilization at room temperature (23 °C, 400 rpm) for 30 min. Afterward, starch was gelatinized at 60 °C (500 rpm), followed by the addition of 20 wt.% glycerol. The PVOH suspension was used as such.

With both suspensions, blends with complementary proportions (m:m) of 1:0, 3:1, 1:1, 1:3, and 0:1 of cationic starch (S) and PVOH (P) were obtained with mechanical agitation (10 min, 400 rpm). Table 1 shows the treatments with their solid content (NBR 8877 - ABNT, 2020), pH measurement (W38 Bel Engineering, Brazil), and viscosity (NBR 9277 - ABNT, 2020) in addition to the control treatment of kraftliner paper without coating (C1) and double wet-and-dry paper (C2) to compare and contrast the effect of water on paper, computing seven treatments. The methodology is summarized in the Figure 1.

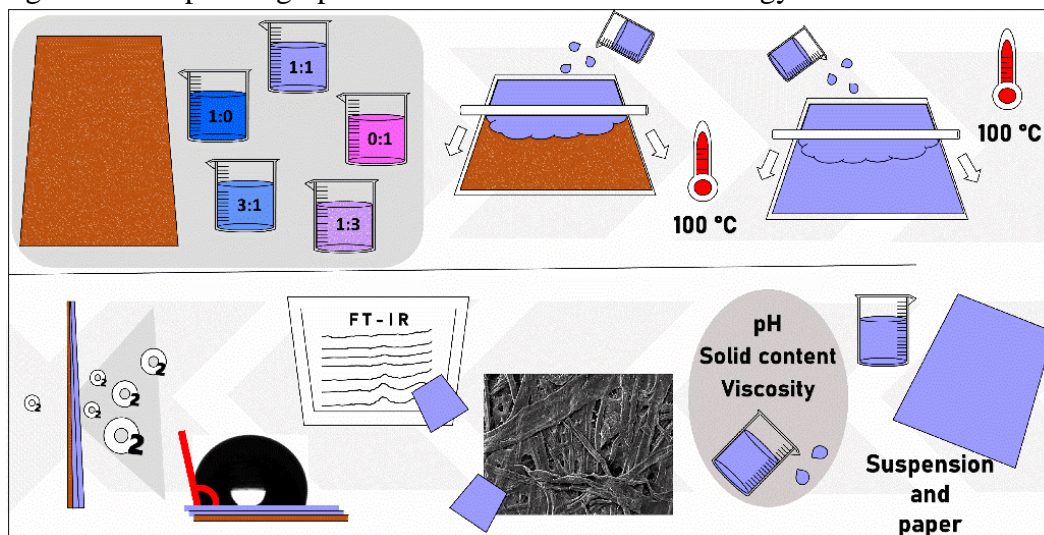
Table 1 - Description of treatments and characterization of pH, solids content, and viscosity of the blend suspension formed by cationic starch and poly(vinyl alcohol).

| Sample | Description | pH | Solid content (%) | Viscosity (cP) |
|--------|--|-----------------|-------------------|--------------------|
| C1 | Control 1 - Without coating | - | - | - |
| C2 | Control 2 - Double wet-and-dry | - | - | - |
| S | Cationic starch | 7.8 ± 0.1^a | 4.2 ± 0.1^a | 4707.7 ± 3.1^a |
| S3:1P | Cationic starch 3:1* Poly(vinyl alcohol) | 6.8 ± 0.1^b | 4.1 ± 0.2^a | 490.3 ± 4.0^b |
| S1:1P | Cationic starch 1:1* Poly(vinyl alcohol) | 6.3 ± 0.1^c | 6.0 ± 0.1^b | 478.7 ± 5.1^c |
| S1:3P | Cationic starch 1:3* Poly(vinyl alcohol) | 6.1 ± 0.1^d | 9.3 ± 0.7^c | 423.0 ± 7.2^d |
| P | Poly(vinyl alcohol) | 6.0 ± 0.1^e | 19.0 ± 0.2^d | 331.3 ± 1.5^e |

* Proportion in m:m. Average value \pm standard deviation. The same letters in the columns do not differ according to the Scott-Knott test at 5% significance.

Source: From the author (2023).

Figure 1 - Simplified graphical abstract with the methodology used in this research.



Source: From the author (2023).

2.1.2 Kraftliner paper coating

The suspension application with two layers in 297x210 mm kraftliner paper was carried out layer-by-layer with a coating machine (4 m/min). The suspension was uniformly spread with a bar with enough amount, which was predetermined by the solid content, to reach a grammage of 7.5 ± 0.3 g/m² (ASTM D646-13, 2013) for the first layer (bar n. 220), followed by drying at 103 ± 2 °C for 5 min. A second layer was applied under similar conditions (bar n. 100), reaching 15.0 ± 0.5 g/m² total, followed by drying. The first layer fills the roughness and porosity of the paper, anchoring the coating, while the second layer evens out the surface, forming a continuous film. The suspension application followed the direction of the fibers in the machine direction (MD) of the kraftliner paper.

2.2 Methods

2.2.1 Physical properties of coated paper

a) *Thickness and density:* The thickness and density of the multilayer paper were measured according to the ISO 534:2011 (ISO, 2011) procedure using a Regmed micrometer (ESP/SA-10, Brazil).

b) *Scanning electron microscopy:* The paper surface and cross-section, cut with liquid nitrogen, and coated with gold using a spray Balzers coating technique (SCD 050), were placed on aluminum stubs with carbon tape on aluminum foil and evaluated by field-emission scanning electron microscopy (SEM) under a Tescan (Clara, Czech Republic) under working conditions of 10 kV and a working distance of 8 mm.

2.2.2 Thermogravimetric analysis (TGA)

TGA is a method used to evaluate the change in mass as a temperature function. This work measured samples using a Netzsch (Perseus® TG 209 F1 Libra®, Japan). An atmosphere of N₂ (20 mL/min) with a heating rate of 10 K/min was used. Measurements for samples between 20 °C (293 K) and 600 °C (873.15 K) were processed using Software provided by Netzsch in a standard Al₂O₃ crucible. Instrument correction used the measurement of an empty crucible. T_{onset} and T_{half} indicate the temperature at the beginning of the thermal event, calculated by extrapolation and at 50% mass loss, respectively.

2.2.3 Fourier transform infrared spectroscopy (FT-IR)

Attenuated total reflectance Fourier transform infrared spectroscopy (ATR FT-IR) was performed to identify the chemical structure of the coating and possible interactions between its components. A Nicolet 6700 FT-IR equipped with a Pike Technologies GladiATR diamond spectrometer (Thermo Scientific, Waltham, MA, USA) collected spectra with an average of 60 scans recorded at 4 cm⁻¹ resolution in the range 4,000 to 500 cm⁻¹ at room temperature of 23 °C. The Origin Pro 8.5 software's Peak Analyze function (OriginLab, USA) was used to establish the baseline. The peaks' bases were marked by 20 points that were connected by a line interpolation and smoothed by the 10 AAV function.

2.2.4 Water barrier property of coated paper

a) *Water contact angle*: Krüss Drop Shape Analyzer - Goniometer DSA25 (Hamburg, Germany) measured the water contact angle with the coated paper surface in triplicate. A camera captures the image of the deionized water drop deposited from 20 mm, analyzing ten average contact angles with the paper by Advance Software at room temperature (23 °C) after water stabilization.

b) *Wettability*: The wettability of multilayer papers followed the procedures proposed by ASTM T 458 cm-04 (ASTM, 2004). This method measures the angle at 5 s after contact with the coated paper and after a period of 55 s (total of 60 s) in triplicate. A higher drop dispersion means a smaller angle after 60 s and, consequently, high wettability. Wettability is calculated using Equation 1.

$$\text{Wettability} = \frac{(A-a)}{55} \quad (1)$$

‘R’ represents wettability in °/s; ‘A’ represents the contact angle with water in 5 s in °; ‘a’ represents the contact angle with the water after 60 s in °; ‘55’ represents the time for the paper to absorb the water in seconds.

c) *Cobb test*: The water absorption test (Cobb test) followed TAPPI T441 om-13 (TAPPI, 2013) with 100 mL of deionized water poured over 15x15 cm samples into a ring instrument for 120 s. A 10 kg roller presses the humid samples between two absorbent papers to remove trapped moisture, weighed before and after the procedure. The Cobb index shows the relationship between the mass of water absorbed by the multilayer paper and the wetted area (g/m²).

d) *Water vapor permeability*: The measurements of water vapor transmission rate (WVTR) and water vapor permeability (WVP) followed the adaptation of the ASTM E96/E96M-16 (2016) standard method, as used by Guimarães Jr. *et al.* (2015) with 16 mm diameter coupled to permeation cells filled with silica in triplicate. These cells, placed in an environment at 38 °C and 90% relative humidity (RH) for eight days, were weighed daily. The 90% RH environment created in a desiccator containing a saturated saline solution followed the ASTM E104-02 (2012) procedure. WVTR (g/m².day) and WVP (g.mm/day.m².kPa) are calculated with Equations 2 and 3 as follows:

$$\text{WVTR} = \frac{(M/t)}{A} \quad (2)$$

$$\text{WVP} = \text{WVTR} \cdot \frac{\text{Th}}{S} \cdot (R^1 - R^2) \quad (3)$$

‘M’ is the mass (g), ‘t’ is the time (d), ‘M/t’ is the angular coefficient from the linear regression of time (day) and mass gain (g), and ‘A’ is the test area (m²). ‘Th’ is the paper thickness (μm), ‘S’ is the saturation vapor pressure at the test temperature (kPa), ‘R¹’ is the relative humidity in the desiccator (90%), and ‘R²’ is the relative humidity of the test environment (0%).

2.2.5 Oil/grease barrier property of the coated paper

a) Kit test: Oil resistance followed T 559 cm-12 (TAPPI, 2012). Kit oil solutions ranging from 1 to 12 contain specific proportions of the following reagents: castor oil, toluene, and n-heptane. Kit test 1 is the solution of only castor oil, while kit test 12 is the solution of toluene and n-heptane, with the lowest surface energy. A kit test drop was applied to the paper at a height of 13 mm, and the excess oil was removed after 15 s. The kit test not absorbed by the paper represents the number of its resistance. A paper with kit test 12 indicates a more oil/grease-resistant coating.

b) Fold kit test: The same procedure was performed on a wrinkle by following the same methodology. The crease simulates a possible discontinuity of the thin coating when folding the multilayer paper, which was created by repeatedly folding the paper.

c) Surface-free energy: Surface-free energy analysis follows the sessile drop method described by Owens and Wendt (1969), Kaelble (1970), and Rabel (1971). Advance Software measures polar and dispersive surface energies, which is expressed in mN/m, from the contact angles formed in the samples by five different solvents (water, glycerol, diiodomethane, ethylene glycol, and 1-bromonaphthalene) at room temperature (23 °C). Polarity is the ratio of polar components to the total free energy of the multilayer paper surface.

2.2.6 Oxygen barrier of the coated paper

Using an oxygen permeation analyzer (Ox-Tran® Model 2/22 L, Mocon Inc., Minneapolis, MN, USA), the oxygen transmission rate (OTR) of the multilayer paper followed

the ASTM D3985-17 (ASTM, 2017) procedure. Aluminum foil covered the coated paper that was placed between two chambers at ambient atmospheric pressure; one chamber was purged with nitrogen at 23 °C and 50% relative humidity, and the other was purged with oxygen at the same temperature and relative humidity. After oxygen was transmitted to the nitrogen stream, a coulometric detector determined the amount of oxygen in 5 test cycles. OTR levels cannot exceed ten cc/mm²·day to meet food packaging requirements.

2.3 Statistical analysis

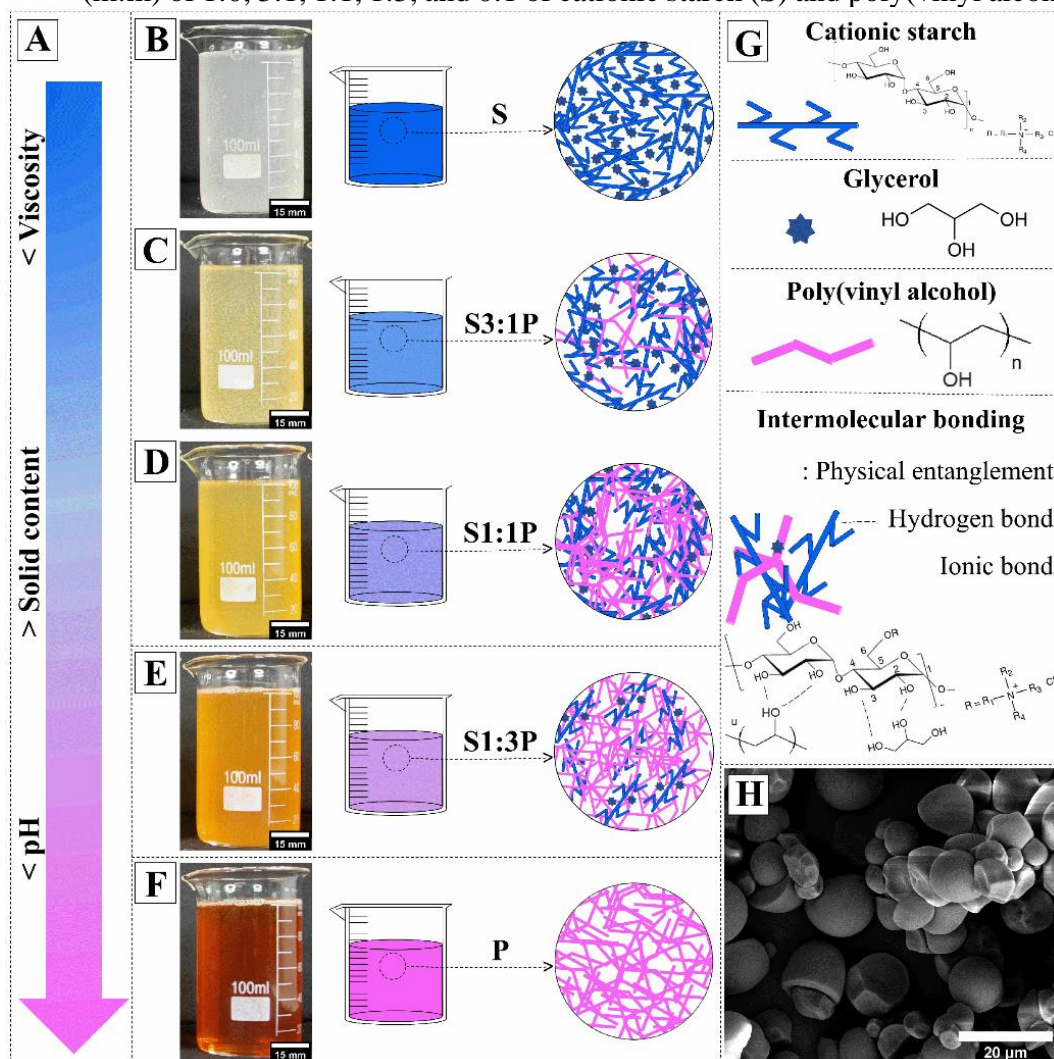
The results were submitted to a one-way analysis of variance (ANOVA) and the Scott–Knott test, at 5% significance, to evaluate the properties of multilayer paper and uncoated kraftliner paper, which was processed by Sisvar 5.6 Software (Ferreira, 2014).

3. RESULTS AND DISCUSSION

3.1 Investigation of suspensions

Starch and PVOH blends have a separation phase due to the short contribution to mixing entropy among these polymers (De Gennes, 1979). However, the cationization of starch and the addition of glycerol to the suspension caused the positive charges to form electrostatic bonds with the negatively charged spots of PVOH. This interaction, with hydrogen bonding among glycerol, PVOH, and water, and physical entanglement resulted in a single-phase suspension for the evaluated blends, showing great synergy (Tian *et al.*, 2017), as indicated in Figure 2. Sin *et al.* (2010) investigated the hydrogen bonding between starch and PVOH through computational modeling and experimental FT-IR, confirming the compatibility and stability of the blend in a water suspension.

Figure 2 - Sketch of blend suspensions in deionized water with complementary proportions (m:m) of 1:0, 3:1, 1:1, 1:3, and 0:1 of cationic starch (S) and poly(vinyl alcohol)(P).



Schematic representation of increase and decrease of pH, solid content, and viscosity when adding poly(vinyl alcohol) to cationic starch/glycerol matrix (A); suspension of: 100% (m/m) cationic starch/glycerol (B), 75% (m/m) cationic starch/glycerol and 25% (m/m) poly(vinyl alcohol) (C), 50% (m/m) cationic starch/glycerol and 50% (m/m) poly(vinyl alcohol) (D), 25% (m/m) cationic starch/glycerol and 75% (m/m) poly(vinyl alcohol) (E), 100% (m/m) poly(vinyl alcohol) (F); chemical representation of cationic starch, glycerol, poly(vinyl alcohol) and their possible intermolecular interactions (G); and scanning electron image of cationic starch granule (H).

Source: From the author (2023).

Cationic starch exhibits high viscosity at low solid contents due to gelatinization with water ingress into the granule structure (Radosta *et al.*, 2004). Ranging from $4.2 \pm 0.1\%$ at $4,707.7 \pm 3.1$ cP to $19.0 \pm 0.2\%$ at 331.3 ± 1.5 cP, with the addition of 25% PVOH to cationic starch the suspension decreased the viscosity dramatically by approximately 4,200 cP (Table 1). Subsequently, the viscosity decreased by 2% when more 25% PVOH was added due to the retrogradation of starch from mechanical agitation and electrostatic bonds between polymers (Ebnesajjad, 2012). Solid content and viscosity conditions affect the formation of film during

the coating process, influencing the quality and mechanical improvement of the multilayer paper. Very viscous suspensions are difficult to spread and require high pumping forces. The less viscous ones favor penetration in the paper, and an appropriate film is not formed (Thébault *et al.*, 2017).

Sakkara *et al.* (2020) studied the effect of pH on the barrier properties of unmodified starch films. The pH influences the properties of permeability to oxygen and water vapor due to increased starch crosslinking. Starch hydrolysis is minimal in suspensions of $\text{pH} \geq 4$ with cure at temperatures ≤ 105 °C (Olsson *et al.*, 2013). The pH values of the suspensions ranged from 6.0 ± 0.1 to 7.8 ± 0.1 within this pH range.

3.2 Physical, morphological, and thermal characterization

Thickness and density directly influence the barrier properties of oil, water, water vapor, and gases, as continuous layers are needed to produce a barrier property (Yang *et al.*, 2022; Heinz, Stephan, and Gambaryan-Roisman, 2021). Pure polymer and blend suspensions formed a uniform film on the kraftliner paper with a low standard deviation for the thickness considering a similar grammage, as shown in Table 2 and Figure 3. The surface of the starch film shows greater roughness and discontinuity, suggesting a lower barrier property (Figure 3G).

Table 2 - Multilayer paper thickness, density, and thermal degradation temperature characterization.

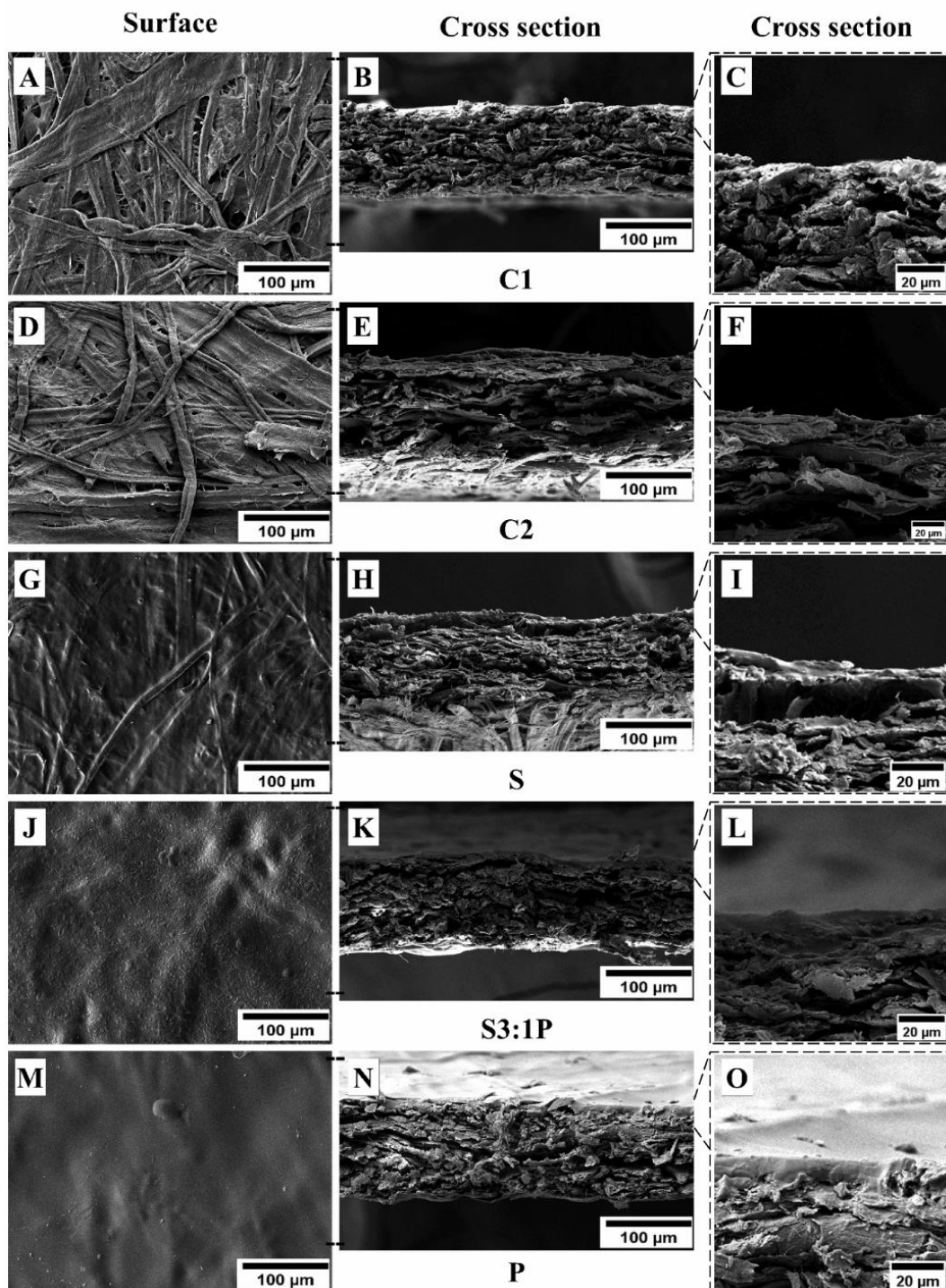
| Sample | Paper thickness (mm) | Paper density (g/cm ³) | T _{onset} (°C) | T _{half} (°C) | Thermodegradation final residues (%) |
|--------|----------------------------|------------------------------------|-------------------------|------------------------|--------------------------------------|
| C1 | 0.125 ± 0.001 ^a | 0.691 ± 0.002 ^a | 308 | 344 | 18.5 |
| C2 | 0.124 ± 0.002 ^a | 0.689 ± 0.003 ^a | 307 | 344 | 18.4 |
| S | 0.147 ± 0.003 ^c | 0.693 ± 0.014 ^a | 303 | 342 | 16.9 |
| S3:1P | 0.143 ± 0.004 ^d | 0.711 ± 0.030 ^b | 306 | 342 | 17.9 |
| S1:1P | 0.141 ± 0.003 ^d | 0.720 ± 0.015 ^b | 298 | 340 | 14.6 |
| S1:3P | 0.138 ± 0.002 ^c | 0.738 ± 0.032 ^c | 302 | 341 | 15.9 |
| P | 0.134 ± 0.003 ^b | 0.756 ± 0.018 ^d | 274 | 332 | 14.5 |

T_{onset}: Temperature at the beginning of the thermal event. T_{half}: Temperature at 50% mass loss.

Average value ± standard deviation. The same letters in the columns do not differ according to the Scott–Knott test at 5% significance. Control treatments with no coating (C1) and double wet-and-dry (C2). Blend treatments with complementary proportions (m:m) of 1:0, 3:1, 1:1, 1:3, and 0:1 of cationic starch (S) and poly(vinyl alcohol) (P).

Source: From the author (2023).

Figure 3 - Typical scanning electron microscopy images of multilayer paper surface (A, D, G, J, M) and cross-section (B, C, E, F, H, I, K, L, N, O).



Control treatments with no coating (C1) (A, B, C) and double wet-and-dry (C2) (D, E, F). Blend treatments with complementary proportions (m:m) of 1:0 (G, H, I), 3:1 (J, K, L), and 0:1 (M, N, O) of cationic starch (S) and poly(vinyl alcohol) (P).

Source: From the author (2023).

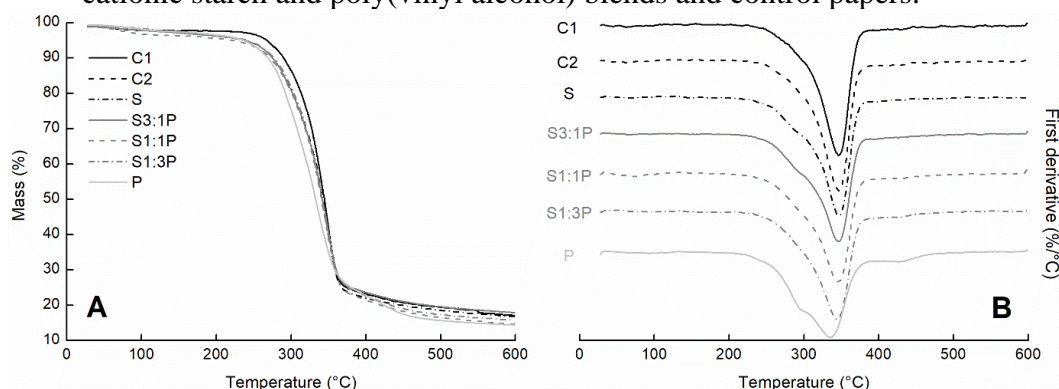
Adding PVOH to cationic starch and pure PVOH generated films with excellent surface uniformity, as seen in Figures 3J and 3M, respectively. The greater package thickness with lower density is observed in packages coated with cationic starch, which results from the high

viscosity of the starch. When dried, the amorphous structures remain separate, decreasing the density of the coated paper. In addition, part of the cationic starch appears to penetrate the paper's pores, pushing the fibers away (Figures 3G, 3H, and 3I). On the other hand, the linear chains of PVOH (Figures 3M, 3N, and 3O) are well adjusted to low viscosity, become less thick after drying and, consequently, exhibit a higher density (Wang *et al.*, 2013). The blends showed intermediate thicknesses and densities between the two pure polymers, as seen in Figures 3J, 3K, and 3L. Finally, an increase in density is observed when PVOH is added to the cationic matrix of starch.

The network of flattened fibers formed by the kraftliner paper creates uneven and porous structures along its entire surface, as suggested in Figures 3A and 3D. Pores transport water, water vapor, oil, and gases through paper (Zhang, Xiao, and Qian, 2014). It is also possible to observe an increase in the paper's pores for the C2 sample, generating an increase in the standard deviation of thickness and density. The pore heterogeneity and the surface (Figures 3E and 3F) can facilitate the displacement of water and gases through the paper. On the other hand, interlacing these fibers contributes positively to the mechanical strength for use as packaging, as well as the thermal response of the paper fibers.

Thermogravimetric analysis was performed to understand the behavior of the multilayer papers with increasing temperature. The thermogravimetric analysis of papers coated with blends of cationic starch and PVOH can be divided into three phases (Figure 4A). The first decay in the thermographic curve refers to the dehydration of the coated paper with physical elimination by vaporization or breaking of trapped water. This process is not considered degradation (Abiral *et al.*, 2019; Mohammadkazemi, Azin, and Ashori, 2015; Liu *et al.*, 2013). After the adsorbed water is lost, the starch-coated paper remains stable until thermal degradation starts at 303 °C, and PVOH-coated paper starts at 274 °C (Table 2). The coated papers analyzed exhibited similar thermal behavior, ending with a temperature close to 375 °C. However, the beginning of mass loss occurred in the paper coated with PVOH before the other coated papers, with a temperature at a maximum degradation rate of approximately 11-14 °C difference (Figure 4B).

Figure 4 - Thermogravimetry curves (A) and the first derivative (B) of multilayer paper with cationic starch and poly(vinyl alcohol) blends and control papers.



Control treatments with no coating (C1) and double wet-and-dry (C2). Blend treatments with complementary proportions (m:m) of 1:0, 3:1, 1:1, 1:3, and 0:1 of cationic starch (S) and poly(vinyl alcohol) (P).

Source: From the author (2023).

The significant mass loss observed for the kraftliner multilayer papers is due to the depolymerization of hemicelluloses, cellulose decomposition, and lignin degradation. Hemicelluloses have amorphous structures with random arrangements, favoring hydrolysis (John and Thomas, 2008; Yang *et al.*, 2006). Cellulose, as a semicrystalline polymer, improves the thermal stability of papers. The crystalline structure break is mainly responsible for mass loss (Mohammadkazemi, Azin, and Ashori, 2015; Vazquez *et al.*, 2013). Due to its crosslinked structure and high molecular weight, the lignin component is difficult to degrade completely and among the last components to degrade (John and Thomas, 2008; Yang *et al.*, 2006).

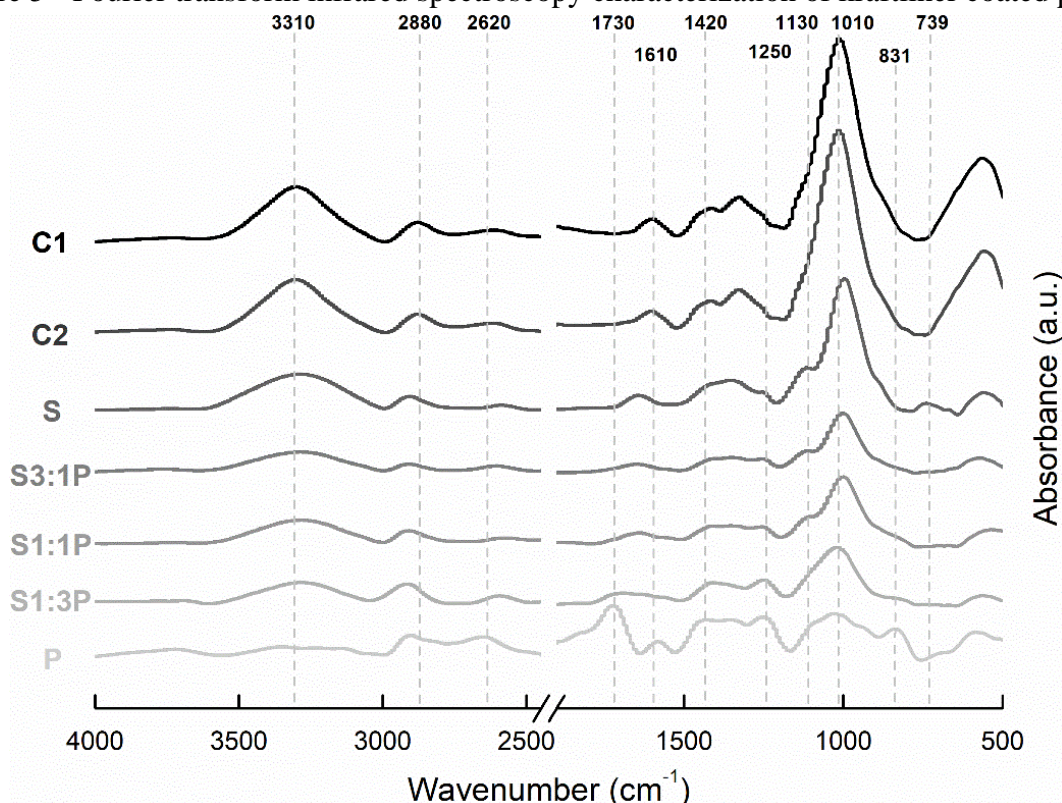
Yang *et al.* (2013) suggested that before starch macromolecules are converted into volatile products with low molecular weights, the macromolecules undergo intermediate physical and chemical changes. For cationic starch, other reactions occur that involve the scission of cationic groups, decreasing the temperature of thermal degradation. Sin *et al.* (2011) evaluated the thermal degradation and activation energy of blends of PVOH with cassava starch. The authors verified that starch presents better thermal resistance due to its cyclic hemiacetal structure, which is less susceptible to thermal attacks. The blends increased the thermal stability of PVOH by 40-50%.

3.3 Fourier transform infrared spectroscopy (FT-IR)

The FT-IR spectra of functional groups found in lignocellulosic materials, such as kraftliner paper (Figure 5), are characterized by peak bands at $3,310\text{ cm}^{-1}$, which are attributed to the stretching of OH from molecules of water, cellulose, starch, glycerol, and PVOH, and a

peak at $2,880\text{ cm}^{-1}$, which is attributed to the stretching vibration of CH groups of cellulose, starch, and PVOH (Han *et al.*, 2013). There is a sequential decrease in the intensity of the OH stretching peak. The blend components' more significant and intense interactions can contribute to this decreased peak. The disappearance of the $3,310\text{ cm}^{-1}$ peak might result from OH group interactions in the molecular chains of PVOH with the kraftliner paper.

Figure 5 - Fourier transform infrared spectroscopy characterization of kraftliner coated paper.



Control treatments with no coating (C1) and double wet-and-dry (C2). Blend treatments with complementary proportions (m:m) of 1:0, 3:1, 1:1, 1:3, and 0:1 of cationic starch (S) and poly(vinyl alcohol) (P).

Source: From the author (2023).

The $1,610\text{ cm}^{-1}$ peak, which was observed in the samples coated with pure PVOH and cationic starch and in control samples C1 and C2, is related to the HOH- stretching vibration of the water adsorbed by hydroxyl groups (Chen *et al.*, 2016). For PVOH, C=O is attributed to the $1,730\text{ cm}^{-1}$ peak and C-O-C to the 831 cm^{-1} peak (Mansur *et al.*, 2008). Both peaks were not observed on kraftliner papers coated with a blend of cationic starch and PVOH. The interaction of cationic starch, PVOH, and glycerol may have masked the appearance of these peaks in samples coated with S3:1P, S1:1P, and S1:3P.

The bands that vary in the $1,610\text{ cm}^{-1}$ and $1,250\text{ cm}^{-1}$ range are characteristic of the uronic ester groups and ester bonds of the carboxylic group of ferulic and p-coumaric acid,

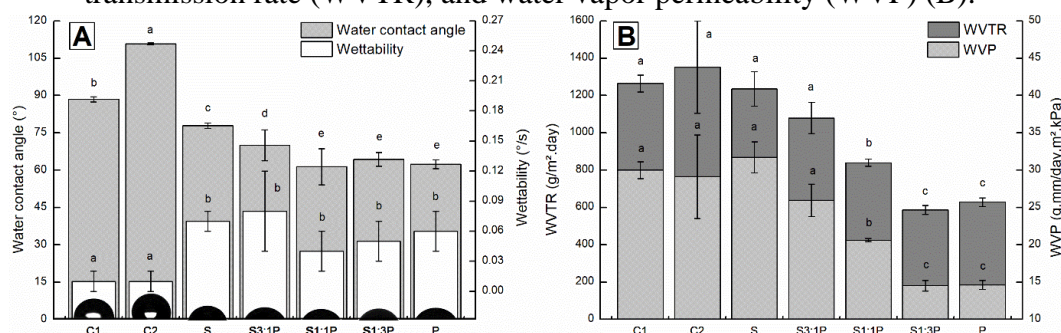
which are present mainly in lignin and hemicelluloses, and are more evident in C1 treatments and C2 since there is no coating in these samples (Miao, Lin, and Bian, 2020; Bian *et al.*, 2019).

An intense peak at 990 cm^{-1} is attributed to the crystalline region of starch (Abdulla *et al.*, 2018). However, the peak is not observed due to starch cationization and irreversible breakage of the crystalline structure during gelatinization. The bands at the peaks at $1,130\text{ cm}^{-1}$, $1,010\text{ cm}^{-1}$, and 739 cm^{-1} are related to the elongation of the starch's CO, COH, and COC bonds (Akhavan, Khoylou, and Ataeviarjovi 2017; Prachayawarakorn *et al.*, 2013). Similar behavior was also observed by Hamdani *et al.* (2022), confirming that the polymers exhibited good interactions and good adhesion to kraft paper.

3.4 Paper water and oil resistance

Barrier properties determine the applicability of multilayer papers; for the water barrier, the contact angle with water and wettability measure the paper's hydrophobicity/hydrophilicity (Figure 6A). Contact angles greater than 90° indicate that the materials are hydrophobic (Bačovská *et al.*, 2016). The highest contact angle was observed for the control paper coated with water. The double drying of the paper caused a process of hornification (Mascarenhas *et al.*, 2022), which caused an increase in the porosity of C2 and in the water contact angle. In addition, the surface roughness generated air trapping between the fiber network of the paper, making its surface more hydrophobic (Samyn, 2013).

Figure 6 - Properties of multilayer paper of water contact angle, wettability (A), water vapor transmission rate (WVTR), and water vapor permeability (WVP) (B).



The same letters for each analysis do not differ according to the Scott–Knott test at 5% significance.

Control treatments with no coating (C1) and double wet-and-dry (C2). Blend treatments with complementary proportions (m:m) of 1:0, 3:1, 1:1, 1:3, and 0:1 of cationic starch (S) and poly(vinyl alcohol) (P).

Source: From the author (2023).

On the other hand, papers coated with PVOH and cationic starch presented contact angles smaller than 90° due to the hydrophilic nature of their polymer chain. Papers with PVOH contents of 50 wt.% or more had an even smaller contact angle with water (close to 64°). PVOH showed a good spread over the paper surface with low thickness, as seen in the previous session. The coated paper's smoothness generated a lower contact angle by facilitating water spread across the surface (Tan, Da Silva, and Demarquette, 2001). Wettability, indicating waterdrop angle absorption as a function of time, was also higher for papers coated with both polymers, reaching 0.08 %/s for the S sample. Measuring the water contact angles applied to coated paper is helpful. However, the paper's barrier to water penetration is influenced by other characteristics, such as surface roughness, porosity, and film formation as a physical block (Samyn, 2013).

Multilayer papers were also evaluated for water vapor resistance (Figure 6B). The parameters of water vapor transmission rate (WVTR) and water vapor permeance (WVP) presented the same behavior. Control samples and samples with starch content greater than 50% showed high WVTR values, with values greater than $1,080 \text{ g/m}^2\cdot\text{day}$. All amorphous and porous polysaccharides with hydrogen bonds are highly susceptible to WVTR due to the disruption of these bonds (Chi and Catchmark, 2018). By adding a ratio of 1:1 cationic starch:PVOH, the WVTR decreased by 38% compared to that of the control treatment. In the proportions of PVOH 1:3 and 0:1, the WVTR still reached 57% less WVTR. The mixture of cationic starch and PVOH in a 1:3 ratio formed a network with a three-dimensional structure with intensified intermolecular bonds, leading to the lowest WVTR of $586\pm 23 \text{ g/m}^2\cdot\text{day}$.

As another water barrier analysis, the Cobb test indicated that water absorption was high for samples containing cationic starch, as the level reached $189\pm 2 \text{ g/m}^2$ (Table 3). Starch has few molecular interactions due to its hydrophilic nature and forms an intrinsic dense interdiffusion film with water barrier properties, splitting the starch chains up and promoting film swelling (Chi, Wang, and Catchmark, 2020). In addition, the porosity and surface roughness of the films can contribute to increased water absorption (Hu *et al.*, 2009). The addition of PVOH caused a decrease in water absorbency, similar to what was found elsewhere (Lago *et al.*, 2021; Rodrigues *et al.*, 2020; Lin *et al.*, 2017), while the pure PVOH coating maintained a Cobb similar to the control treatments.

Table 3 - Water absorbency and oil resistance of multilayer paper.

| Sample | Cobb test (g/m ²) | Oil kit test* | |
|--------|-------------------------------|---------------|------|
| | | Surface | Fold |
| C1 | 37 ± 1 ^a | 0 | 0 |
| C2 | 36 ± 1 ^a | 0 | 0 |
| S | 189 ± 2 ^e | 10 | 0 |
| S3:1P | 138 ± 9 ^d | 12 | 1 |
| S1:1P | 115 ± 5 ^c | 12 | 1 |
| S1:3P | 68 ± 17 ^b | 12 | 1 |
| P | 34 ± 1 ^a | 12 | 1 |

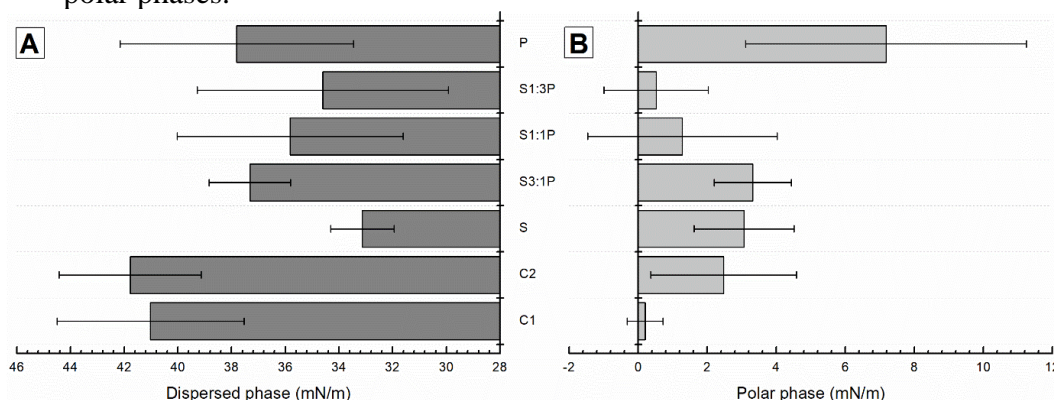
* Oil kit test number according to T 559 cm-12 (TAPPI, 2012). Average value ± standard deviation. The same letters do not differ according to the Scott–Knott test at 5% significance. Control treatments with no coating (C1) and double wet-and-dry (C2). Blend treatments with complementary proportions (m:m) of 1:0, 3:1, 1:1, 1:3, and 0:1 of cationic starch (S) and poly(vinyl alcohol) (P).

Source: From the author (2023).

On the other hand, the blends showed a sound oil barrier (Table 3) due to both polymers' polarity and cohesive energy (Chen *et al.*, 2021). Paper is a porous material with high oil permeation, causing a decrease in packaging quality (Zhang, Xiao, and Qian, 2014). Tests were performed on multilayer paper surfaces and folds, imitating the use of packaging. The starch presented the kit oil n. 10, with zero resistance when paper is folded. When PVOH was added to cationic starch for all proportions, the coated papers increased the oil resistance to kit n. 12 for the surface, maximum resistance, and kit n. 1 for folded coated paper samples. PVOH is a well-known oil-resistant polymer (Spagnol *et al.*, 2018), promoting suitable packaging for oil resistance.

As a surface characterization, the surface free energy relates to the barrier properties of multilayer papers (Figure 7). Higher surface free energy promotes more efficient ink dispersion in coated paper, reducing the use of paint in the paper industry, hence eliminating the requirement of corona charge treatment (Mascarenhas *et al.*, 2022; Shenoy and Shetty, 2022; Lopes *et al.*, 2018). The polar phase of the surface free energy expresses the presence of available polar groups, such as hydroxyls (Shahbazi, Rajabzadeh, and Sotoodeh, 2017). The lowest value of the polar phase was observed by the C1 control with 0.2±0.5 mN/m, in which the hydroxyl groups were unavailable. The paper hydroxyl groups were again accessed by double wet-and-dry (Samyn, 2013). The hydrophilic functional groups present in PVOH and starch influence the increase in the polar phase of free energy, reaching 7.2±4.1 mN/m for 100% PVOH. For all samples, the dispersed phase was considerably higher than the polar phase, which was also found by Żółek-Tryznowska and Holica (2020).

Figure 7 - Properties of multilayer coated paper surface free energy with their dispersed and polar phases.



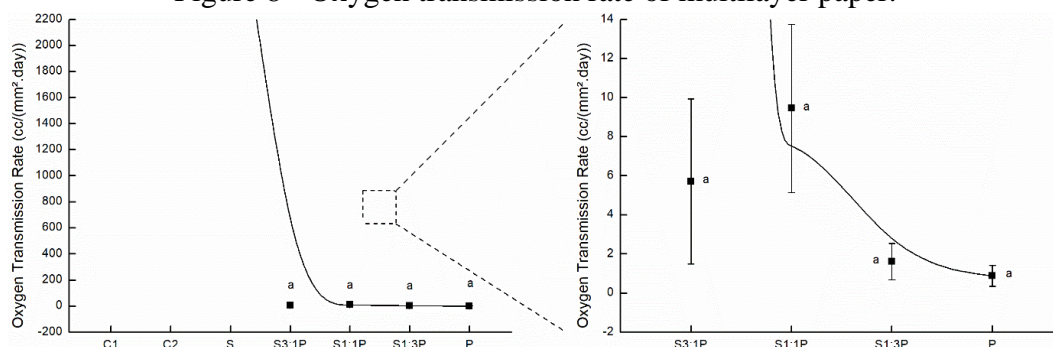
Control treatments with no coating (C1) and double wet-and-dry (C2). Blend treatments with complementary proportions (m:m) of 1:0, 3:1, 1:1, 1:3, and 0:1 of cationic starch (S) and poly(vinyl alcohol) (P).

Source: From the author (2023).

3.5 Oxygen barrier

Uncoated papers C1 and C2 have a shallow oxygen barrier due to their high porosity, which was confirmed by SEM images, with values above 10,000 $\text{cm}^3/(\text{m}^2 \cdot \text{day})$, as shown in Figure 8. The starch-coated paper also exhibited a low oxygen barrier. The rupture of intramolecular and intermolecular hydrogen bonds favors the permeation of oxygen molecules (Gao *et al.*, 2012). As seen in Section 3.2, the cationic starch film still shows discontinuities in the kraftliner paper. Furthermore, the starch chains are randomly disorganized in the amorphous regions, allowing the diffusion of oxygen molecules (Liu *et al.*, 2016; 2022). The crystalline structure of natural starch is impermeable to small molecules; however, the gelatinization process irreversibly disrupts this structure (Yilmaz *et al.*, 2004).

Figure 8 - Oxygen transmission rate of multilayer paper.



The same letters do not differ according to the Scott–Knott test at 5% significance. Control treatments with no coating (C1) and double wet-and-dry (C2). Blend treatments with complementary proportions (m:m) of 1:0, 3:1, 1:1, 1:3, and 0:1 of cationic starch (S) and poly(vinyl alcohol) (P).

Source: From the author (2023).

PVOH coatings, on the other hand, have a high oxygen barrier under low drying conditions, which decreases in highly humid environments (Tsurko *et al.*, 2017). Oxygen is a nonpolar molecule and does not establish significant interactions with the PVOH hydroxyl groups. Furthermore, the polymeric fit increases the hydrogen bonds between the PVOH chains (Peng *et al.*, 2006). Grunlan *et al.* (2004) confirmed more than 500% increase in O₂ permeability with an increase in relative humidity from 0% to 55%. The starch and PVOH blends maintained the oxygen barrier property of PVOH with up to 75 wt.% cationic starch, with average values lower than 10 cm³/(mm².day). Coating paperboard with starch and PVOH, Javed, Ullsten, and Järnström (2017) found that samples containing glycerol contained defects in the coating bilayers, increasing the OTR of the paper. Furthermore, the authors verified that by using citric acid as a plasticizer, the film remained free of defects and the OTR remained lower than 1 cm³/(mm².dm³ay), which was confirmed by Javed *et al.* (2016) and Olsson *et al.* (2013), even in high humidity.

OTR values close to zero are desirable for food packaging, such as packaging for fresh meats, cheeses, soluble coffee, seeds, baked goods, vegetables, and fruits (Stocchetti, 2012). Wang *et al.* (2018) suggested that for low OTR and WVTR values between 100 and 1000 g/(m².day), packaging should be used for cheese, baked products, fruits, vegetables, and salads. Considering the water resistance presented by the PVOH and cationic starch blends, using multilayer paper is more suitable with dried products.

The addition of cationic starch in blends with PVOH as a coating on kraftliner paper, which was presented in this article and obtained similar results to starch-PVOH blends, exhibits potential for reducing nonrenewable material and potential for biodegradability, contributing to the production of ecological packaging.

4. CONCLUSION

The present work contributes with detailed information about the application and performance of different cationic starch/glycerol:PVOH blends as paper coating for different functional barriers (oil/grease, water, water vapour, and O₂). Suspensions of cationic starch and PVOH blends showed good synergy. The suspension viscosity decreased with the addition of PVOH to the starch matrix, which may have been caused by starch retrogradation and adjustment to PVOH chains. Papers coated with more than 25 wt.% cationic starch showed increased temperature at the maximum degradation rate. In addition, the coatings showed good adhesion to the paper without spaces in the interface, as confirmed by SEM images, while filling

the pores of the kraftliner paper in the coating area. The coated paper showed low water resistance by water contact angle tests, wettability tests, and Cobb tests due to the hydrophilic nature of both polymers. On the other hand, compared to the control paper, the kraftliner coated papers showed resistance to oil/grease and decreased water vapor permeability. The addition of cationic starch up to 75 wt.% to the PVOH matrix did not decrease the oxygen resistance of the PVOH, assisting in the incorporation of renewable material in the manufacture of kraftliner coated paper with a barrier function. However, the water vapor permeability remained low due to the proportion of 25 wt.% cationic starch. Therefore, blends formed by high-viscosity cationic starch, glycerol, and PVOH showed great potential for kraftliner coating, which are related to the PVOH ratio in those blends, mainly for packaging applications that require reduced O₂ permeability and resistance to oil/grease, as used in kraftliner coated paper for non-moistened products. This study has contributed with more detailed knowledge about chemical interactions of cationic starch and PVOH, microstructure, about performance of the ensuing coated papers, to the search for more sustainable packaging and consists of data support for theoretical studies. Additional work is still valuable for optimizations of performance, to improve the relationship between biodegradable and renewable materials, the waterproof properties and for maintaining paper as low-cost solutions for the packaging sector.

ACKNOWLEDGMENT

This study was financed in part by the Coordenação de Aperfeiçoamento de Pessoal de Nível Superior – Brasil (CAPES) – Finance Code 001. The authors are grateful for the support of the Laboratory BioNano from the Federal University of Pelotas - UFPel, the Laboratory of Electron Microscopy and Analysis of Ultrastructural from the Federal University of Lavras - UFLA, and FINEP, FAPEMIG, CNPq, Rede RELIGAR, and CAPES for supplying the equipment and technical support for experiments involving electron microscopy. The authors are also thankful for the Wood Science and Technology graduate program at the Federal University of Lavras – UFLA, the Forest, Nature, and Biomass section, and the Niels Bohr Institute at the University of Copenhagen - UCPH. Likewise, Klabin S/A for supplying commercial kraft paper and some characterization.

REFERENCES

- ABDULLA, A.H.D.; PUDJIRAHAR, S.; KARINA, M. *et al.* Fabrication and characterization of sweet potato starch-based bioplastics plasticized e work reported in this p with glycerol. **Journal of Biological Sciences**, v. 19, p. 57–64, 2018.
- ABNT NBR 8877 (2020) Adhesives - Determination of solids content. **Associação Brasileira de Normas Técnicas**, São Paulo, SP, 2020.
- ABNT NBR 9277 (2020) Adesivos - Determinação da viscosidade - Método do viscosímetro Brookfield, **Associação Brasileira de Normas Técnicas**, São Paulo, SP, 2020.
- ABRAL, H.; KADRIADI; MAHARDIKA, M. *et al.* Characterization of disintegrated bacterial cellulose nanofibers/PVA bionanocomposites prepared via ultrasonication. **International Journal of Biological Macromolecules**, v. 135, p. 591-599, 2019.
- AKHAVAN, A.; KHOYLOU, F.; ATAEIVARJOVI, E. Preparation and characterization of gamma irradiated Starch/PVA/ZnO nanocomposite films. **Radiation Physics and Chemistry**, v. 138, p. 49–53, 2017.
- ASTM D3985-17 (2017) Standard Test Method For Oxygen Gas Transmission Rate Through Plastic Film And Sheeting Using A Coulometric Sensor. **ASTM International**, West Conshohocken, PA, 2017.
- ASTM D646-13 (2013) Standard Test Method for Grammage of Paper and Paperboard (Mass Per Unit Area). **ASTM International**, West Conshohocken, PA, 2013.
- ASTM T 458 cm-04 (2004) Surface Wettability Of Paper (Angle Of Contact Method). **ASTM International**, West Conshohocken, PA, 2004.
- ASTM E104-02 (2002) Standard Practice For Maintaining Constant Relative Humidity By Means Of Aqueous Solutions. **ASTM International**, West Conshohocken, PA, 2002.
- ASTM E96 / E96M-16 (2016) Standard Test Methods for Water Vapor Transmission of Materials. **ASTM International**, West Conshohocken, PA, 2016.
- BAČOVSKÁ, R.; WISIAN-NEILSON, P.; ALBERTI, M. *et al.* Phenyl-methyl phosphazene derivatives for preparation and modification of hydrophobic properties of polymeric nonwoven textiles. **Reactive and Functional Polymers**, v. 100, p. 53-63, 2016.
- BASIAK, E.; LENART, A.; DEBEAUFORT, F. How Glycerol and Water Contents Affect the Structural and Functional Properties of Starch-Based Edible Films. **Polymers**, v. 10, n. 4, p. 412, 2018.
- BASSI, S. A.; BOLDRIN, A.; FARACA, G. *et al.* Extended producer responsibility: How to unlock the environmental and economic potential of plastic packaging waste? **Resources, Conservation and Recycling**, v. 162, p. 105030, 2020.

BIAN, H., GAO, Y., LUO, J. *et al.* Lignocellulosic nanofibrils produced using wheat straw and their pulping solid residue: from agricultural waste to cellulose nanomaterials. **Waste Management**, v. 91, p. 1–8, 2019.

BIERMANN, C. J. **Handbook of Pulping and Papermaking**. 2nd Edition, 1996.

BYRNE, D.; BOEIJE, G.; CROFT, I. *et al.* Biodegradability of Polyvinyl Alcohol Based Film Used for Liquid Detergent Capsules: Biologische Abbaubarkeit der für Flüssigwaschmittelkapseln verwendeten Folie auf Polyvinylalkoholbasis. **Tenside Surfactants Detergents**, v. 58, n. 2, p. 88-96, 2021.

CHEN, L.; DOU, J.; MA, Q. *et al.* Rapid and near-complete dissolution of wood lignin at $\leq 80^\circ\text{C}$ by a recyclable acid hydrotrope. **Science Advances**, v. 33, n. 9, p. 1701735, 2017.

CHEN, L.; SUN, X.; HANG, J. *et al.* Large-Scale Fabrication of Robust Superhydrophobic Coatings with High Rigidity and Good Flexibility. **Advanced materials interfaces**, v. 3, p. 1500718, 2016.

CHEN, Y.; DUAN, Q.; ZHU, J. *et al.* Anchor and bridge functions of APTES layer on interface between hydrophilic starch films and hydrophobic soyabean oil coating. **Carbohydrate Polymers**, v. 272, p. 118450, 2021.

CHI, K.; CATCHMARK, J. M. Improved eco-friendly barrier materials based on crystalline nanocellulose/chitosan/carboxymethyl cellulose polyelectrolyte complexes. **Food Hydrocolloids**, v. 80, p. 195-205, 2018.

CHI, K.; WANG, H.; CATCHMARK, J. M. Sustainable starch-based barrier coatings for packaging applications. **Food Hydrocolloids**, v. 103, p. 105696, 2020.

CHRISTOPHLIEMK, H.; ULLSTEN, H.; JOHANSSON, C. *et al.* Starch-poly(vinyl alcohol) barrier coatings for flexible packaging paper and their effects of phase interactions. **Progress in Organic Coatings**, v. 111, p. 13-22, 2017.

CONTI, E.M. The content of heavy metals in food packaging paper boards: An atomic absorption spectroscopy investigation. **Food Research International**, v. 30, p. 343-348, 1997.

DANG, K. M.; YOKSAN, R. Thermoplastic starch blew films with improved mechanical and barrier properties. **International Journal of Biological Macromolecules**, v. 188, p. 290-299, 2021.

DE GENNES, P.G. Scaling concepts in polymer physics. **Cornell University Press**. p. 58, 1979.

DEY, A.; NEOGI, S. Oxygen scavengers for food packaging applications: A review. **Trends in Food Science and Technology**, v. 90, p. 26-34, 2019.

DILKES-HOFFMAN, L. S.; PRATT, S.; LANT, P. A. *et al.* 19 - The Role of Biodegradable Plastic in Solving Plastic Solid Waste Accumulation. In: AL-SALEM, S. M. **Plastics to Energy**. **William Andrew Publishing**, p. 469-505, 2019.

EBNESAJJAD, S. Handbook of Biopolymers and Biodegradable Plastics: Properties, Processing and Applications. **Elsevier Science**, 1204 p., 2012.

FERREIRA, D. F. Sisvar: a Guide for its Bootstrap procedures in multiple comparisons. **Ciência e agrotecnologia**, v. 38, n.2, 2014.

GAO, W.; DONG, H.; HOU, H. *et al.* Effects of clays with various hydrophilicities on properties of starch–clay nanocomposites by film blowing. **Carbohydrate Polymers**, v. 88, n. 1, p. 321-328, 2012.

GAO, W.; WU, W.; LIU, P. *et al.* Preparation and evaluation of hydrophobic biodegradable films made from corn/octenylsuccinated starch incorporated with different concentrations of soybean oil. **International Journal of Biological Macromolecules**, v. 142, p. 376-383, 2020.

GARAVAND, Y.; TAHERI-GARAVAND, A.; GARAVAND, F. *et al.* Starch-Polyvinyl Alcohol-Based Films Reinforced with Chitosan Nanoparticles: Physical, Mechanical, Structural, Thermal and Antimicrobial Properties. **Applied Sciences**, v. 12, n. 3, p. 1111, 2022.

GE, C.; LANSING, B.; LEWIS, C. L. Thermoplastic starch and poly(vinyl alcohol) blends centered barrier film for food packaging applications. **Food Packaging and Shelf Life**, v. 27, p. 100610, 2021.

GIUSEPPE, F.; COFFIGNIEZ, F.; AOUF, C. *et al.* Activated gallic acid as radical and oxygen scavenger in biodegradable packaging film. **Food Packaging and Shelf Life**, v. 31, p. 100811, 2022.

GÓMEZ-ALDAPA, C. A.; VELASQUEZ, G.; GUTIERREZ, M. C. *et al.* Effect of polyvinyl alcohol on the physicochemical properties of biodegradable starch films. **Materials Chemistry and Physics**, v. 239, p. 122027, 2020.

GRUNLAN, J. C.; GRIGORIAN, A.; HAMILTON, C. B. *et al.* Effect of clay concentration on the oxygen permeability and optical properties of a modified poly(vinyl alcohol). **Journal of Applied Polymer Science**, v. 93, n. 3, p. 1102–1109, 2004.

GUIMARÃES JR., M.; BOTARO, V.R.; NOVACK, K.M. *et al.* Preparation of cellulose nanofibrils from bamboo pulp by mechanical defibrillation for their applications in biodegradable composites. **Journal of Nanoscience and Nanotechnology**, v. 15, p. 6751–6768, 2015.

GUO, Z.; GOU, Q.; YANG, L. *et al.* Dielectric barrier discharge plasma: A green method to change structure of potato starch and improve physicochemical properties of potato starch films. **Food Chemistry**, v. 370, p. 130992, 2022.

HAKKE, V. S.; LANDGE, V. K.; SONAWANE, S. H. *et al.* The physical, mechanical, thermal and barrier properties of starch nanoparticle (SNP)/polyurethane (PU) nanocomposite films synthesised by an ultrasound-assisted process. **Ultrasonics Sonochemistry**, v. 88, p. 106069, 2022.

HAMDANI, S. S.; LI, Z.; RUOGI, P. *et al.* Oxygen and water vapor barrier properties of polyvinylalcohol and zein bilayer-coated paper. **Journal of Applied Polymer Science**, v. 139, n. 7, p. e51707, 2022.

HAN, J.; ZHOU, C.; WU, Y. *et al.* Self-assembling behavior of cellulose nanoparticles during freeze-drying: effect of suspension concentration, particle size, crystal structure, and surface charge. **Biomacromolecules**, v. 14, p. 1529–1540, 2013.

HAY, J. M.; LYON, D. Vinyl Alcohol: a Stable Gas Phase Species? **Nature**, v. 216, p. 790-791, 1967.

HEINZ, M.; STEPHAN, P.; GAMBARYAN-ROISMAN, T. Influence of nanofiber coating thickness and drop volume on spreading, imbibition, and evaporation. **Colloids and Surfaces A: Physicochemical and Engineering Aspects**, v. 631, p. 127450, 2021.

HU, Z.; ZEN, X.; GONG, J. *et al.* Water resistance improvement of paper by superhydrophobic modification with microsized CaCO₃ and fatty acid coating. **Colloids and Surfaces A: Physicochemical and Engineering Aspects**, v. 351, n. 1-3, p. 65-70, 2009.

ISO 534:2011 (2011) Paper And Board - Determination Of Thickness, Density And Specific Volume, **International Organization for Standardization**, Washington, DC, 2011.

JAVED, A.; ULLSTEN, H.; JÄRNSTRÖM, L. Effects on Oxygen-barrier Properties of Pretreating Paperboard with a Starch–Poly(Vinyl Alcohol) Blend before Polyethylene Extrusion. **Packaging and Technology Science**, v. 30, p. 399-410, 2017.

JAVED, A.; ULLSTEN, H.; JÄRNSTRÖM, L. *et al.* Study of starch and starch-PVOH blends and effects of plasticizers on mechanical and barrier properties of coated paperboard. **Nordic Pulp and Paper Research Journal**, v. 31, n. 3, p. 499-510, 2016.

JOHN, M.; THOMAS, S. Biofibres and biocomposites. **Carbohydrate Polymers**, v. 71, n. 3, p. 343–364, 2008.

KAELBLE, D. H. Dispersion-polar surface tension properties of organic solids. **The Journal of Adhesion**, v. 2, p. 66–81, 1970.

KAN, M.; MILLER, S. A. Environmental impacts of plastic packaging of food products, **Resources, Conservation and Recycling**, v. 180, p. 106156, 2022.

KHAZAEI, A.; NATEGHI, L.; ZAND, N. *et al.* Evaluation of Physical, Mechanical and Antibacterial Properties of Pinto Bean Starch–Polyvinyl Alcohol Biodegradable Films Reinforced with Cinnamon Essential Oil. **Polymers**, v. 13, n. 16, p. 2778, 2021.

KOCHKINA, N.E.; BUTIKOVA, O.A.; LUKIN, N.D. Ecofriendly films based on low-substituted starch acetate enhanced by polyvinyl alcohol additions. **Iranian Polymer Journal**, v. 31, p. 1361–1371, 2022.

- KUMAR, P.; TANWAR, R.; GUPTA, V. *et al.* Pineapple peel extract incorporated poly(vinyl alcohol)-corn starch film for active food packaging: Preparation, characterization and antioxidant activity. **International Journal of Biological Macromolecules**, v. 187, p. 223-231, 2021.
- LAGO, R. C.; OLIVEIRA, A. L. M.; DOS SANTOS, A. A. *et al.* Addition of wheat straw nanofibrils to improve the mechanical and barrier properties of cassava starch-based bionanocomposites. **Industrial Crops and Products**, v. 170, p. 113816, 2021.
- LEE, S.; ZHANG, M.; WANG, G. *et al.* Characterization of polyvinyl alcohol/starch composite films incorporated with p-coumaric acid modified chitosan and chitosan nanoparticles: A comparative study. **Carbohydrate Polymers**, v. 262, p. 117930, 2021.
- LIN, D.; KUANG, Y. CHEN, G. *et al.* Enhancing moisture resistance of starch-coated paper by improving the film forming capability of starch film. **Industrial Crops and Products**, v. 100, p. 12-18, 2017.
- LIU, D.; DANG, S.; ZHANG, L. *et al.* Corn starch/polyvinyl alcohol based films incorporated with curcumin-loaded Pickering emulsion for application in intelligent packaging. **International Journal of Biological Macromolecules**, v. 188, p. 974-982, 2021.
- LIU, S.; CAI, P.; LI, X. *et al.* Effect of film multi-scale structure on the water vapor permeability in hydroxypropyl starch (HPS)/Na-MMT nanocomposites. **Carbohydrate Polymers**, v. 154, p. 186-193, 2016.
- LIU, S.; LIU, L.; LI, B. *et al.* Size effect of carnauba wax nanoparticles on water vapor and oxygen barrier properties of starch-based film. **Carbohydrate Polymers**, v. 296, p. 119935, 2022.
- LIU, X.; WANG, Y.; YU, L. *et al.* Thermal degradation and stability of starch under different processing conditions. **Starch–Stärke**, v. 65, p. 48–60, 2013.
- LOPES, T. A.; BUFALINO, L.; CLARO, P. I. C. *et al.* The effect of surface modifications with corona discharge in Pinus and Eucalyptus nanofibril films. **Cellulose**, v. 25, p. 5017–5033, 2018.
- MANSUR, H.S.; SADAHIRA, C.M.; SOUZA, A.N. *et al.* FT-IR Spectroscopy Characterization of Poly(vinyl alcohol) Hydrogel with Different Hydrolysis Degree and Chemically Crosslinked with Glutaraldehyde. **Materials Science and Engineering: C**, v. 28, p. 539-548, 2008.
- MASCARENHAS, A. R. P.; SCATOLINO, M. V.; DIAS, M. C. *et al.* Association of cellulose micro/nanofibrils and silicates for cardboard coating: Technological aspects for packaging. **Industrial Crops and Products**, v. 188, n. 1, p. 115667, 2022.
- MIAO, X.; LIN, J.; BIAN, F. Utilization of discarded crop straw to produce cellulose nanofibrils and their assemblies. **Journal of Bioresources and Bioproducts**, v. 5, p. 26–36, 2020.

- MITTAL, A.; GARG, S.; BAJPAI, S. Fabrication and characteristics of poly (vinyl alcohol)-starch-cellulosic material based biodegradable composite film for packaging application. **Materials Today: Proceedings**, v. 21, n. 3, p. 1577-1582, 2020.
- MOHAMMADKAZEMI, F.; AZIN, M.; ASHORI, A. Production of bacterial cellulose using different carbon sources and culture media. **Carbohydrate Polymers**, v. 117, p. 518-523, 2015.
- MUTHU, S.S. Environmental Footprints of Packaging. **Springer Singapore**, v. 1, n. 1, 192 p. 2016.
- OLSSON, E.; MENZEL, C.; JOHANSSON, C. *et al.* The effect of pH on hydrolysis, cross-linking and barrier properties of starch barriers containing citric acid. **Carbohydrate Polymers**, v. 98, n. 2, p. 1505-1513, 2013.
- OWENS, D. K.; WENDT, R. C. Estimation of the surface free energy of polymers. **Journal of Applied Polymer Science**, v. 13, p. 1741–1747, 1969.
- PATIL, S.; BHARIMALLA, A. K.; MAHAPATRA, A. *et al.* Effect of polymer blending on mechanical and barrier properties of starch-polyvinyl alcohol based biodegradable composite films. **Food Bioscience**, v. 44, n. 1, p. 101352, 2021.
- PATIL, S.; BHARIMALLA, A. K.; NADANATHANGAM, V. *et al.* Nanocellulose reinforced corn starch-based biocomposite films: Composite optimization, characterization and storage studies. **Food Packaging and Shelf Life**, v. 33, p. 100860, 2022.
- PENG, Z.; KONG, L.X.; LI, S.D. *et al.* Poly (vinyl alcohol)/silica nanocomposites: morphology and thermal degradation kinetics. **Journal of nanoscience and nanotechnology**, v. 6, n. 12, p. 3934-3938, 2006.
- PETERSEN, K.; NIELSEN, P.V.; BERTELSEN, G. *et al.* Potential of biobased materials for food packaging. **Trends in Food Science and Technology**, v. 10, p. 52-68, 1999.
- PRACHAYAWARAKORN, J.; CHAIWATYOTHIN, S.; MUEANGTA, S. *et al.* Effect of jute and kapok fibers on properties of thermoplastic cassava starch composites. **Materials and Design**, v. 47, p. 309–315, 2013.
- QIN, Y.; YUN, D.; XU, F. *et al.* Smart packaging films based on starch/polyvinyl alcohol and Lycium ruthenicum anthocyanins-loaded nano-complexes: Functionality, stability and application. **Food Hydrocolloids**, v. 119, p. 106850, 2021.
- RABEL, W. Einige Aspekte der Benetzungstheorie und ihre Anwendung auf die Untersuchung und Veränderung der Oberflächeneigenschaften von Polymeren. **Farbe und Lack**, v. 77, p. 997–1005, 1971.
- RADOSTA, S.; VORWERG, W.; ELBERT, A. *et al.* Properties of Low-substituted Cationic Starch Derivatives Prepared by Different Derivatisation Processes. **Starch**, v. 56, p. 277–287, 2004.

RODRIGUES, L. D. A.; HURTADO, C. R.; MACEDO, E. F. *et al.* Colloidal properties and cytotoxicity of enzymatically hydrolyzed cationic starch-graft-poly(butyl acrylate-co-methyl methacrylate) latex by surfactant-free emulsion polymerization for paper coating application. **Progress in Organic Coatings**, v. 145, p. 105693, 2020.

ROY, S.; RHIM, J. Antioxidant and antimicrobial poly(vinyl alcohol)-based films incorporated with grapefruit seed extract and curcumin. **Journal of Environmental Chemical Engineering**, v. 9, n. 1, p. 104694, 2021.

SAKKARA, S.; NATARAJ, D.; VENKATESH, K. *et al.* Effect of pH on the physicochemical properties of starch films. **Journal of Applied Polymer Science**, p. 48563-48563, 2020.

SAMYN, P. Wetting and hydrophobic modification of cellulose surfaces for paper applications. **Journal of Material Science**, v. 48, p. 6455–6498, 2013.

SHAHBAZI, M.; RAJABZADEH, G.; SOTOODEH, S. Functional characteristics, wettability properties and cytotoxic effect of starch film incorporated with multi-walled and hydroxylated multi-walled carbon nanotubes. **International Journal of Biological Macromolecules**, v. 104, n. 1, p. 597-605, 2017.

SHENOY, R.; SHETTY, P. New eco-friendly coating formulations for recycled paperboards: effect on print quality and ink volume consumption. **Progress in Color, Colorants and Coatings**, v. 15, p. 175–189, 2022.

SIN, L. T.; RAHMAN, W. A. W. A.; RAHMAT, A. R. *et al.* Computational modeling and experimental infrared spectroscopy of hydrogen bonding interactions in polyvinyl alcohol–starch blends. **Polymer**, v. 51, n. 5, p. 1206-1211, 2010.

SIN, L. T.; RAHMAN, W. A. W. A.; RAHMAT, A. R. *et al.* Determination of thermal stability and activation energy of polyvinyl alcohol–cassava starch blends. **Carbohydrate Polymers**, V. 83, N. 1, P. 303-305, 2011.

SPAGNOL, C.; FRAGAL, E. H.; WITT, M. A. *et al.* Mechanically improved polyvinyl alcohol-composite films using modified cellulose nanowhiskers as nano-reinforcement. **Carbohydrate Polymers**, v. 191, p. 25-34, 2018.

STOCCHETTI, G. Technology that bridges the gap. **Packaging Films**, v. 3, n. 1, p. 16–18, 2012.

SUHAG, A.; BISWAS, K.; SINGH, S. *et al.* Crosslinking effect on polyvinyl alcohol resin for barrier properties of barrier biaxial orientation films. **Progress in Organic Coatings**, v. 163, p. 106662, 2022.

TAN, I. H.; DA SILVA, M. L. P.; DEMARQUETTE, N. R. Paper surface modification by plasma deposition of double layers of organic silicon compounds. **Journal of Materials Chemistry**, v. 11, n. 4, p. 1019-1025, 2001.

TAPPI T 559 cm-12 (2012) Grease Resistance Test for Paper and Paperboard. **Technical Association of the Pulp and Paper Industry**, Peachtree Corners, GA, United States, 2012.

TAPPI T441 om-13 (2013) Water absorptiveness of sized (non-bibulous) paper, paperboard, and corrugated fiberboard (Cobb test). **Technical Association of the Pulp and Paper Industry**, Peachtree Corners, GA, United States, 2013.

THÉBAULT, M.; KANDELBAUER, A.; MÜLLER, U. *et al.* Factors influencing the processing and technological properties of laminates based on phenolic resin impregnated papers. **European Journal of Wood and Wood Products**, v. 75, p. 785–806, 2017.

TIAN, H.; YAN, J.; RAJULU, A. V. *et al.* Fabrication and properties of polyvinyl alcohol/starch blend films: Effect of composition and humidity. **International Journal of Biological Macromolecules**, v. 96, p. 518-523, 2017.

TOMASIK, P.; SCHILLING, C.H. Chemical modification of starch. **Advances in Carbohydrate Chemistry and Biochemistry**, v. 59, p. 175-403, 2004.

TORRES, F.I.; DA SILVA, J.C.; VIEIRA, O. *et al.* Eukalinertm: the first 100% hardwood kraftliner in the world. In: 53RD ABTCP INTERNATIONAL PULP AND PAPER CONGRESS AND EXHIBITION AND 9TH. 2020. São Paulo, **Anais [...]** São Paulo: ABCTP, 2020.

TSURKO, E. S.; FEICHT, P.; HABEL, C. *et al.* Can high oxygen and water vapor barrier nanocomposite coatings be obtained with a waterborne Formulation? **Journal of Membrane Science**, v. 540, p. 212–218, 2017.

VAZQUEZ, A.; FORESTI, M. L.; CERRUTTI, P. *et al.* Bacterial Cellulose from Simple and Low Cost Production Media by *Gluconacetobacter xylinus*. **Journal of Polymers and the Environment**, v. 21, p. 545–554, 2013.

VINCI, G.; D'ASCENZO, F.; ESPOSITO, A. *et al.* Glass beverages packaging: innovation by sustainable production in trends in beverage packaging. **Academic Press**, v. 16, p. 105–133, 2019.

WANG, J.; GARDNER, D. J.; STARK, N. M. *et al.* Moisture and Oxygen Barrier Properties of Cellulose Nanomaterial-Based Films. **ACS Sustainable Chemistry and Engineering**, v. 6, p. 49–70, 2018.

WANG, L.; DONG, Y.; MEN, H. *et al.* Preparation and characterization of active films based on chitosan incorporated tea polyphenols. **Food Hydrocolloids**, v. 32, n. 1, p. 35-41, 2013.

WANG, X.; HOU, X.; ZOU, P. *et al.* Cationic starch modified bentonite-alginate nanocomposites for highly controlled diffusion release of pesticides. **International Journal of Biological Macromolecules**, v. 213, p. 123-133, 2022.

WU, F.; ZHOU, Z.; LI, N. *et al.* Development of poly(vinyl alcohol)/starch/ethyl lauroyl arginate blend films with enhanced antimicrobial and physical properties for active packaging. **International Journal of Biological Macromolecules**, v. 192, p. 389-397, 2021.

XU, Q.; FANG, D.; ZHANG, X. *et al.* Etch the borosilicate glass to form a straight through-glass-via based on the FLACE technology. **Journal of Micromechanics and Microengineering**, v. 32, p. 055008, 2022.

YANG, H.; YAN, R.; CHEN, H. *et al.* In-Depth Investigation of Biomass Pyrolysis Based on Three Major Components: Hemicellulose, Cellulose and Lignin. **Energy Fuels**, v. 20, n. 1, p. 388–393, 2006.

YANG, J.; ZHAO, K.; WANG, G. *et al.* Influence of coating thickness on microstructure, mechanical and LBE corrosion performance of amorphous AlCrFeTiNb high-entropy alloy coatings. **Surface and Coatings Technology**, v. 441, p. 128502, 2022.

YAO, X.; QIN, Y.; ZHANG, M. *et al.* Development of active and smart packaging films based on starch, polyvinyl alcohol and betacyanins from different plant sources. **International Journal of Biological Macromolecules**, v. 183, p. 358-368, 2021.

YILMAZ, G.; JONGBOOM, R. O. J.; FEIL, H. *et al.* Permeation of Volatile Compounds through Starch Films. **Biomacromolecules**, v. 5, n. 2, p. 650–656, 2004.

YOU, Y.; YANG, L.; SUN, X. *et al.* Synthesized cationic starch grafted tannin as a novel flocculant for efficient microalgae harvesting. **Journal of Cleaner Production**, v. 344, p. 131042, 2022.

ZHANG, W.; XIAO, H.; QIAN, L. Enhanced water vapour barrier and grease resistance of paper bilayer-coated with chitosan and beeswax. **Carbohydrate Polymers**, v. 101, p. 401-406, 2014.

ŻOŁEK-TRYZNOWSKA, Z.; HOLICA, J. Starch films as an environmentally friendly packaging material: Printing performance. **Journal of Cleaner Production**, v. 276, p. 124265, 2020.

SIXTH PART

1. THESIS CONCLUSIONS

The process of manufacturing coatings for kraftliner paper to create packaging with a physical barrier to gases and liquids was compared in this work by adding various polymers and natural ingredients to a cationic starch matrix. To assess how water, water vapor, oil/grease, and oxygen affect the performance of coatings, carnauba wax (W), bentonite (B), and poly(vinyl alcohol) (P) were added to cationic starch (S) and compared to uncoated paper (C1), as well as a double dry and wet paper (C2).

The modified starch biopolymer and natural carnauba wax composite displayed good compatibility (paper 1). Through retrogradation, their contact reduced the viscosity of the starch. Additionally, the composite raised the melting point of the wax, preventing it from completely entering the paper's pores and producing a layer on top of the kraftliner paper. Adding carnauba wax to the starch enhanced the surface free energy of the coated sheets' water contact angle and decreased its dispersion and polar phases. On the other hand, starch boosted the material's oil resistance while lowering the wettability introduced by the wax. The introduction of glycerol and polysorbate 80 was a likely reason why the water vapor permeability rate did not change. Although the water absorption produced by the starch/wax interaction remained lower than that of the different polymers, it was not less than that of the kraftliner control papers. Regarding the mechanical strength, it appears that the reduction in tensile strength and Tensile stiffness of the coated sheets introduced by hornification was predominantly caused by water in the suspensions.

The cationic starch biopolymer and bentonite added together interacted well (paper 2). The suspension viscosity was reduced due to the bentonite exfoliation procedure. In addition, compared to a pure cationic starch coating, adding bentonite to the starch reduced the wettability and water absorption of the coated paper in the Cobb test. By reducing the polar phase of the surface energy and increasing the dispersed phase, 7 wt.% of bentonite increased the oil resistance of the oil kit coating from 10 to 12. Regarding the mechanical strength, it is also confirmed that the water in the suspensions played a major role in lowering the tensile strength and the Tensile stiffness of the coated sheets induced by the hornification.

Blends of cationic starch and poly(vinyl alcohol) demonstrated good synergy, with suspension viscosity falling as poly(vinyl alcohol) was added to starch (paper 3). At the maximal degradation rate, papers coated with more than 25 wt.% cationic starch showed an

elevated temperature. Additionally, as shown by scanning electron microscopy images, the coatings filled the pores of the kraftliner paper in the coating region. The coatings strongly adhered to the paper without causing voids in the interface. Due to the hydrophilic properties of both polymers, the coated paper showed low water resistance in water contact angle tests, wettability tests, and Cobb tests. In contrast, the multilayer papers displayed lower water vapor permeability and oil/grease resistance than that of the control paper. The use of renewable material in creating multilayer paper with a barrier function was made possible by adding cationic starch up to 75 wt.% to poly(vinyl alcohol). However, the water vapor permeability remained low because there was a fraction of 25 wt.% cationic starch. Blends made of cationic starch, glycerol, and poly(vinyl alcohol) demonstrated significant potential for multilayer packaging for nonmoisturized goods using kraftliner coating.

The interaction between biodegradable and renewable materials, such as waterproof and affordable packaging, still needs much improvement. There is certainly room for improvement in terms of achieving excellent barriers. However, we are aware that finding a biodegradable substance made from a cost-effective renewable resource to produce high-quality packaging takes time and effort.

Future research should focus on increasing the solids content while maintaining the pH levels of all suspensions above four and the viscosities between 1,000 and 3,000 cP. To promote spreading, it is also essential to mix starch into carnauba wax with the least amount of emulsifier possible and raise the solids content of both starch and poly(vinyl alcohol). To increase the wettability of papers, poly(vinyl alcohol) and starch could be applied as a first layer and a hydrophobic coating as a second layer. To minimize packaging problems and enhance packing performance, an elastic substance or polymer, such as micro/nanofibrils, should be added to improve the fold of the kit oil.

To foster a positive relationship between people and the environment and create more environmentally friendly packaging for a bright future, we aspire to improve our understanding of green materials and cationic starch.